

**STUDY AND CHARACTERIZATION OF NON-ORGAN
SPECIFIC BIOPOTENTIAL SIGNALS ACQUIRED
FROM THE HUMAN SYSTEM**

Thesis submitted by

Aditi Roy (Bhattacharya)

Doctor of Philosophy (Engineering)

Department of Instrumentation and Electronics Engineering

Faculty Council of Engineering & Technology

Jadavpur University

Kolkata, India

2018

JADAVPUR UNIVERSITY

KOLKATA - 700 032, INDIA

INDEX NO.238/11/E

1. Title of the Thesis: **STUDY AND CHARACTERIZATION OF
NON-ORGAN SPECIFIC
BIOPOTENTIAL SIGNALS
ACQUIRED FROM THE HUMAN SYSTEM**

2. Name, Designation &
Institution of the
Supervisors: **Dr. Ratna Ghosh**
Professor
Dept. of Instrumentation and
Electronics Engineering
Jadavpur University
Salt Lake Campus
Kolkata - 700 098
West Bengal, India

Dr. Bhaswati Goswami
Professor
Dept. of Instrumentation and
Electronics Engineering
Jadavpur University
Salt Lake Campus
Kolkata - 700 098
West Bengal, India

3. List of Publications:

I. List of papers published in Journals:

1. Aditi Bhattacharya, Dibyendu Basu, Bhaswati Goswami, Ratna Ghosh, A reliable signal conditioning circuit to acquire human biopotentials, International Journal on Smart Sensing and Intelligent Systems, VOL. 6, NO. 3, pp.1116-1132, June 2013.

II. List of papers published in International Conference Proceedings :

1. Aditi Bhattacharya, Dibyendu Basu, Bhaswati Goswami, Ratna Ghosh, Measuring Human Biopotentials to Ascertain Parameters for Health, In Communication and Industrial Application (ICCIA), 2011 International Conference on, pp.1-4. IEEE, 2011.
2. Aditi Bhattacharya, Nilanjan Mandal, Dibyendu Basu, Bhaswati Goswami, Ratna Ghosh, A Signal Conditioning Circuit to measure Human Biopotentials, In Sensing Technology (ICST), 2012 Sixth International Conference on (pp.794-799). IEEE, 2012.
3. Arindam Sarkar, Aditi Bhattacharya, Ratna Ghosh, Bhaswati Goswami, A Comparative Study of Biopotentials Acquired from Left and Right Hands of Human Subjects, In Advanced Computational and Communication Paradigms 2018 (pp. 110-117). Springer, Singapore.

4. List of Patents: Nil

5. List of Presentations in National/International/Conferences/Workshops:

1. Aditi Bhattacharya, Dibyendu Basu, Bhaswati Goswami, Ratna Ghosh, Measuring Human Biopotentials to Ascertain Parameters for Health, In Communication and Industrial Application (ICCIA), 2011 International Conference on, pp.1-4. IEEE, 2011.

2. Aditi Bhattacharya, Nilanjan Mandal, Dibyendu Basu, Bhaswati Goswami, Ratna Ghosh, A Signal Conditioning Circuit to measure Human Biopotentials, In Sensing Technology (ICST), 2012 Sixth International Conference on (pp.794-799). IEEE, 2012.

Certificate from the Supervisors

This is to certify that the thesis entitled **STUDY AND CHARACTERIZATION OF NON-ORGAN SPECIFIC BIOPOTENTIAL SIGNALS ACQUIRED FROM THE HUMAN SYSTEM** submitted by **Smt. Aditi Roy (Bhattacharya)**, who got her name registered on December 02, 2011 for the award of Ph.D.(Engg.) degree of Jadavpur University, is absolutely based upon her own work done under the supervision of Prof. Ratna Ghosh and Prof. Bhaswati Goswami and that neither her thesis nor any part of the thesis has been submitted for any degree/ diploma or any other academic award anywhere before.

(Dr. Ratna Ghosh)
Professor
Dept. of Instrumentation &
Electronics Engineering
Jadavpur University
Kolkata 700098, India

(Dr. Bhaswati Goswami)
Professor
Dept. of Instrumentation &
Electronics Engineering
Jadavpur University
Kolkata 700098, India

ACKNOWLEDGEMENT

Completion of this doctoral dissertation would not have been possible without the guidance, assistance, appreciation and the support of several individuals who in one way or another contributed and extended their valuable assistance in the preparation and completion of this study. I would like to express my sincere gratitude to all of them.

First and foremost, with immense gratitude, I acknowledge the support and help extended by my supervisors, Dr. Ratna Ghosh and Dr. Bhaswati Goswami, Professors, Instrumentation and Electronics Engineering Department, Jadavpur University whose encouragement, supervision and support from the preliminary to the concluding level enabled me to develop an understanding of the research problem. They always made themselves available to clarify my doubts, despite their busy schedule and I consider it a great opportunity to do my doctoral programme under their guidance and to learn from their research expertise.

Apart from academic aspects, I would cherish all the moments shared in discussions with them, which helped me grow as a more matured person and also to develop the understanding about the lessons of life from different perspectives, more precisely and in an assertive way.

I would like to express my sincere gratitude to Mr. Sajal Badopadhyay, Wingard Research whose work on Gyrosonics and ZED Science helped conceptualise the present research study.

I express my deepest gratitude to Mr. Dibyendu Basu, who always stood beside me as my elder brother and provided me moral support and suggestions, whenever I needed, in all the academic and non-academic issues.

I owe my sincere gratitude to Arindam Sarkar for his active help in Matlab programming which immensely helped in inferring the experimental results.

I would like to acknowledge Jadavpur University, for providing me the required financial support as fellowship during the entire period of this research work.

I am grateful to Head of the Department and all the staff and faculty members of

the Department of Instrumentation and Electronics Engineering, Jadavpur University for their direct and indirect cooperation and assistance towards completion of this work. I sincerely acknowledge the support and help received from Somali Nandi, Somen Biswas and all other research fellows and students working in the research laboratory during this tenure of my work.

I also want to thank all the individuals who gave consent in participating the research work and were *Subjects* of my research study.

This thesis would not have been possible without the support from my parents, Sailen Roy and Bani Roy, and other family members, who provided constant support and encouragement throughout this time period. A special thanks goes to my husband, Bhaskar Bhattacharya, for supporting me in every aspect during my research work and to my elder daughter Debarati Bhattacharya, 3rd year MBBS student, for providing suitable inputs while formulating the chapter on experimental design and also to my younger daughter Rituja Bhattacharya for putting up with my work schedule.

I also owe it all to Almighty God for granting me the wisdom, health and strength to undertake this research task and enabling me to complete it.

November, 2018

Aditi Roy (Bhattacharya)

ABSTRACT

The present research aims to determine the qualitative and quantitative features and parameters of biopotentials that are measured simultaneously from both hands of healthy human subjects using endosomatic EDA technique. These are to be used to characterise healthy human subjects at rest and to devise a procedure using a minimal set of the identified parameters to synthesise realistic pairs of biopotentials.

For this study, real-time data has been acquired from healthy subjects only, such that the measured signals are due to internal causes only, without any explicit external disturbances. Accordingly, the experiment has been designed meticulously, particularly in terms of the inclusion and exclusion criteria of subjects as well as conditions necessary for maintaining an identically comfortable experimental environment.

A simple, yet safe, instrumentation system, without any additional filter or filtering technique, has been used for the study. The instrumentation system consists of two pairs of EDA sensors (Ag-AgCl electrodes) connected to two fingers of left hand (LH) and right hand (RH) simultaneously. The sensor locations are away from any major organ in the human body such that the measurement will provide the response without encountering any organ-specific information. These sensors are connected to a pair of RISH Multi 18S digital multimeters that transmit the data online to a laptop or a PC. The static characteristics of this total acquisition system was analysed to ensure the compatibility of the system with the sensors for this application.

The research study has been conducted in two phases during different times of the year with 16 subjects in Phase1 and 14 subjects in Phase2 . The subjects belong

to eastern region of India and are within the age group of 20 to 58 years. Data was recorded in single (Phase1) and multiple (Phase2) sets of 2 minutes duration at 0.05sec interval; the number of samples in each set was 2400. A total of 715 LH and RH pairs of data have been considered in the two phases, 384 pairs in Phase1 and 331 pairs in Phase2. In a span of 2 minutes, the signals vary almost monotonically only within few tens of mV. Hence, these signals are slowly changing baseline biopotentials of human subjects.

It was found that both LH and RH signals vary continuously for same or different subjects, at same or different dates. Despite this variability, all the recorded LH and RH biopotentials remain bounded in a limited range of $\pm 300\text{mV}$ in both phases. The interdependency indicated between the measured LH and RH signals has been explored by proposing two new sets of derived signals, termed as the Gap and the Pair sum (PS) signals. All types of polarity and trends occurred in the acquired and derived signals in the two phases, along with that different patterns exhibited by a pair of LH and RH signals. The statistical analysis of the 4 signals has also been performed at overall, subjectwise and then setwise levels.

This study showed that a prolonged duration of rest in Phase2 causes the polarity of the data to be more Negative, with an associated increase in occurrence of Constant trend, than in Phase1. It is also evident that the Phase2 data are in general more tightly clustered.

A comparison of the overall and setwise characteristics established that the setwise mean, $Mean_{set}$, is a representative parameter of the corresponding signal for all four signals. It is further observed that the LH signals are more consistent over both the phases. A comparative study of the polarity and trends of the Gap and PS signals established that the PS signals are more representative of the baseline nature of the interdependence of the measured signals.

In order to provide a common basis for studying the time-series characteristics of these 4 signals, the $Mean_{set}$ has been deducted from each signal and the resulting set has been termed as the Deviation signal. It is observed that the total range

of Deviation signals is limited within $\pm 30\text{mV}$ in all cases. It is also observed that prolonged rest stabilizes the Deviation signals also, yet, motor disturbances due to sleep affect the Deviation signals, particularly those of RH.

A further study shows that these Deviation signals have a quasilinear pattern with the signals crossing zero typically in the middle epoch, indicative of the location of the setwise mean. This led to a linear regression model of these signals in terms of two parameters, namely, Zero Crossing Instant (ZCI) of the signal and the corresponding slope (m) of the trendline fitted through ZCI. It is observed that the calculated coefficient of variation, R^2 , are mostly greater than 0.5 and the Residuals are restricted mostly within $\pm 4\text{mV}$. A further analysis of the interrelationship of the ZCI and m values showed that the ZCI and m values mostly lie within the ZCI2M2 class, with $\text{ZCI} \in [801, 1600]$ and m within $\pm 0.01 \text{ mV/instant}$. It was also established that the stochastic Residuals mostly belong to a 4 parameter beta distribution.

Using the identified features and parameters, a procedure has been proposed in this study to synthesise a realistic pair of LH and RH signals using a 2 layer structural hierarchy where the surface layer is defined by the deterministic setwise mean values and the stochastic Residuals, while the inner layer is marked by the values of the ZCI and slopes of the acquired LH and the interdependent PS Deviations. It has been established that while the proper choice of the ZCI and slopes in the LH and PS Deviation signals yields the trends and pairwise patterns for the LH and RH signals, the choice of their respective setwise means provides the signal polarities and the selection of suitable sets of stochastic Residuals guarantees the uniqueness of each signal. Thus, it is established that a simple 2 layer structural hierarchy leads to the plethora of functional complexity observed in the endosomatic EDA biopotentials recorded simultaneously from the left and right hand of human subjects.

Contents

1	Introduction	1
1.1	Review of Literature	2
1.1.1	Electrical Activity in Human Systems	2
1.1.2	Acquisition of Biopotentials	4
1.1.3	Non-organ Specific Studies of the Human System	8
1.1.4	Measurement of Electrodermal Activity (EDA)	10
1.2	Aim and Organisation of the Thesis	12
1.3	List of Contributions	15
2	Conditions and Methodology for acquiring Human Biopotentials	19
2.1	Introduction	19
2.2	Conditions specified for experiment	20
2.2.1	Subject selection	21
2.2.2	Environment of experiments	22
2.2.3	Technique used	22
2.3	Instrumentation System	23
2.3.1	Measurement procedure:	23
2.3.2	Building blocks	25
2.3.3	Static characteristics	29
2.4	Experimental Methodology	36
2.4.1	Protocols followed	36

2.4.2	Placement of electrodes	39
2.4.3	Health parameters measured	40
2.4.4	Acquisition of bio-potentials	41
2.5	Discussions	42
3	Analysis of Human Biopotentials	45
3.1	Introduction	45
3.2	Qualitative analysis of the signals:	47
3.2.1	General Characteristics:	47
3.2.2	Classifying the left and right hand (LH and RH) signals: . . .	52
3.2.3	Classifying the pair of LH and RH signals:	59
3.2.4	Two New Proposed Signals: Gap and Pair Sum (PS):	63
3.3	Quantitative analysis of the signals:	69
3.3.1	Overall analysis:	70
3.3.2	Subject-wise analysis:	73
3.3.3	Analysis of the anomaly in Phase2 RH signals	76
3.3.4	Setwise analysis	79
3.4	Discussions	87
4	Characterisation of the Deviation Signals	93
4.1	Introduction	93
4.2	General Characteristics:	94
4.2.1	Trends in Deviation Signals:	103
4.2.2	Pairs of LHdev and RHdev Signals:	107
4.3	Modelling the Deviation Signals:	110
4.3.1	Zero Crossing Instant (ZCI):	111
4.3.2	Slope m of the Trendline:	112
4.3.3	Instantaneous Residuals:	113
4.4	Analysis of the regression model	115
4.4.1	Characteristics of ZCI	115

4.4.2	Characteristics of slope m	118
4.4.3	Characteristics of Residuals:	120
4.5	Interrelationship between ZCI and m :	125
4.6	Discussions:	133
5	Synthesis of a pair of biopotential signals using representative features	137
5.1	Introduction	137
5.2	Identification of representative features	138
5.3	Synthesis of LH and RH biopotentials:	140
5.4	Validation of Synthesis Procedure	143
5.4.1	Quantitative Analysis:	144
5.4.2	Qualitative Analysis:	150
5.5	Discussions	153
6	Conclusions and Scope for Future Work	155
6.1	Conclusions:	155
6.2	Scope for future work	163

Abbreviations and Nomenclature

List of Abbreviations

fsd	Full scale deflection
rmse	Root mean square error
df	Degrees of freedom
cdf	Cumulative distribution function
EDA	Electrodermal Activity
TV	True Value
MV	Measured value
SE	Static error
RE	Relative error
RA	Relative accuracy
$\%RA_{fsd}$	Percent RA with respect to fsd
SD	Standard deviation
R^2	Goodness of fit factor, Coefficient of variation
GSR	Galvanic skin response
SPL	Skin potential level
PR	Pulse rate
BP	Blood pressure
SpO ₂	Oxygen saturation level in blood
LH	Left Hand
RH	Right Hand

List of Nomenclature and Variables

i, k	time instant
x_k	True input voltage at k th instant
x_{out_k}	Measured output voltage at k th instant
x_i	Potential at the i th instant
x_1	Potential at the 1st instant in a set
x_{2400}	Potential at the 2400th (last) instant in a set
Diff	$x_1 - x_{2400}$ of a signal set
x_{LHi}	Left hand potential at the i th instant
x_{RHi}	Right hand potential at the i th instant
d_1	First difference, $x_{LH1} - x_{RH1}$
d_{2400}	Last difference, $x_{LH2400} - x_{RH2400}$
Gap	Gap signal, $\{x_{LHi} - x_{RHi}\} \forall i \in [1, 2400]$
PS	Pair sum signal, $\{x_{LHi} + x_{RHi}\} \forall i \in [1, 2400]$
$Mean_{overall}$	Overall mean of all data in all sets in a phase
$SD_{overall}$	Overall SD of all data in all sets in a phase
$Mean_{set}$	Setwise Mean
SD_{set}	Setwise SD
$Mean_{Mean_{set}}$	Mean of all setwise mean values
$SD_{Mean_{set}}$	SD of all setwise mean values
LHmean	mean value of LH signal, $Mean_{set}(LH)$
RHmean	mean value of RH signal, $Mean_{set}(RH)$
LHdev	LH Deviation signal, $LH - Mean_{set}(LH)$
RHdev	RH Deviation signal, $RH - Mean_{set}(RH)$
Gapdev	Gap Deviation signal, $Gap - Mean_{set}(Gap)$
PSdev	PS Deviation signal, $PS - Mean_{set}(PS)$
DiffDev	$x_1 - x_{2400}$ of a Deviation signal set

ZCI	Zero crossing Instant of the Deviation signal
m	slope of the fitted trendline
ZCI2M2	Class of signals with $ZCI \in [801,1600]$ and slope m within ± 0.01 mV/instant
y_k	Value of Deviation signal trendline at k th instant
y_{actual_k}	Value of actual Deviation signal at k th instant
Residuals	$\{y_{actual_k} - y_k\} \forall i \in [1, 2400]$
LHdevZCI	ZCI of LHdev signal
LHdev m	m of LHdev signal
PSdevZCI	ZCI of PSdev signal
PSdev m	m of PSdev signal
PSdevSim	Synthesised trendline of PSdev signal
LHdevSim	Synthesised trendline of LHdev signal
RHdevSim	Synthesised trendline of RHdev signal
LHSim	Synthesised trendline of LH signal
RHSim	Synthesised trendline of RH signal
LHRealistic	Synthesised realistic LH signal
RHRealistic	Synthesised realistic RH signal
LHSimRes	Residuals of synthesised LHSim
RHSimRes	Residuals of synthesised RHSim
LHRes	Residuals of trendlines fitted to acquired LH signal
RHRes	Residuals of trendlines fitted to acquired RH signal

List of Figures

2.1	Data acquisition setup showing both hands fitted with electrodes connected to multimeter and connection of multimeter to adapter	24
2.2	Schematic block diagram of the instrumentation system	25
2.3	Representative biopotentials acquired from human fingers of each hand for two subjects (LH-left hand in blue, RH-right hand in red)	29
2.4	Plot of mean static errors at input voltages within $\pm 300\text{mV}$ with minimum and maximum static errors shown in errorbar	33
2.5	Plot of mean $\%RA_{f_{sd}}$ at input voltages within $\pm 300\text{mV}$	33
2.6	Plot of mean of measured voltages at different input voltages in the range $\pm 300\text{mV}$	34
2.7	Plot of SD of measured voltages at different input voltages in the range $\pm 300\text{mV}$	35
2.8	Output voltage recorded for 30 minutes at $+300\text{mV}$ input	37
2.9	First 10 samples of measured voltage at $+300\text{mV}$ input	37
2.10	Condition of the subject maintained during recording of biopotentials	38
2.11	Location of electrode placement for EDA measurement	39
3.1	Time plot of a typical signal shown along with its zoomed plot for 10s (between 201 to 400th instants)	46
3.2	Time series plots of left and right hand (LH and RH) biopotentials acquired in Phase1 and Phase2	48

3.3	Large variations in recorded biopotentials	49
3.4	Typical characteristics of acquired LH and RH biopotentials	50
3.5	Representative time series plots of different subjects on same date . . .	51
3.6	Representative time series plots of same subject on different dates . . .	51
3.7	Bar graph depicting polarity counts of the LH and RH biopotentials in Phase1(blue) and Phase2(red)	54
3.8	Bar graph depicting Trends of LH and RH biopotentials in Phase1 (blue) and Phase2 (red)	56
3.9	Representative time series plots of a pair of signals, LH in blue and RH in red, acquired from 4 different subjects at different times	59
3.10	Typical patterns in pairs shown with different colors for each pair of four different subjects observed at different times	60
3.11	Bar graph depicting count of patterns in a pair of LH and RH biopo- tentials in Phase1(blue) and Phase2(red)	62
3.12	Representative plots of observed trends and polarities in Gap and PS signals	64
3.13	Bar graph depicting polarity counts of the Gap and PS biopotentials in Phase1(blue) and Phase2(red)	65
3.14	Bar graph depicting Trends for Gap and PS signals in Phase1 (blue) and Phase2 (red)	67
3.15	Cdf plots of LH, RH, Gap and PS biopotentials recorded in Phase1 and Phase2	70
3.16	Subject-wise and overall cdf of LH and RH biopotentials recorded in Phase1 and Phase2	75
3.17	LH and RH biopotentials recorded in Phase2 on specific and other dates	76
3.18	Typical setwise mean and SD of Phase2 RH potentials for one subject	77
3.19	Cdf plots of Phase2 RH biopotentials	78
3.20	Typical plot of $Mean_{set}$ and SD_{set} for one subject:Phase1	80
3.21	Typical plot of $Mean_{set}$ and SD_{set} for one subject:Phase2	81

3.22	Cdf plots of $Mean_{set}$ of all 4 signals in Phase1 and Phase2	82
3.23	Cdf plots of SD_{set} of all 4 signals in Phase1 and Phase2	82
4.1	Sample time-series plots of LH and RH Deviation signals in sets of Phase1 and initial and final sets of Phase2	96
4.2	Time-series plots of all LH, LHdev, RH and RHdev signals in Phase1 and Phase2	99
4.3	Time-series plots of all Gap, Gapdev, PS and PSdev signals in Phase1 and Phase2	100
4.4	Cdf plots of LH, RH, Gap and PS Deviation signals in Phase1 and Phase2	102
4.6	Cdf plots of SD of LH signals for all subjects	102
4.5	Zoomed plots of cdf of Deviation signals within ± 10 mV	103
4.7	Cdf plots of SD of RH signals for all subjects	103
4.8	Observed Trends in all 4 types of Deviation signals	105
4.9	Sample LH and RH signal patterns and their corresponding Deviation signal pairs:Phase1	108
4.10	Sample LH and RH signal patterns and their corresponding Deviation signal pairs:Phase2	109
4.11	LH and RH Deviation signals of a typical subject	111
4.12	Sample fit plots and their Residuals	114
4.13	Cdf plots of Zero Crossing Instants (ZCI) of Deviation signals	115
4.14	Zoomed cdf plots of ZCI of Deviation signals in the middle epoch	116
4.15	Cdf plots of slopes, m, of trendlines fitted to Deviation signals	118
4.16	Zoomed cdf plots of slopes, m, within ± 0.01 mV/instant	118
4.17	Cdf plots of R^2 values obtained for trendlines of all 4 Deviation signals	121
4.18	Cdf plots of instantaneous Residuals for all 4 Deviation signals	123
4.19	Zoomed cdf plots of instantaneous Residuals within ± 4 mV	123
4.20	Scatter plots: m vs. ZCI for LHdev and RSdev signals	126
4.21	Scatter plots: m vs ZCI for Gapdev and PSdev signals	127

4.22	Cdf plots of Fit factor R^2 of trendlines in the class ZCI2M2, R^2_{ZCI2M2}	129
4.23	Cdf plots of Residuals for ZCI2M2 class (Residuals _{ZCI2M2})	130
4.24	Zoomed cdf plots of Residuals _{ZCI2M2} within $\pm 4\text{mV}$	130
5.1	Synthesis of pair of Deviation trendlines	142
5.2	Synthesised pair of signal trendlines and corresponding Residuals . .	142
5.3	Cdf plots of LHSimRes, RHSimRes, LHSimRes4, RHSimRes4, LHRes and RHRes	146
5.4	Sample synthesised pairs of signals	152

List of Tables

1.1	Some Typical Bioelectric Signals Sensed by Biopotential Electrodes and Their Sources [1], [2]p215	6
2.1	Static Error and Relative Accuracy for different input voltages	31
3.1	Occurrence of signals with specific polarity	53
3.2	Occurrence of trends and corresponding minimum Diff and maximum Diff of acquired biopotentials	56
3.3	Occurrence in % of trends in a pair of LH and RH signals	58
3.4	Occurrence of patterns in a pair of recorded biopotentials	62
3.5	Occurrence of derived signals with specific polarity	65
3.6	Occurrence of trends and corresponding minimum Diff and maximum Diff of derived signals	67
3.7	Basic statistical parameters of biopotentials	71
3.8	Subject-wise mean and span	74
3.9	Statistical parameters of Phase2 RH biopotentials	78
3.10	Chi-square test for ($Mean_{set}$) values	83
3.11	Statistical characteristics of setwise mean, $Mean_{set}$ of LH, RH, Gap and PS signals	84
3.12	Statistical characteristics of setwise standard deviations, SD_{set} of LH, RH, Gap and PS signals	85

4.1	Statistical characteristics of Deviation signals	104
4.2	Trends in Deviation signals	106
4.3	Occurrence, in % count, of Trends in LHdev and RHdev signals	107
4.4	Statistical characteristics of Zero Crossing Instant (ZCI)	116
4.5	Slopes m , in mV/instant, of fitted trendlines	119
4.6	Mean, Median and SD of the fit factor (R^2) for trendlines of all 4 Deviation signals	121
4.7	Instantaneous Residuals in mV	122
4.8	Occurrence of types of Pearson distribution for Residuals	125
4.9	% count of ZCI and m in the Deviation signals	128
4.10	Statistical characteristics of R_{ZCI2M2}^2	129
4.11	Statistical characteristics of Residuals $_{ZCI2M2}$	131
4.12	Type of Pearson distribution for Residuals $_{ZCI2M2}$ with % count	131
5.1	Parameter ranges for Trendline generation	144
5.2	Statistical characteristics of Residuals of synthesised and actual signals	147
5.3	Comparative Pearson distribution test results for Residuals of actual and synthesised signals	149

Chapter 1

Introduction

Biopotential signals are generated by the electrochemical activity of cells. Under normal steady state conditions, these cells exhibit a resting potential [3], while certain class of cells exist that are capable of generating action potentials on being stimulated. Biopotential signals such as Electroencephalogram (EEG) and Electrocardiogram (ECG) are the resultant of several action potentials produced by a combination of such cells [4]. It is known that the EEG measures the electrical activity of the brain, while the ECG is the measure of the electrical activity of the heart. On the other hand, passive reception of electrical activity of the dermal substrate is possible using the endosomatic method of measurement of electrodermal activity (EDA) [5](p79). Thus, a huge variety exists in the type of biopotentials that can be recorded from a human subject.

For measuring these signals, electrodes are placed on predefined locations in various parts of the body: on the scalp, near the brain, for the EEG; on the chest, in the vicinity of the heart, for the ECG; and typically on the arm or the fingers for the EDA. So, it is expected that while the EEG and the ECG biopotentials carry brain or heart specific information respectively, the EDA signals are likely to be free of such organ specific information.

Typically, the concept in the health industry was to determine the illness per-

taining to a particular organ [6] and then the treatment was done accordingly to restore the health of that specific organ. Various organ specific signals, in particular the ECG, have been well studied using this approach with numerous applications in the health industry. In essence, being healthy was an objective concept that meant stability and balance; wholeness or completeness and means to restore it [7], [8]. This notion of health has been superseded presently by the notion of wellness, which is defined by the World Health Organisation (WHO) as the optimal state of health of a human being [9], [10], [11]. This includes the physical, mental as well as social well being of the subject and several researchers are performing studies on these various aspects and their interrelations that substantiate this viewpoint [12], [13].

In the present study, the total human system has been treated as a holistic entity and its normal steady state behaviour has been studied using the non-organ specific and passive endosomatic EDA technique. The focus of this work is to acquire the EDA biopotentials from the healthy human system, and then to characterize them structurally and functionally. Thus, it is necessary to study the state of art in the aspects of electrical activities of cells and their relation to biopotentials; signal acquisition techniques of biopotentials; the non-organ specific studies used for monitoring the human condition; and the measurement of EDA signals.

1.1 Review of Literature

1.1.1 Electrical Activity in Human Systems

The origins of the biopotentials manifested by the various organs in the human body can be traced to the electrical activity at the cellular level [14], [15], [16]. The difference in ionic concentration across the cell membrane produces the resting potential [17]. Some of the cells in the body, like the heart muscles and brain cells, are excitable and produce an action potential. This action potential results from a rapid flux of ions across the cell membrane in response to an electric stimulation or

transient change in the electric gradient of the cell [18].

One characteristic feature of all living cells is the control of the flow of specific electrically charged ions across the cell membrane [19]. Bioelectricity influences cellular processes as fundamental as the control of the cell cycle, cell proliferation, cancer-cell migration, electrical signalling in the adult brain, embryonic neuronal cell migration, axon outgrowth, spinal-cord repair, epithelial wound repair, tissue regeneration and establishment of left-right body asymmetry [20]. It is well established that biological processes should be viewed as electrodynamic processes, as is done in the cases of electrocardiogram (ECG), electroencephalogram (EEG) and electromyogram (EMG) that record the activities of the specific organs and organ systems of heart, brain and muscles [19]. A study has also been reported on the influence of a special sound perception technique on the autonomic nervous system of healthy subjects by analyzing heart rate variability (HRV) derived from the ECG [21], [22]. On the other hand, the electrodermal activity (EDA), usually recorded as an exosomatic conductance response to low voltage electrical excitation [23], is the result of local processes in the skin and these have been primarily ascribed to submotor activity and the activity of sweat glands [2]p85. Some researchers ascribe the fast components of the recorded EDA to rapid membrane polarizations and depolarizations [24], [25].

Several early studies also exist on the potentials recorded using endosomatic EDA technique [26], [27], [2], [28], although detailed studies using multiple subjects and conditions are not available in several cases. In general, the electrical excitation of any cell generates currents in the surrounding volume conductor and this manifests itself as a potential at some location inside or on the body. However, a large proportion of these almost time-invariant, low amplitude cellular level signals are associated with phenomena that are yet to be used in clinical medicine [29].

Thus, there exists a scope for a detailed study of these generic EDA biopotentials and their characterisation.

1.1.2 Acquisition of Biopotentials

The recording of biopotentials requires a relatively simple transducer with a simple acquisition device. The unifying principles for acquisition of all types of biopotentials involve the following aspects:

1. Design of the transducer suitable for the application and its attachment to the acquisition device.
2. Signal processing unit like amplifier circuit design for suitable amplification of the signal and rejection of noise and interference.
3. Good measurement practices to mitigate artifacts, noise, and interferences.
4. Suitable recorder for recording and storing the data and in case of sophisticated devices, the provision of automatic analysis of the data and diagnosis.

The electrical conduction in the biologic medium is done by means of ions, while the conduction in the measurement system is by electrons. Thus, picking up biopotentials involves interacting with these ionic charge carriers and transducing the small ionic currents into electrical currents efficiently so that these can be processed using electronic instrumentation. The electrodes used for the purpose should have specialised characteristics that interface to the organ or a particular region of the body and transduce them into low-noise, artifact-free signals [30]. The design should be pragmatic to reduce cost and allow for good manufacturing and reliable long-term use. These practical considerations determine whether high quality but reusable electrodes made of silver or gold or cheaper disposable electrodes are used [31].

The conventional wet adhesive silver/silver chloride (Ag/AgCl) electrodes, used almost universally in clinical applications today, are known to produce the lowest and most stable junction potentials [32], [33]. These types of electrodes are chosen because they are almost perfectly non-polarisable with low impedance and low artifacts [2], [34]. They can be easily fabricated for use in many biomedical applications [14] and are recommended for measurements involving very low voltages.

The design of these electrodes consists of the highly conductive silver metal interfaced to its salt, silver chloride, and connected via an electrolytic gel to the human

body. Even for acquiring EDA signals, sintered silver/silver chloride (Ag/AgCl) electrodes are practically the only standard EDA electrodes in use in recent times [33]. Such electrodes display the smallest possible bias potentials and are nonpolarisable to a high degree [14]. Zinc/zinc sulfate (Zn/ZnS) electrodes and zinc/zinc chloride (Zn/ZnCl₂) are also known to be simple to construct nonpolarizable electrodes, but these are not commercially viable or recommended because of problems with the exact composition for an adequate electrode cream as well as with their maintenance [33], [35]. However, it is known that measurement of EDA biopotentials has the major advantage that polarizability of the electrodes does not affect the measurement [2].

In the present work, sintered Ag/AgCl wet electrodes have been used for acquiring the EDA biopotentials from the human subjects.

The next aspect is the choice of suitable signal processing circuits that can extract the low level biopotential signals from the human body efficiently as it is known that the EDA biopotentials recorded from the human body are in the millivolt range [28](p97). In order to do so, it is necessary to know some preliminary details, like the typical range and frequency, of the biopotentials to be measured. The typical characteristics of biopotentials recorded from different organs are tabulated in Table 1.1 [1], [2]p215. It must be noted here that the skin potential level (SPL) is only one of the several signals grouped in the class of EDA signals. It is observed from this Table that the amplitudes of biopotentials are typically in the range of 10 μ V to hundreds of mV, while the frequency of these signals vary from dc to several hundred Hz [15], [36].

The most noteworthy problems of acquisitions of low voltage are the presence of biological interference (from skin, electrodes, motion, etc.) and noise from environmental sources (power line, radio frequency, electromagnetic, etc.) [2]p140. Theoretically, there should be no interference between channels of the recording device

if these involve direct connections between differential amplifiers and pairs of electrodes. However, in practice, it is observed that interfering factors arise in such scenarios [27] and so, the use of multiple circuits before acquisition are likely to change the signal levels.

Table 1.1: Some Typical Bioelectric Signals Sensed by Biopotential Electrodes and Their Sources [1], [2]p215

Bioelectric Signal	Abbreviation	Biologic Source	Frequency range(Hz)	Dynamic range
Electro-cardiogram	ECG	Heart surface	0.05-100	1 – 10mV
Electro-myogram	EMG	Muscle	500-10000	1 – 10 μ V
Electro-encephalogram	EEG	Brain surface	0.5-100	2 – 100 μ V
Electro-oculogram	EOG	Eye-dipole field	dc-100	10 μ V – 5mV
Electro-retinogram	ERG	Eye-retina	0.2-200	0.5 μ V – 1mV
Skin Potential Level	EDA	Skin		10mV – (-70)mV
Action Potential	-	Nerve or muscle	100-2000	10 μ V – 100mV

In the present work, direct differential measurements have been taken using suitable meters for recording the actual signals from the skin, as per the guidelines stated in [27].

In conventional clinical biological signal measurement systems, it was preferable to store the data in the next stage, prior to its analysis and subsequent diagnosis [27]. However, presently, unconstrained biological signal monitoring is emerging as an alternative where the principal goal is to sustainably monitor health related information through biological signals without interrupting the subjects ordinary daily activities and without requiring additional operations or cooperation in order to make signal measurements. This method enables daily recording of normal health status, and application of these data for health care purposes with minimal inconvenience to the patient. Eventually, the huge amount of data gathered from unconstrained continuous monitoring would be used to understand daily changes in health information that occur in response to disease, medication, infection, or stress [37].

In the present work, however, unconstrained data acquisition has not been done. Instead, the data has been recorded into a laptop for its subsequent study and characterization.

Generally, studies with humans or animals involve a control group and one or more intervention group(s) to study the effect of a single or multiple intervention(s) done on the other group(s) with reference to the results obtained for the control group [38], [39], [40]. In certain rare cases, studies on single subjects are also done, as in the case of a magnetoencephalographic study of the brain to observe the effect of gyrosound on a single subject [41]. Another type of study involves the whole community, like a study of community-based prevention of coronary heart disease [42]. However, in a few instances, some specific studies have also been done by researchers while considering only healthy subjects [21], [22], [43].

In the present work, biopotentials have been acquired from several healthy human subjects as a single large group, without considering a separate control group and one or more additional groups.

1.1.3 Non-organ Specific Studies of the Human System

As mentioned earlier, WHO presently defines health as a state of complete physical, mental, and social well-being and not merely the absence of disease or infirmity [44], [10], [45], [46]. It can be interpreted that in every healthy individual, a complex dynamic process successfully adapts and maintains the required biological stability of the human system in the midst of ever-changing conditions. It has been established that structurally, a complex system might be made up of a large number of simpler components, or it might be formed from hierarchies of smaller numbers of interacting subsystems, whose functional behaviour is more than a mere sum of the parts [47], [48]. It can thus be inferred that the overall adaptability of the complex human system depends on the health of the individual organs and organ systems, yet is not a mere sum of these individual components. Several researchers engage in the tasks of studying the trends, regression fits, statistical characteristics as well as feature identification of these biosignals [49], [50] with the objective of characterizing certain specific conditions of the organ or organ systems. Studies have also been reported on decoding and eventual modeling of specific biological systems using recorded signals [51]. However, similar research into the non-organ specific signals are still in the nascent stage.

Thus, there exists a scope to analyze the structural complexity in some generic signals recorded from the human system using standard signal analysis techniques and to relate it to the expected functional variations manifested in the recorded signals.

Certain clinical parameter measurements and biochemical assays are used to monitor (detect or estimate) specific pathological/physiological states for purposes of diagnosis and evaluating therapy. The measurement of various clinical parameters like blood pressure [52], [53], [54], oxygen saturation level, pulse rate [55], [56], photoplethysmogram [57], [58], [59], [60] and body temperature [61] are used to monitor the overall condition of the body. As mentioned earlier, various biochemical assays

are also used to monitor different conditions. Auto-immune diseases are monitored using tests like Ig testing, HLA profiling, ELISA test; allergy to various allergens are tested by assessing the IgE level; while the most common routine examination is the complete haemogram [62].

Some researchers have used electrical measurements to study the functional aspects of certain non-organ specific biomedical processes. Detection and measurement of small potential differences are used for the detection of ovulation, oestrous cycle, menopause and pregnancy in mammals [63]. Surface electromyography, which infers the pattern of production of force by skeletal muscles, has been used for diagnosing low back pain [64]. The interpretation of muscle function from the electromyogram (EMG) is challenged by the fact that factors such as type of muscle fiber, muscle length, and muscle velocity can all influence the relationship between electrical and mechanical activity of a muscle [65]. There are also studies that various types of EDA signals are good indicators of pain [43], generalized anxiety, panic disorders, emotional changes as well as neurological or physiological arousal [66] [67], [2], [28], [68].

The human system is known to exhibit morphological as well as functional bilaterality with respect to the sagittal plane [69], [70], [71]. Researchers have studied the bilateral symmetry to identify health related characteristics [72], to detect calm/distress conditions [73], to investigate human performance [74], to differentiate left and right-handedness [75], to investigate the relationships of excitatory and inhibitory circuits of the left vs. right primary motor cortex with peripheral electrodermal activity (EDA) [76] and also human infirmities [77]. Indices like BSI [78] and BBSI [79] have also been proposed to study the bilateral symmetry of brain signals. Studies on cerebral asymmetry have been used to explain a large variety of behaviours, like reading disability, schizophrenia, stuttering, gender-related difference in spatial ability, infantile autism, generation gap; as well as to review the evidence pertaining to cerebral asymmetries in the intact human brain. [80]. A study using GSR measurements reports the stabilization effects of a specific sound signal

on the left and right hemispheric brain signaling in psychosomatic patients with healthy subjects as a control group [81]. However, the general characterization of the bilaterality of these signals have not been properly established.

Thus, there exists a scope to study the effect of bilaterality in the structural and functional organization of EDA biopotentials.

1.1.4 Measurement of Electrodermal Activity (EDA)

There are two approaches of measurement of EDA: endosomatic and exosomatic. The endosomatic recordings do not use an external current, since only potential differences originating in the skin itself are recorded [2], [23]. Methods of exosomatic recording apply either direct current (DC) or alternating current (AC) to the skin [82]. In DC measurement, if voltage is kept constant, EDA is recorded directly in skin conductance (SC) units, while skin resistance (SR) units are obtained when current is kept constant. Accordingly, if effective voltage is kept constant in AC measurement, EDA is recorded directly as skin admittance (SY), while the appliance of constant effective current results in skin impedance (SZ) recordings [83]. The exosomatic DC recording, which involves applying electrical signals to the subjects, is by far the most commonly used method [2]. On the other hand, the endosomatic method of measurement of EDA consists of passive reception of electrical activity of the dermal substrate [5](p79).

In the present work, the endosomatic EDA technique is adopted, which has the advantage that it is non-invasive and does not involve any electrical stimulation of the subject. Moreover, the measurement is taken from two extreme ends of the body i.e, two fingers of each hand of the human body and thereby it is assumed that there is no major organ overlay on these measurements and therefore the measurement is non-organ specific.

It has been reported [28] that the usefulness of electrodermal measures depends in a major way upon technical aspects of methodology, like subject selection, experimenter, and environmental variables, and these require prior consideration [84]. The study variables considered for subject selection typically include age, sex, race and also characteristics that affect any possible interaction with the experimenter [28]p49. On the other hand, specifications of the environment of the experiments involve the physical aspects such as temperature or humidity [85], which could have direct effects on electrodermal phenomena; and also consideration of its social aspects such as experimenter behavior and interactions with subjects, which could have a range of indirect effects on electrodermal phenomena [28]p49, [86], [87], [88], [89], [90]. It is known that familiarity of the subject with the experimental environment and procedure reduces the experimental stress on the subject. Such repeated testing also allows the experimenter to become familiar with the subjects' characteristic physiological profiles, including the recordable electrodermal levels. In such scenarios, the appearance of an atypical record often provides valuable leads for future research. Hence, it is suggested by Venables and Christie [28]p56 that care must be taken to retain equipment and furniture in identical positions; constant heat, humidity, and noise levels should be maintained and a low-level illumination, rather than total darkness, should be maintained so that subjects may relax completely.

In this study, emphasis has been given to the subject selection criteria, format of interactions with the experimenter and to the proper design of the experimental study environment and setup.

The choice of location of electrodes, area of contact and use of electrolyte may also affect the EDA signals [2]p115. The usual practice in case of endosomatic recordings is to use an active and an inactive site, while two active sites are used for exosomatic recordings [2]. Most researchers make use of the palms or the volar surfaces of the fingers as active sites for electrodermal recording. Venables and Christie (1980) [91]

recommended the medial phalanges of the index and middle fingers for bipolar placement of electrodes. This placement appears to have minimum interference and no preparation of the skin site is required other than washing [28]. Furthermore, the medial phalanges are less prone to scarring and to movement effects than the proximal ones, and the distal phalanges as well as the phalanges of other fingers provide smaller areas for electrode fixing [2]. It is, however, important that the two active sites should be on the same limb, otherwise heart artifact will be apparent.

In the present case, bipolar placement of electrodes on the suggested two active sites, medial phalanges of the index and middle fingers, of both hands has been used for endosomatic EDA recordings. A pair of such electrodes have been used on both hands of the subject for simultaneous measurement, since the effect of bilaterality is to be studied.

1.2 Aim and Organisation of the Thesis

The aim of this study is to determine the qualitative and quantitative features and parameters of biopotentials that are measured simultaneously from both hands of healthy human subjects using endosomatic EDA technique. These are to be used to characterise healthy human subjects at rest and to devise a procedure using a minimal set of the identified parameters to synthesise realistic pairs of biopotentials.

Accordingly, the subsequent chapters of the thesis have been organised as follows.

The conditions and methodology to acquire human biopotentials is stated in Chapter 2. The introduction to this Chapter is stated in Section 2.1. The details of the specific conditions in terms of the subject selection criteria, the environmental conditions and the experimental technique are described in Section 2.2. The instrumentation system used is described in detail in Section 2.3. This includes the

details of its static characteristics, which are determined in order to ascertain the compatibility of the system and the sensors used for the specific application. The methodology used for the acquisition of the biopotentials is described in Section 2.4. This includes the protocols to be maintained, the procedure for acquiring the biopotentials and the health parameters which are measured initially and in every session. The endosomatic EDA signals are acquired passively from both hands of various human subjects while the subject is at rest without any external disturbance. Details of the acquisition of these signals in two phases, Phase1 and Phase2, in which the duration of the rest has been altered, has also been stated in this Section. The Chapter discussions are stated in Section 2.5.

The focus of Chapter 3 is to analyze all the passively measured biopotentials from left hand (LH) and right hand (RH) with the objective of identifying certain qualitative and quantitative attributes of these signals. The introduction to this Chapter is stated in Section 3.1, followed by the qualitative analysis of the signals in both phases in Section 3.2. This includes the description of the general characteristics of the acquired LH and RH signals in Section 3.2.1. This is followed by the characterisation and determination of the prevalence of the possible polarities and trends of the individual LH and RH signals in Section 3.2.2 and of the possible patterns in the pairs of LH and RH signals in Section 3.2.3. It has been observed that the measured LH and RH signals are time varying and yet they vary within a certain range. This feature has been interpreted in terms of their interdependence and two new derived signals, Gap and Pair sum (PS) signals, have been proposed to study this aspect in Section 3.2.4. The study of the polarities and trends of these new signals have also been provided in this Section in a manner similar to that for the individual LH and RH signals. The quantitative statistical analysis of the individual as well as the derived signals in both phases are stated in Section 3.3. This is done at an overall level in Section 3.3.1, followed by a subjectwise analysis in Section 3.3.2. In both these studies, an anomaly is observed in the RH signals in Phase2, which is analysed

in detail in Section 3.3.3. This is followed by the setwise analysis of all data in both phases in Section 3.3.4. The Chapter discussions are stated in Section 3.4.

The analysis in Section 3.3.4 indicates that the setwise mean is a characteristic feature of any acquired or derived signal.

Chapter 4 deals with the subsequent analysis of the Deviation signals for all four types of signals, which are obtained by subtracting the setwise mean values from each of the time-series signals. The Chapter introduction is stated in Section 4.1. The general characteristics of all four types of Deviation signals, including their statistical characteristics, are described in Section 4.2. The trends of these Deviation signals are studied in detail in Section 4.2.1, while this is followed by a detailed study of the pairs of LH and RH Deviation signals in Section 4.2.2.

This study is followed by the modelling of the Deviation signals in terms of the zero crossing instant (ZCI) of the signals, the slope (m) of the fitted trendline and the stochastic instantaneous Residuals in Section 4.3. The detailed statistical analysis of the validity of the regression model is provided in Section 4.4 in terms of the characteristics of the ZCI, the m as well as the Residuals for all data sets in both phases. Thereafter, the interrelationship between ZCI and m has been explored in Section 4.5 with supporting statistical analysis of the parameters ZCI, m and Residuals in the identified common class ZCI2M2. The Chapter discussions are stated in Section 4.6.

Chapter 5 deals with the synthesis of a pair of LH and RH biopotentials. The introduction to this Chapter is stated in Section 5.1. From the signal features and parameters identified in Chapter 3 and Chapter 4, a minimal set of deterministic and stochastic parameters, which are required for the synthesis of any realistic pair of LH and RH biopotentials, is identified in Section 5.2. The procedure for synthesis of the LH and RH biopotentials using the representative features is discussed in Section 5.3 and this is validated in Section 5.4 for signals in the class ZCI2M2 in both phases.

The validation is done in two stages: quantitative and qualitative. The quantitative analysis is stated in Section 5.4.1 in order to establish the structural components of the pair of signals. Thereafter, a qualitative study of the generated signals has been done in Section 5.4.2 to ascertain the functional similarity of the synthesized realistic signals with the acquired signals. The Chapter discussions are stated in Section 5.5.

Chapter 6 contains the conclusions of the study in Section 6.1, while the scope for future work is stated in Section 6.2.

1.3 List of Contributions

1. The proforma as well as the conditions to be used for this experimental study, conducted in two phases, has been meticulously and independently designed, as mentioned in Section 2.2.
2. A simple, yet safe, instrumentation system was devised without any additional filter or filtering technique for recording data for this human study, as mentioned in Section 2.3, and the compatibility of the system with the sensors was ensured for this application, as discussed in Section 2.3.3.
3. The time-series signals measured from left and right hands (LH and RH) of human subjects have been characterised individually in terms of their general nature; Positive, Negative or Transitive polarity; Increasing, Decreasing or Constant trends; as well as their general statistical characteristics. The pairs of signals have also been characterized in terms of their possible patterns, namely Converging, Diverging, Parallel or Crossing. These are discussed in Section 3.2, Section 3.3 and Section 3.2.3 respectively.
4. Two new signals, the Gap signal and the Pair Sum (PS) signal, have been proposed and studied to explore the interdependence between the LH and RH signals, as mentioned in Section 3.2.4.

5. The effect of short and extended durations of rest, as studied in Phase1 and Phase2 respectively, on a pair of bilateral endosomatic EDA signals has been established, both qualitatively and quantitatively in Section 3.2 and in Section 3.3. It is established that the longer duration of rest in Phase2 data sets corroborates with a significant increase in the counts of Negative polarity and Constant trend mentioned in Section 3.2.2 and also the Parallel pairs of signals are significantly more in Phase2 as mentioned in Section 3.2.3.
6. The mean value of an acquired or derived time series signal, termed as its setwise mean ($Mean_{set}$), has been established to be its representative static feature in both types of measurement scenarios for all subjects, as detailed in Section 3.3.4. Subsequently, Deviation signals, obtained by subtracting the $Mean_{set}$ from each signal, have been proposed and studied in Section 4.2 to explore the time-series nature of all types of signals. These Deviation signals have been modeled using a linear regression model, as mentioned in Section 4.3. For this, a new parameter, Zero Crossing Instant (ZCI), of the Deviation signal has been proposed and the corresponding slope (m) of the trendline has been fitted through ZCI. It is established that the model, which has been validated for all Deviation signals in Section 4.4, has stochastic Residuals.
7. It has been established that most of the Deviation signals can be well represented by trendlines with ZCI and slope (m) values belonging to a restricted class, ZCI2M2, and associated Residuals belonging to a 4 parameter beta distribution in a limited range. This is detailed in Section 4.5.
8. A procedure has been proposed and established in this study to synthesise a realistic pair of LH and RH signals using a upper deterministic mean cum stochastic Residual layer and an inner deterministic Deviation signal layer. This is detailed in Section 5.3.
9. It has been established that a simple two layer structural hierarchy leads to the plethora of functional complexity observed in the endosomatic EDA biopotential

tials recorded simultaneously from the left and right hand of human subjects, mentioned in Section 5.4.

Chapter 2

Conditions and Methodology for acquiring Human Biopotentials

2.1 Introduction

This chapter deals with the conditions under which the biopotentials of the human body have been acquired and the methodology that has been adopted to record these signals. The inclusion and exclusion criteria for the human subjects needed special consideration since the objective is to study healthy subjects. Thereafter, the locations on their body from where the signals have been acquired also required some consideration since it is known that these non-organ specific EDA biopotentials from the human body are in the millivolt range [28](p97).

The prime objective of this work is to acquire the low voltage endosomatic EDA signals in inherent raw form without any use of filter or signal conditioning circuits. This is done without any external excitation to the healthy human subject in order to record the signals truthfully with minimal processing. In order to record these biopotentials and thereafter, to capture the inherent characteristics of the human system, a proper instrumentation system is selected and its characteristics has been studied in details. It is also essential that there is minimum disturbance imposed on

the subject and in the acquisition system. So, it was necessary to maintain similar conditions of the subject(s) as well as the environment. Here, healthy subject means the subject who is generally fit and well without, or with, medication and is present at his/her respective tasks in the institute as a student, faculty, staff or research scholar.

The chapter is organised as follows. The conditions specified for all experimental studies are stated in Section 2.2. The instrumentation system used is specified in Section 2.3, along with the details of its static characteristics in Section 2.3.3. The methodology adopted for these studies is described in Section 2.4 and the discussions are stated in Section 2.5.

2.2 Conditions specified for experiment

It is well known that any signal acquired from a single or multiple human subject(s) at different times are not identical and differ from each other, leading to large diversity in nature. In this study, this diversity is considered as an essential feature of the human system and is of prime interest. In order to ensure that this diversity is attributable primarily to internal causes only, some standard conditions have been maintained in terms of subject selection, environment of experiments and the technique used for the data acquisition.

It is known that familiarity of the subject with the experimental environment and procedure reduces the experimental stress on the subject, while maintaining an identical environment with equipment and furniture in identical positions; constant heat, humidity, and noise levels and a low-level illumination allow the subjects to relax completely [28]p59.

The details of these aspects, as maintained in the present study, have been stated hereafter.

2.2.1 Subject selection

- **Population:** Subjects present and available in the Jadavpur University, Salt Lake campus, Kolkata, India.
- **Inclusion criterion:** Subjects of either sex, of age within 20 to 60 years, who are apparently healthy [44], [10], [45], [46], and who gave informed consent.
- **Exclusion criterion:** Subjects with known psychiatric illness or who are institutionalized, cognitively impaired, seriously ill people, pregnant women, minors, prisoners and those who did not give consent.
- **Study Variables:** The selected subjects considered belong to the following groups
 - a) Age - 20 to 58 years
 - b) Sex - both male and female
 - c) Weight-55 to 90 kgs
 - d) Height - 148 to 180 cms
 - e) Residency- both urban and rural localities in eastern part of India
 - f) Family - both nuclear and joint
 - g) Education - Higher secondary and above
 - h) Occupation - skilled workers, academicians and students
 - i) Addiction - Smoking and betel (paan) chewing in some cases, no alcohol or narcotics addiction
 - j) Medical comorbidities - Persons with hypertension [92], diabetes mellitus [93], high cholesterol [94] and thyroid [95].

2.2.2 Environment of experiments

- **Study Area:** A research laboratory in the Department of Instrumentation and Electronics Engineering, Jadavpur University, Salt Lake Campus, Kolkata, India.
- **Location used:** A bed is kept in a closed environment inside the research laboratory, aligned with the geographical North-South, with the placement of the head of the subject towards the North. This bed location and the subject alignment are kept fixed for all recordings.
- **Environment:** The closed cubicle is well ventilated, low lit, silent and the temperature and humidity are maintained at comfortable levels using air-conditioners at particular settings.

2.2.3 Technique used

- **Materials and methods** [96]
 - a) Type of study - Observational analytical: The observations from a fixed number of human subjects are acquired using suitable non-invasive, contact type, passive sensors and these recorded data are studied analytically.
 - b) Study design - Longitudinal: Data have been acquired repeatedly from each of the subjects over a certain period of time.
- **Instrumentation System used:** The measurement system used is explained in Section 2.3. The static characteristics of this system has been analyzed to ensure the compatibility of the system with the sensor.
- **Methodology used:** The experimental methodology used is detailed in Section 2.4. The protocols used, the location of electrodes, conditions of the subjects maintained at every recording and the other health parameters recorded are stated in this Section.

- **Subject sampling technique:** The subject sampling technique used is non-randomised purposive, in which the subjects were chosen as per their availability and convenience with mutual consent regarding the time, duration and tenure of the experimental work.
- **Study tools:** A structured proforma has been designed in the first stage on the basis of similar study materials and preliminary trials. This pretested proforma has been followed for a set of studies. Thereafter, it has been suitably modified based on the previous records and objectives of the work. This second proforma has then been followed for another set of studies.
- **Study technique:** The subjects were placed in supine position in controlled environment with simultaneous continuous measurement of biopotentials from a pair of fingers of both the hands.
- **Sample size:** Study done in two phases with 16 subjects in Phase1 and 14 subjects in Phase2 during different times of the year.

2.3 Instrumentation System

The instrumentation system has been used to acquire the endosomatic EDA biopotentials from an easily accessible location and to store the data for offline analysis. The details of this system are discussed hereafter. In order to ensure its suitability for the desired purpose, the static characteristics of this system has also been studied and this is stated subsequently in this Section.

2.3.1 Measurement procedure:

As shown in Figure 2.1, the input signals are taken from two designated fingers of each hand of the human subject using electrodes which are connected via cables to the respective multimeters. A pair of left hand electrodes are connected to one

multimeter, while the pair of right hand electrodes are connected to another multimeter (Figure 2.11) as detailed in Section 2.4.2. Two adapters are attached to the two multimeters which are kept in DC mode and are switched to online data transmission mode during measurement. The addresses of the adapters are provided manually for communication prior to transmission of signals from each hand. The adapters transfer the data received from the multimeters to the laptop over RS 232 serial interface. The data values are obtained in datalogger form and are stored in the laptop for further analysis.

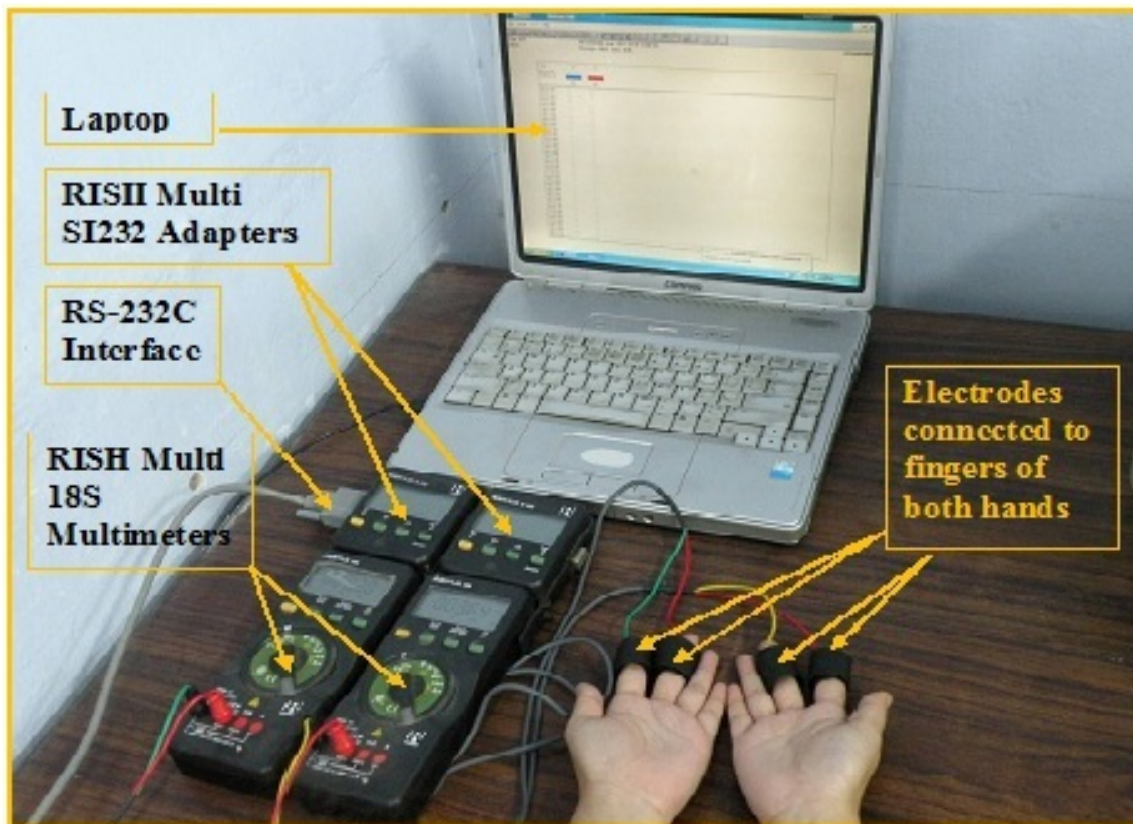


Figure 2.1: Data acquisition setup showing both hands fitted with electrodes connected to multimeter and connection of multimeter to adapter

2.3.2 Building blocks

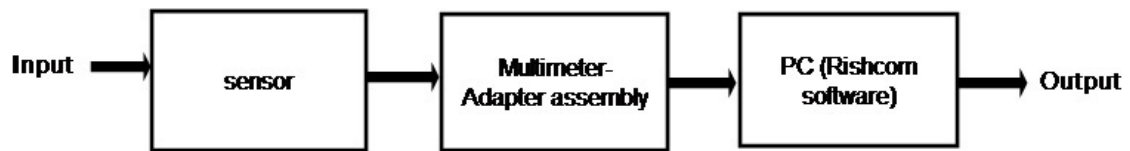


Figure 2.2: Schematic block diagram of the instrumentation system

The instrumentation system thus essentially comprises of three blocks, which are shown in Figure 2.2. The details of the input, the component blocks and typical output are described hereafter.

- **Input:** The input signal is a differential bioelectrical potential, which is recorded from the skin surface of the human body. This is chosen as the input because it is passive and non-invasive. The locations of the placement of the sensors are the skin surface of a pair of fingers from both hands. This is chosen because this location is easily accessible and at two of the extreme ends of the body.
- **Sensor:** The bio-potentials from both hands are measured using identical pairs of sensor electrodes connected to a pair of fingers on each hand. The sensors used are wet silver-silver chloride (Ag-AgCl) electrodes, typically electrodes, which are recommended for measurements involving very low voltages [32], [14], [33], [14]. The wet electrodes use a gel type electrolyte between the electrode and the surface of the skin, thus providing the necessary interface between the skin surface and the electronic measuring apparatus as detailed in Section 2.4.2.
- **Multimeter:** A pair of digital multimeters (Make: Rishabh Instruments, model-RISH Multi 18S) [97], [98] are used to acquire the sensor voltages from both hands. Connection of (i) both hands fitted with electrodes and multimeter and ii) connection of multimeter and adapter are shown in the Figure 2.1. The RISH Multi 18S multimeter has 5 ranges of measurement for potentials. The

range and the resolution are automatically selected in the multimeter depending on the measured value. The multimeter output is displayed or transmitted after every 10th measured value.

In the present study, a pair of electrodes from one hand are connected in differential mode to the input terminals of each multimeter as mentioned in Section 2.4.2. This ensures that the common mode signals in the multimeters get attenuated to levels $>120\text{dB}$, effectively nullifying them. The meter is also inherently compensated for power line interference.

The RISH Multi 18S multimeter sends out the interface signals with every measurement and 20 data packets are transmitted per second [99](Section 6.3, page22). This means sampling frequency is 20Hz in terms of data packets. Here, each data packet refers to each measured voltage value represented as a 6 bit data and 20 such voltage values are transmitted per second.

- **Adapter:** Each RISH Multi SI232 storage adapter is attached to a Rish Multi 18S multimeter using their respective male-female connectors. This arrangement permits the optically isolated transmission of measured data from multimeter to adapter. In this study, two Rish Multi 18S multimeters are cascaded with two RISH Multi SI232 adapters and each of the measurement values from each multimeter is transmitted via infrared light to the SI 232 storage adapter through the closed, electrically isolated RISH Multi housing. This, thus, ensures the safety of the subject from any exposure to current more than 5mA, which is harmful for human beings [100]. The device is provided with safety extra-low voltage as per DIN VDE 0411 for electrical safety. The data is synchronized by an integrated clock for real time applications [98].
- **PC with serial interface:** The RISH Multi SI232 storage adapters are connected via a serial RS-232C interface cable to a dedicated PC for transmission of the measured values. Nearly all parameters for this connection can be set either manually or from the PC using the interfacing RISHCOM100 software.

This software is used for the processing and representation of the measured data. In online mode, the adapter transfers data received from the multimeters to the PC. The software allows for the recording of the acquired data which is continuously shown on the monitor. A maximum of 2 lakh samples can be measured in a single set.

RISH Multi SI232 adapter has an LCD-segment-display unit and 4 keys for configuration settings. The four keys used are the yellow colored ESC key and three green keys, namely ON/OFF or ENTER-Key, UP-Key and DOWN-Key. ESC-Key is used for escaping from the respective menu level used at the time and returning to the next higher menu level. ON/OFF or ENTER Key is used for switching on/off and for input acknowledgement of menu item. UP-Key is used for choosing single menu items in the direction of flow and for increasing values and DOWN-Key is used for choosing single menu items against the direction of flow and for decreasing values.

For online transmission of the measured signals, the multimeters are switched to data transmission mode by pressing the DATA and ON buttons simultaneously. Before anything is transmitted to the PC, the address of the memory adapter is set and the adapter is adjusted to the transmission mode. For this the ON/OFF Key is pressed and then by pressing the UP-Key twice, the display address is obtained and then again ENTER-Key is pressed. Thereafter, the address is set by suitable pressing of the UP-Key and DOWN-Key followed by ENTER-Key for confirmation. Then, the PC is switched on and the software program is started. The memory adapters are addressed via the serial interface and a bidirectional connection is automatically established with the PC.

In the sub-menu Setup/Channels, the appropriate interface is set as serial link and the number of channels to be displayed is selected as 2 for both hands. Then, for performing the measurement, Setup/Memory Adapters is clicked and all the connected adapters are switched into online mode. Thereafter, the measurement values are transmitted to the PC by selecting File/Measuring

and displayed as selected in the Setup menu [101].

In the present case, two RISH Multi 18S multimeters are connected to two RISH Multi SI232 adapters, one each for the two hands, as shown in Figure 2.1. The sampling time is set at 50ms to ensure maximum storage of data. In order to facilitate online direct transmission of the measured data from the multimeters to PC, each adapter is manually provided with a specific address for communication. The two storage adapters are connected to each other via one of the two inbuilt RS 232C interface ports available on each device. The inbuilt multiplexer communicates and stores the data in a laptop or a desktop PC in an EXCEL file. In this study, a laptop is used in place of a desktop PC and the acquisition system is operated with batteries in order to enhance subject safety.

- **Output:** As mentioned earlier, a number of sets of biopotentials were preliminarily acquired at random times from a number of subjects in order to decide the sensing scheme to be used for all studies and to ascertain the suitability of the range and resolution of the instrumentation system for recording the data. Figure 2.3 shows two sample recordings of a pair of signals using this system, wherein the lines shown in blue and red signify the signals from left hand (LH) and right hand (RH) respectively and a set means 2400 samples of biopotentials acquired from each hand of the subjects in 2 minutes. Since the sampling frequency is 20 Hz, hence the sampling time is 50ms. Thus, the 400th sample corresponds to 20s ($= 400 \times 50/1000$) and so on with 2400 instants corresponding to 120s of elapsed time.

From the signals tested, it was seen that the signal levels of the various sets of data vary between $\pm 300\text{mV}$ but in a particular set, the signals vary only slightly from a mean value, typically a few tens of millivolts. This passively acquired signal, which is about three times of the standard action potentials (-65mV) and/or resting membrane potential of large nerves (-90mV) [102], can thus be considered as a baseline potential with a slowly varying nature, which

needs to be characterized independently.

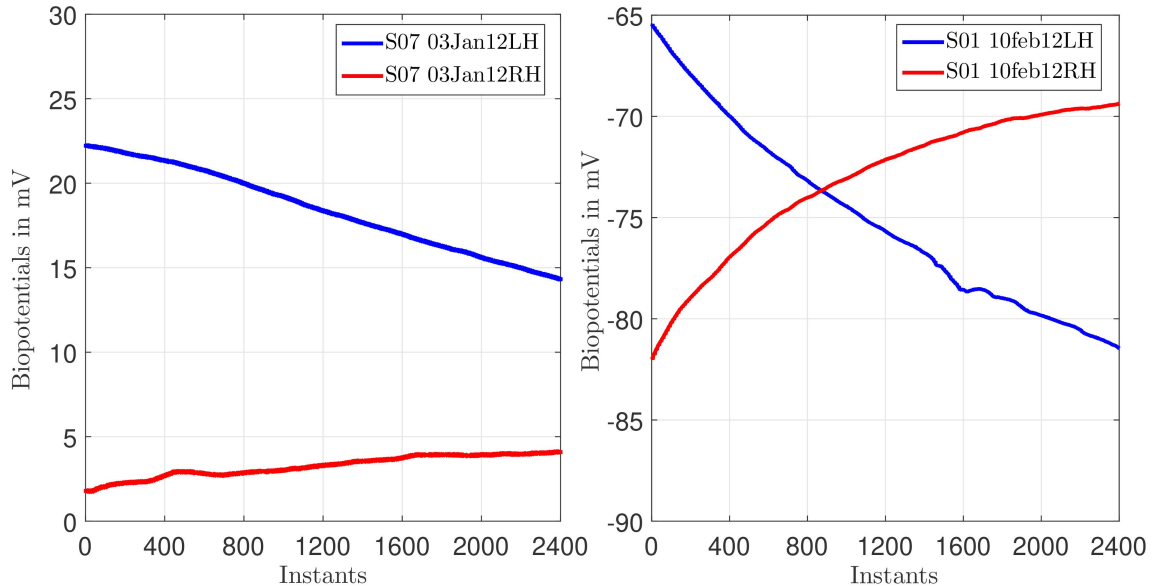


Figure 2.3: Representative biopotentials acquired from human fingers of each hand for two subjects (LH-left hand in blue, RH-right hand in red)

2.3.3 Static characteristics

These slowly changing biopotentials have been acquired in the multimeter in the dc mode since no explicit external input is applied to the subjects. Hence, it was essential to study the static characteristics of the instrumentation system for the aforementioned range of inputs, specifically $\pm 300\text{mV}$, prior to the systematic acquisition and characterization of the biopotentials from various human subjects.

In the multimeter, the range is automatically selected depending on the measured value and as per the specification of the meter, the resolution in the range of $\pm 300\text{mV}$ is $10\mu\text{V}$. The performance of the sensing system has been characterized in terms of accuracy, precision, linearity, sensitivity and drift in time, also referred as baseline

wander [103], [19]. For this purpose, the outputs of the instrumentation system to standard static inputs have been recorded.

2.3.3.1 Data acquisition of static inputs

Constant voltages of various magnitudes, as given in Table 2.1, within $\pm 300\text{mV}$ have been applied as an input to Rish-Multi 18S multimeters from a standard digital millivolt calibrator (Libratherm make, Model-LC-05). It is to be noted that in order to apply negative voltages, the terminals have been reversed. The calibrator provides a resolution of 0.01mV , when used in the range 00.00 to 60.00mV , while the resolution is 1mV in the range setting 0 to 10V . The stated overall accuracy is better than $\pm 0.2\%$ of the range used [97].

As mentioned earlier, the Rish-Multi 18S multimeter is used in dc mode [5](p80). Its sampling frequency is set at 20Hz , yielding a sampling time of 50ms , throughout the experiment. Each multimeter has been used along with its adapter to record the data for a typical duration of 120s . Data from a pair of multimeters have been acquired as a set of 2400 data samples, which have been stored in a laptop. The multimeter readings have been recorded repeatedly in increasing and decreasing order for 10 times for each input value ranging from -300mV to $+300\text{mV}$. The standard input voltages have been considered here as true values (TV) and the acquired voltages have been considered as measured values (MV). The same calibration procedure has been followed for every input voltage.

2.3.3.2 Accuracy

In this study, identical electrodes are used as sensors on both fingers of both hands for acquisition of the signals. A pair of multimeters measure the differential voltage between two fingers of a hand in dc mode, thus minimizing the common mode signals. The overall accuracy of the instrumentation system comprising of the sensors, the meters and the adapters have been studied in this scenario and their static error and relative accuracy have been determined.

Table 2.1: Static Error and Relative Accuracy for different input voltages

True value mV	Measured value (mean) mV	Static Error			Mean Relative Accuracy $\%RA_{fsd}$
		Min mV	Max mV	Mean mV	
-300.00	-299.83	0.14	0.19	0.17	100.03
-200.00	-199.65	0.32	0.37	0.35	100.06
-100.00	-99.75	0.23	0.28	0.25	100.04
-50.00	-49.88	0.10	0.15	0.13	100.02
-25.00	-24.88	0.11	0.14	0.13	100.02
-10.00	-9.9	0.09	0.11	0.10	100.02
-2.00	-1.91	0.08	0.11	0.09	100.02
-1.00	-0.92	0.07	0.10	0.08	100.01
-0.50	-0.47	0.01	0.05	0.03	100.01
-0.20	-0.18	0.00	0.04	0.02	100.00
-0.10	-0.07	0.02	0.05	0.03	100.01
-0.05	-0.02	0.01	0.04	0.03	100.00
-0.02	0.00	0.00	0.05	0.02	100.00
-0.01	0.01	0.00	0.04	0.02	100.00
0.00	0.03	0.02	0.05	0.03	100.01
0.01	0.04	0.02	0.05	0.03	100.01
0.02	0.05	0.01	0.04	0.03	100.00
0.05	0.08	0.01	0.05	0.03	100.00
0.10	0.13	0.01	0.05	0.03	100.00
0.20	0.23	0.01	0.05	0.03	100.01
0.50	0.52	-0.01	0.04	0.02	100.00
1.00	1.08	0.06	0.09	0.08	100.01
2.00	2.07	0.05	0.08	0.07	100.01
10.00	10.04	0.02	0.06	0.04	100.01
25.00	25.00	-0.02	0.02	-0.00	100.00
50.00	49.97	-0.05	-0.01	-0.03	99.99
100.00	99.81	-0.22	-0.17	-0.19	99.97
200.00	199.55	-0.52	-0.42	-0.45	99.93
300.00	299.57	-0.47	-0.40	-0.43	99.93

Static error (SE) is defined as the difference between TV and MV [104] [105], while the corresponding terms, relative error and % relative accuracy in terms of the full scale deflection (fsd) [106] are defined as follows:

$$\text{Relative Error (RE)} = \frac{SE}{TV} = \frac{TV-MV}{TV}$$

$$\% \text{ Relative Accuracy with respect to fsd, } \%RA_{fsd} = \frac{TV-MV}{fsd} \times 100\%$$

For each input voltage, the mean of the measured values for all the 24000 samples acquired over 10 sets of reading and the corresponding mean static error has been calculated. The mean $\%RA_{fsd}$ at each input voltage has been calculated considering the mean static error and the fsd . The fsd is considered to be 300 in this case. The mean of the measured values, the minimum, maximum and mean values of the static errors and the corresponding mean $\%RA_{fsd}$ at various input voltages in the range $\pm 300\text{mV}$ have been tabulated in Table 2.1. The plot of the mean static errors, along with errorbars depicting maximum and minimum static errors, for the different input voltages is shown in Figure 2.4 and the corresponding plot for mean $\%RA_{fsd}$ is shown in Figure 2.5.

It is observed that at the input voltage level of 25mV, the nature of the static errors reverses from positive for smaller input voltages to negative for input voltages larger than 25mV. This is valid for all measured values, as is evident from the fact that the span of the static errors at any input voltage is very small, within $\pm 0.07\text{mV}$. Furthermore, in terms of the input voltage magnitudes, the static error is lesser for smaller magnitudes than for the larger magnitudes, as is to be expected. These characteristics are reflected in the case of mean $\%RA_{fsd}$ also, which is within $\pm 0.07\%$ of 100% for the total input range.

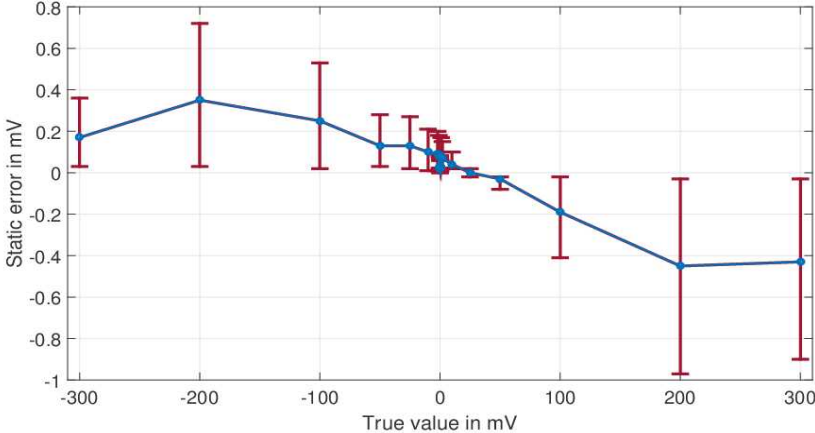


Figure 2.4: Plot of mean static errors at input voltages within $\pm 300\text{mV}$ with minimum and maximum static errors shown in errorbar

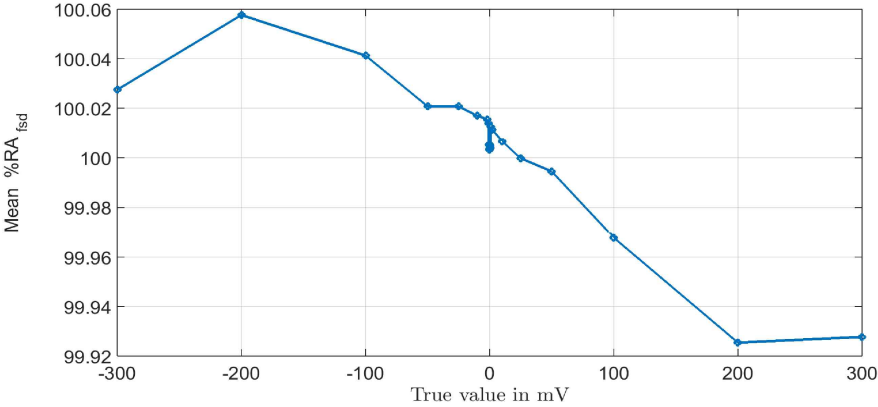


Figure 2.5: Plot of mean $\%RA_{fsd}$ at input voltages within $\pm 300\text{mV}$

2.3.3.3 Precision

Precision, which indicates the degree of refinement of the measured values, can be quantified in terms of the standard deviation (SD) around the mean measured value. The mean and SD of the measured voltages for different input voltages are plotted in Figure2.6 and Figure2.7 respectively.

It is to be noted that the mean measured voltages plotted in Figure 2.6 have been stated in Table 2.1, where the mean static error as well as the mean $\%RA_{fsd}$ have been calculated using these values.

It is observed from Figure 2.7 that the standard deviation of this Rish Multi 18S multimeter is 0.01mV for all the input voltages in the range $\pm 300\text{mV}$, which matches the specifications [97]. This is also the resolution limit of the meter in this range of operation. Since the true value at a particular input voltage level is fixed, so it can further be inferred that the span of the measured data at that particular input voltage is identical to the corresponding span of the static errors. As evident from the maximum and minimum static errors stated in Table 2.1, this is within $\pm 0.07\text{mV}$ for all input voltages in the operating range.

Based on these findings, it can be said that the instrument is very precise in the range of operation, with very small deviations that are well within limit.

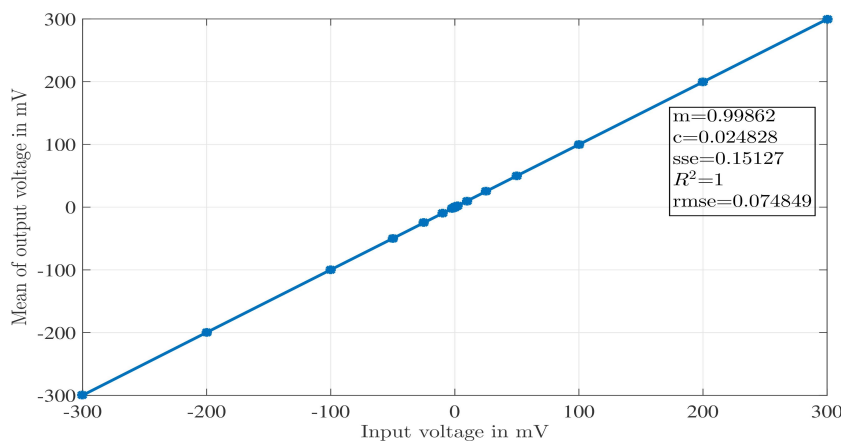


Figure 2.6: Plot of mean of measured voltages at different input voltages in the range $\pm 300\text{mV}$

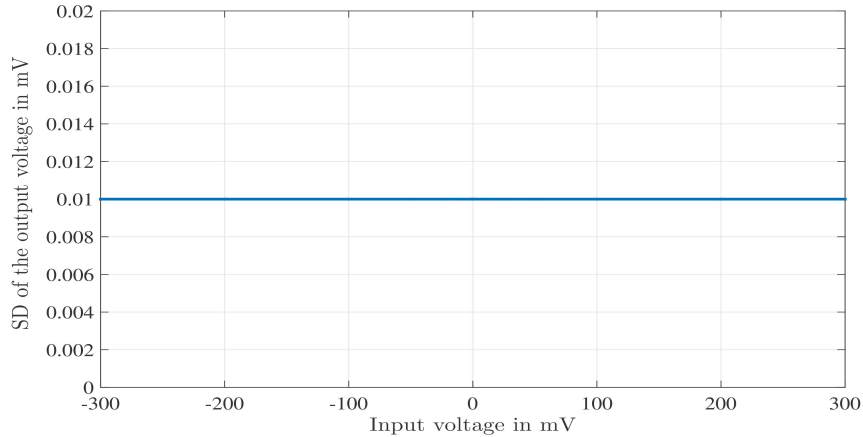


Figure 2.7: Plot of SD of measured voltages at different input voltages in the range $\pm 300\text{mV}$

2.3.3.4 Linearity, Sensitivity and Drift

From Figure 2.6, it is evident that the input and mean output voltages follow a linear relationship with mean relative accuracy close to 100% as shown in Figure 2.5. Also, since the SD is same for all voltages, as seen from Figure 2.7, it can be inferred that this observation is true for all measured voltages. A linear regression algorithm of MATLAB software is used to determine the best fit line, using which the goodness of fit (R^2) and the root mean squared error (rmse) are obtained as 1 and 0.0748 respectively. So, the functional relation between the true input and measured output voltages may be written as $x_{out_k} = 0.999 x_k + 0.025$ where x_{out_k} denotes measured output voltage in mV and x_k denotes true input voltage in mV. It is observed that the system has a very small effective bias of +0.025mV.

It is to be mentioned that since the input-output characteristics is linear for the total operating range, therefore the slope of the best fit line and sensitivity of the instrument are synonymous in this case. Since this instrument is to be used under controlled ambient conditions, so its drift characteristics have been noted with respect to time only. It has been observed from the analysis of the multiple sets of data acquisitions that the data values did not show any perceptible zero or sensitivity

drift.

Additionally, the baseline wander of the instrument has been checked by recording the instrument outputs for a duration of 30 minutes at various input voltages. It has been observed in all cases that the measured data do not show any baseline wander. Instead, the output value is constant all throughout the time, as evident from the time response at the specific input of +300mV shown in Figure 2.8. From the zoomed plot of the output for the first 10 instants shown in Figure 2.9, it can additionally be inferred that there is no observable transients at the sampling rate of 20Hz. So, it is observed that the instrument provides baseline stability and this ensures that a constant output value is obtained for a constant input without any drift in time [19].

2.4 Experimental Methodology

The research study has been conducted in two phases, denoted as Phase1 and Phase2, using the layout design shown in Figure 2.10. The details of the methodology followed for recording the data in both the phases are stated hereafter.

2.4.1 Protocols followed

The study involves human subjects and hence, some protocols have been maintained to ensure the objectivity of the study as well as subject privacy. No compensation or remuneration in any form were given to any of the subjects for their participation in the research study. Also, since the data were collected personally from each of the subjects, the confidentiality of the research data has been ensured even during data analysis and publication/presentation of results. Informed consent in a pre-determined proforma was obtained from each of the subjects and all the subjects signed the consent form after they were detailed about the procedures involved in the study.

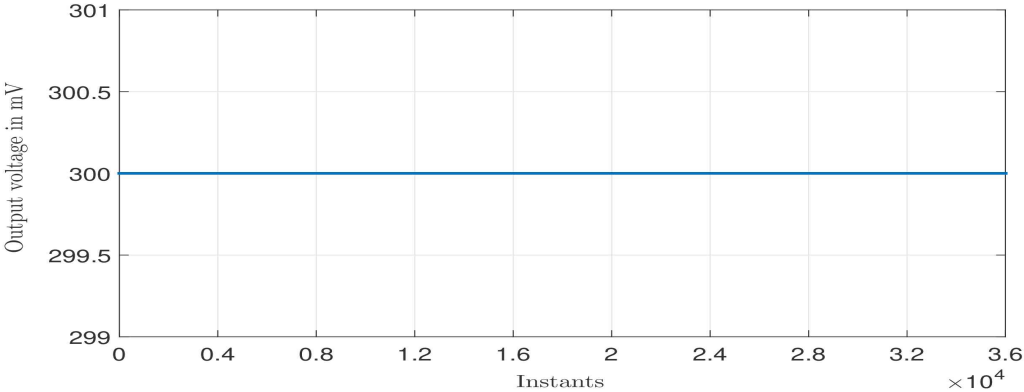


Figure 2.8: Output voltage recorded for 30 minutes at +300mV input

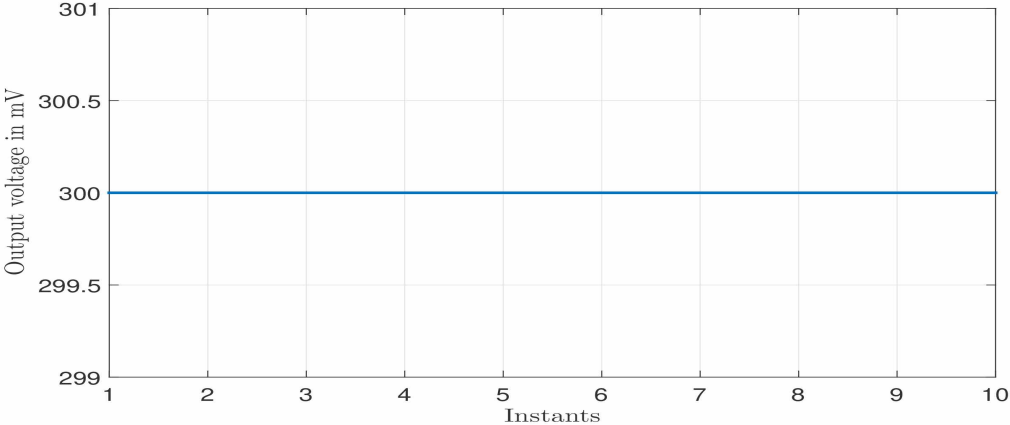


Figure 2.9: First 10 samples of measured voltage at +300mV input



Figure 2.10: Condition of the subject maintained during recording of biopotentials

The following steps were followed for each and every recording:

- a) Subjects participating have been assigned a number and a blindfold study has been performed so the identity of the participants cannot be traced from the assigned numbers by any third person, apart from authorized members of the research group.
- b) A formal informed consent for recording their biopotentials was taken from all the subjects for the undertaken research work. The term *formal informed consent* refers to the fact that the subjects were made aware of the details of the procedures, measurement techniques and objectives of the research study prior to measuring their biopotentials and their written consent was obtained for performing the experiments. This is a pre-requisite for any study involving human subjects in the medical fraternity.
- c) Before undergoing the experimental tests, a proforma was filled to record their

essential identity details, any known past and present medical conditions as well as some essential physical parameters, namely height, weight, waist and hip measurements. Besides this, every time before the recording, the perception of the subjects about their general health condition was also noted.

- d) The research data was saved in files by the participant number and not by name. All recordings and files were stored in a secured location, password protected that can only be accessed by authorized researchers.

2.4.2 Placement of electrodes

The placement of electrodes on the body is an important factor which changes the nature of the signal. It is known that the human system is bimodal in nature and in that, the hands are located at the lateral extremities on either side.

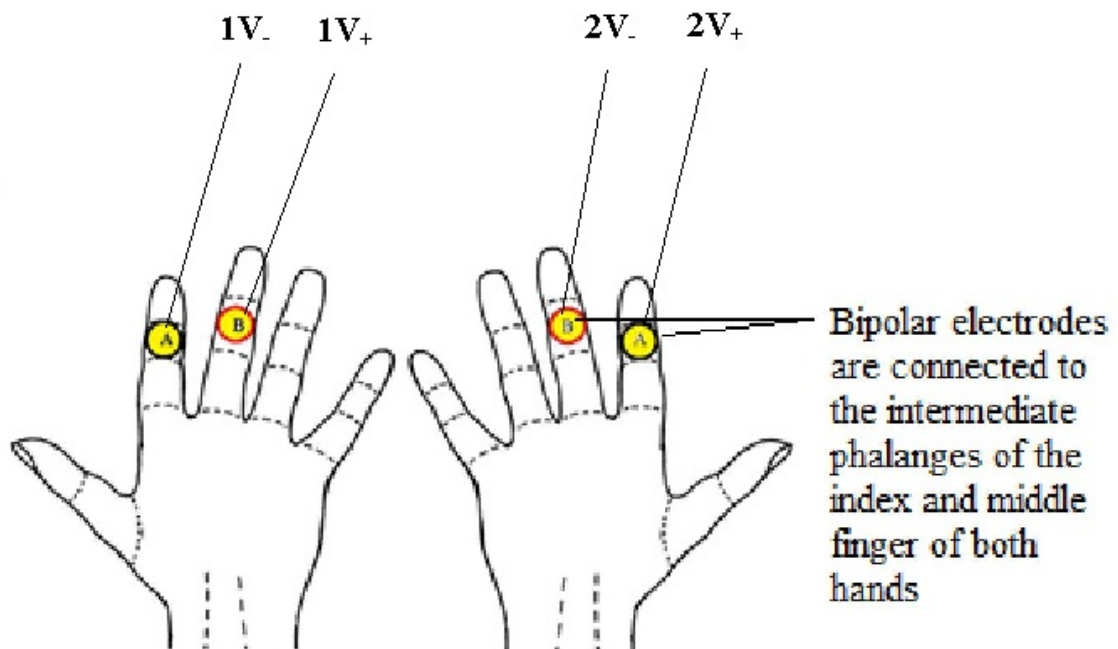


Figure 2.11: Location of electrode placement for EDA measurement

Furthermore, any biopotential recorded from the hands can be expected to have minimal effect of any vital organ or organ system. Hence, as stated earlier, two pairs of EDA sensors (Ag-AgCl electrodes), one pair of sensors for each hand, were used for measuring the biopotentials from the left and right hands of the human subject. Out of the several possible locations mentioned for acquiring EDA signals, [2], the fingers on both hands were chosen as the preferred locations as shown in Figure 2.11. The two sensors of one pair of electrodes were connected to the middle phalanges of the two adjacent fingers, namely middle finger and fore finger, of the same hand, as is suggested for typical GSR measurements [2]. In Figure 2.11, $1V_-$ and $1V_+$ indicate the connections to the negative and positive terminals of multimeter1 respectively, while $2V_-$ and $2V_+$ indicate the respective connections to the negative and positive terminals of multimeter2. The biopotential acquired and recorded using a pair of sensors is thus a differential voltage with minimal effect of the common mode interference signal, as stated earlier.

2.4.3 Health parameters measured

Before recording the biopotentials, the standard available health parameters of pulse rate (PR), oxygen saturation in blood (SpO_2) and blood pressure (BP) were measured while the subject was in the supine position. The PR and SpO_2 were recorded using CONTEC make pulse oximeters (Model CMS50D) on the index fingers. The BP measurements were taken using an OMRON make automatic Blood Pressure Monitor with digital display (Model HEM-7201), which was calibrated periodically. Prior to each recording, it was ascertained that the health parameters are within the standard range, specifically 60-100bpm for PR and more than 94% for SpO_2 [107]. Also, it was ascertained that the BP of the subjects remained within 140/90 as per JNC-8 scale [92].

2.4.4 Acquisition of bio-potentials

The biopotentials were recorded in two phases during different times of the year from a number of human subjects, who were between 20 to 58 years and from both genders. In all cases, the biopotentials were recorded with the subject in supine condition on the experimental bed, as shown in Figure 2.10. The subject under test was allowed to settle down for about a minute in calm, temperature controlled environment before recording the data. The environmental conditions of the closed cubicle were maintained for all the recordings of all the subjects, taken at different times of the year.

For each session, the data was recorded in the form of dc voltage signals from the two hands simultaneously for a time span of 2 minutes with 50ms sampling interval, yielding 2400 samples using the RISH-MULTI meters [97]. This is henceforth referred to as a set of recorded data. This procedure was identical in both the phases of measurement. The biopotentials were recorded in a laptop in data logger form (.mdf format), which was converted to text format (EXCEL) for further analysis.

The details of the records taken in both the phases are as follows:

- A) **First Phase** Sixteen subjects (11 male and 5 female) were chosen for measuring the biopotentials. One set of data was recorded once a day, tentatively about twice a week over a span of about 4 months from 24 Nov 2011 to 30 Mar 2012 for each subject. Therefore, a subject typically rested for about 2-3 min in a set of measurement. PR, SpO₂ and BP were measured before recording the biopotentials. A total number of 388 pairs of such data sets were recorded. This phase is named as Phase1. PR, SpO₂ and BP were measured before recording the biopotentials. A total number of 388 pairs of such data sets were recorded. This phase is named as Phase1.

- B) **Second Phase** Fourteen subjects (9 male and 5 female) were chosen for this phase of recordings. In this phase, five (5) to ten (10) sets of data were recorded at a time, twice a week, for a subject. Therefore, a subject could rest for at

least 10 min ($=5 \times 2min$) to 20 min ($=10 \times 2min$) duration in each case during this phase of measurement. The data for different subjects was recorded over a span of 2 months from 27 February 2014 to 25 April 2014. Simultaneous continuous measurement of SpO₂ and PR was done from both the hands along with the biopotential record. The PR and SpO₂ were acquired at a sampling rate of 1Hz. In all cases, BP was measured from both hands after acquiring the biopotentials. A total number of 341 pairs of data sets were recorded. This phase is named as Phase2.

2.5 Discussions

The present research aims to study and characterize the passive EDA biopotentials acquired from both hands of various human subjects with the objective of identifying certain attributes of the signal. To achieve this purpose, it was necessary to conduct systematic experiments to acquire suitable data. The proper subject and environmental conditions that have been maintained and the experimental methodology that has been adopted for this study has been specified in this Chapter.

In this study, the biopotentials acquired from healthy subjects have been characterised. Hence, a suitable subject selection criteria, which includes the inclusion and exclusion criteria, has been determined for this study. This is a blindfold study with informed consent of the participants, which ensures the confidentiality and privacy of the subjects and all records pertaining to the study.

The study has been done in two phases. In both cases, the study design adopted is longitudinal, observational analytical type where the repeated acquisition of data is done from each of the subjects over certain period of time followed by qualitative and quantitative analysis of the observed data. A suitable structured proforma for both the phases of the study have been designed using preliminary trials. These trials were also used to fix the study design, which ensures that the subjects are rested and not subjected to undesirable external inputs. For this, the signals have been

recorded with the subjects in supine condition at regular intervals over a number of days under controlled conditions, which were maintained in both the phases of measurement.

For this study, it is essential to ensure the integrity of the instrumentation system being used since the signals are typically within $\pm 300\text{mV}$ and they vary within a few mV only in the duration of 2 minutes for which the data sets have been recorded. The instrumentation system comprises of two pairs of identical EDA sensors (Ag-AgCl electrodes), one pair of sensors for each hand, for measuring the biopotentials from the left and right hands, LH and RH, of the human subject. The measurement system used consists of two RISH Multi 18S digital multimeters cascaded with two adapters. The sampling time is set at 50ms. The cascaded set of two adapters are connected via a serial RS-232C interface to a dedicated laptop for transmission of the measured values using the interfacing RISHCOM100 software. The software allows recording of the acquired data in data logger form simultaneously from the two meters.

The systematic characterization of this system for various static input voltages indicates that the instrument provides an accurate, precise and linear output with no drift or baseline wander. This instrument is capable of recording input voltages in the required range of $\pm 300\text{mV}$ with a resolution of $10\mu\text{V}$, which is suitable for acquiring the biopotentials of human subjects.

Based on these preliminary and subsequent observations, these endosomatic EDA signals, termed in this study as non-organ specific biopotentials, have been treated as a valid baseline biopotential of human subjects, which need to be characterised and analysed systematically.

Chapter 3

Analysis of Human Biopotentials

3.1 Introduction

The experimental methodology, the protocols followed, the various conditions of the experiment like the inclusion and exclusion criteria for the choice of subjects as well as the details of the instrumentation system used for the present study have been described in detail in Chapter 2. In the experimental methodology detailed in Section 2.4, it is mentioned that these biopotentials have been acquired passively from various human subjects. During the data acquisition, the subjects were resting in supine position without any external disturbance. It was noted in Section 2.3 that these signals are smoothly changing in nature and typically vary within 20mV in the duration of 2 minutes. This is evident from the plot of a typical signal, along with its zoomed time plot for 10s, in Figure 3.1.

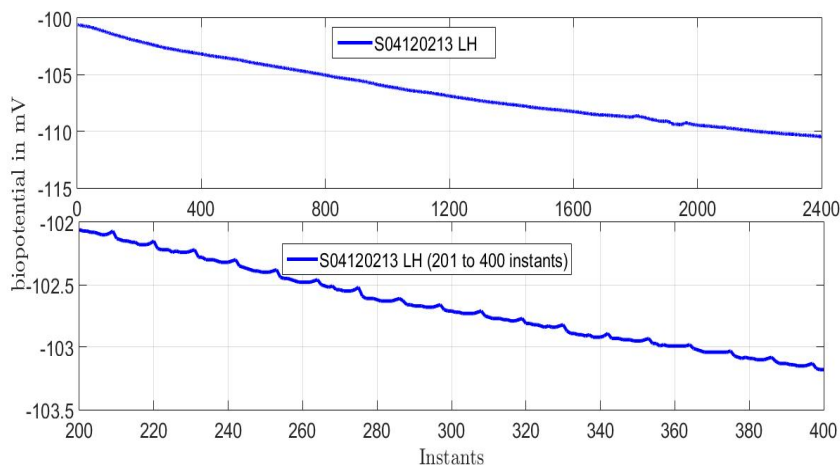


Figure 3.1: Time plot of a typical signal shown along with its zoomed plot for 10s (between 201 to 400th instants)

These signals, which may be treated as slowly changing baseline biopotentials of human subjects, were recorded in two phases, detailed in Section 2.4.4, in which the durations of rest were different.

The focus of the present chapter is to study the qualitative and quantitative features of these baseline endosomatic EDA potentials and to characterize the signals for identifying certain representative features in them. It is expected that the change in the duration of rest will be featured in some of these characteristics.

The chapter is organized as follows. The qualitative analysis of the signals acquired from the left and right hands of the subjects is given in Section 3.2. This includes the description of the general characteristics of these signals in Section 3.2.1, followed by the characterization of a signal from a single hand in Section 3.2.2. Thereafter, the pairs of acquired signals have been characterized in Section 3.2.3, which leads to the definition of two new derived signals and their characterization in Section 3.2.4. The quantitative analysis of the individual as well as derived signals are stated in Section 3.3. This is done at an overall level in Section 3.3.1, followed by further subject-wise analysis in Section 3.3.2. An anomaly in the characteristics of RH signals is studied in Section 3.3.3, followed by a setwise analysis in terms of

the identified features in Section 3.3.4. In general, all these have been studied considering the signals in the two phases separately in order to identify the effect of rest on these aspects. The overall discussions are stated in Section 3.4.

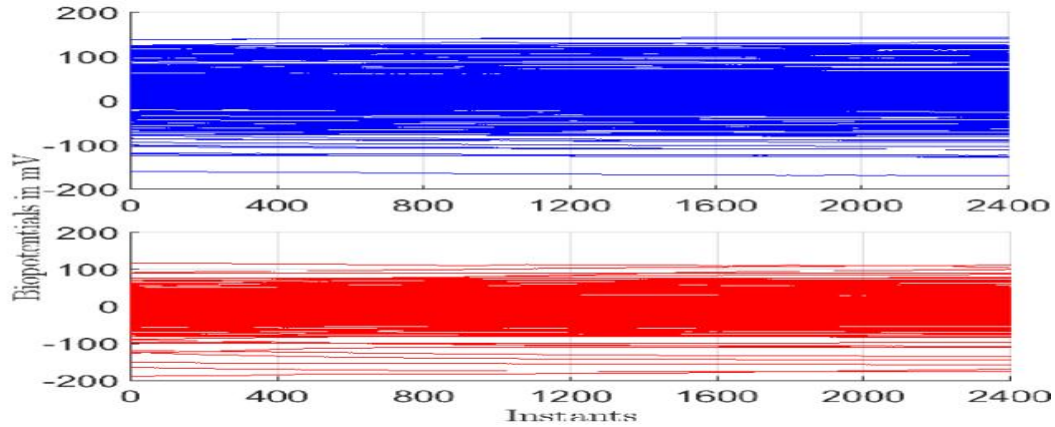
3.2 Qualitative analysis of the signals:

As stated in Section 2.4, the amplitude of the biopotentials, in mV, have been recorded from the left hand (LH) and the right hand (RH) of all subjects in two phases, Phase1 and Phase2, in a single set or in multiple sets acquired sequentially. The total number of samples recorded for every data set for a duration of 2 minutes is 2400, with a time interval of 0.05s. A total of 729 such sets of data have been recorded in the two phases, 388 sets in Phase1 and 341 sets in Phase2.

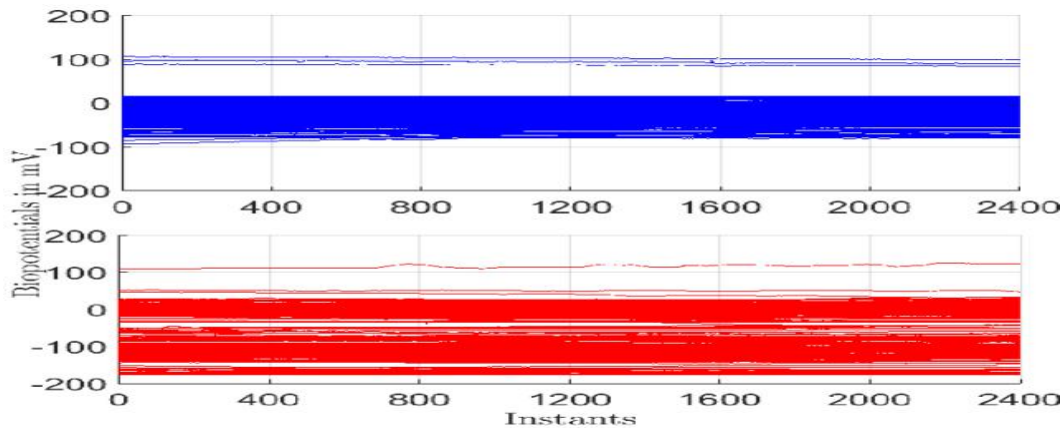
3.2.1 General Characteristics:

Prior to determining the essential features of these biopotentials, it is necessary to observe their general characteristics. A superimposed plot of the sets of data recorded from all the subjects, for each hand and in the two phases, are shown as time-series plots in Figure 3.2. It is observed that the overall data lies within $\pm 300\text{mV}$ in all cases. As noted in Section 2.3, these signals are smoothly changing in nature and typically vary within 20mV in the duration of 2 minutes.

However, in certain cases, it is seen that there is an abrupt change of more than 20mV within a short span of about 2s or 40 consecutive instants in any one, or both, of the sets of data in a pair of the acquired signals. This is shown in the 4 representative plots shown in Figure 3.3.



(a) Biopotentials recorded in Phase1 from 16 subjects; blue-LH, red-RH

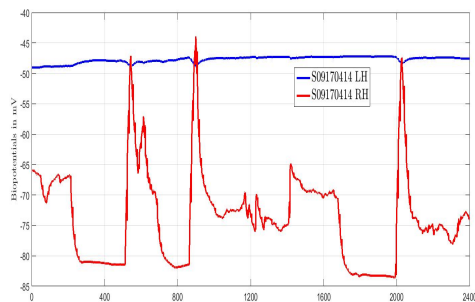


(b) Biopotentials recorded in Phase2 from 14 subjects; blue-LH, red-RH

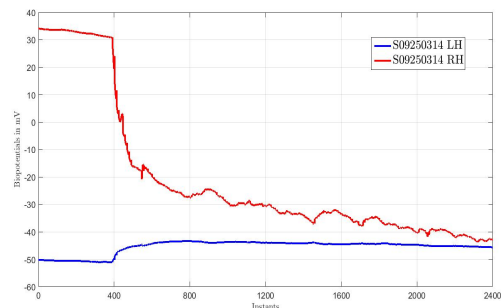
Figure 3.2: Time series plots of left and right hand (LH and RH) biopotentials acquired in Phase1 and Phase2

It may be noted in Figure 3.3(b) that in this pair of signals, the LH signal shows a rise at the 400th instant, but that is within 10mV. However, a much larger variation is present in the RH signal. Such disturbances are observed in a total of 14 data sets (4 sets in Phase1 and 10 sets in Phase2) out of a total of 715 sets from both the phases, which is about 2% of the acquired data. These disturbances in the dataset

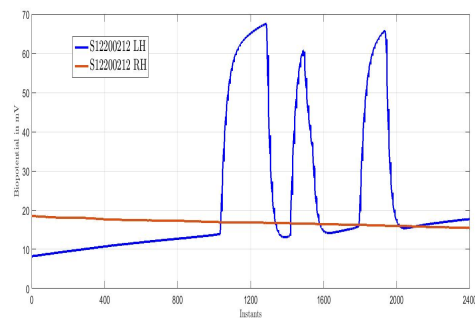
must be due to some unknown atypical cause, whether internal or external to the system. In all such cases the pair of signals, which include the disturbed set and its pair from the other hand, have been totally discarded from further analysis. This is done since it is intended to study the general characteristics of the class of passive baseline EDA potentials recorded from the fingers of both hands, both individually for each hand and also as a pair of signals together.



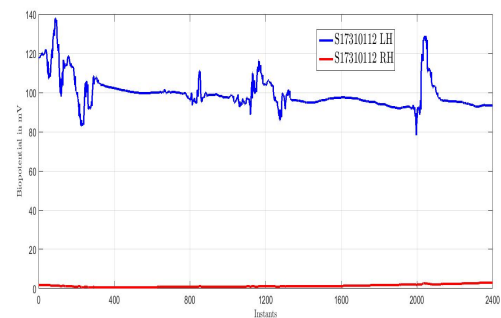
(a) Abrupt variations in RH



(b) Sudden drop in RH



(c) Abrupt variations in LH



(d) Large variability in LH

Figure 3.3: Large variations in recorded biopotentials

The subsequent study has thus been performed for a total of 715 pairs of biopotentials, specifically 384 pairs of biopotentials recorded in Phase1 and 331 pairs recorded in Phase2. A few representative time-series plots of these 715 pairs of biopotentials are shown in Figures Figure 3.4-Figure 3.6. Data sets recorded for different subjects on different dates, are shown in Figure 3.4, different subjects on same date are shown

in Figure 3.5 and same subject on different dates are shown in Figure 3.6.

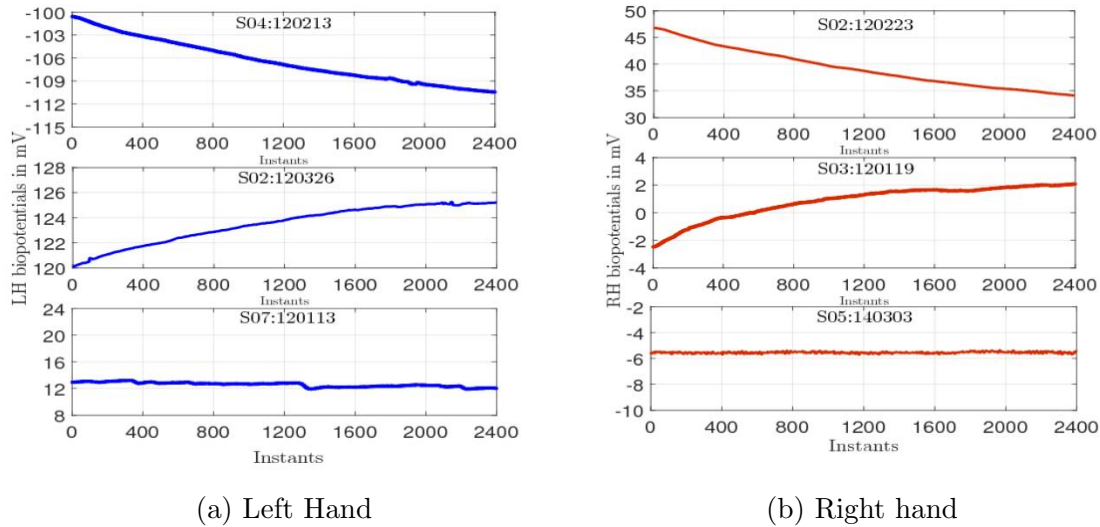


Figure 3.4: Typical characteristics of acquired LH and RH biopotentials

The subject identifier format used in this work is SXXDDMMYY, where the first three letters SXX denotes the subject identifier and the last six letters denotes the date of measurement in DDMMYY format. Hence, the label S04120213 indicates that the data was measured from subject S04 on 12 February, 2013.

Figure 3.5 shows some representative LH and RH plots recorded on 01Mar2012 from different subjects namely, S01, S02, S05, S06, S08 and S15. The figure shows that the biopotentials are different for all the subjects even when measured on the same day.

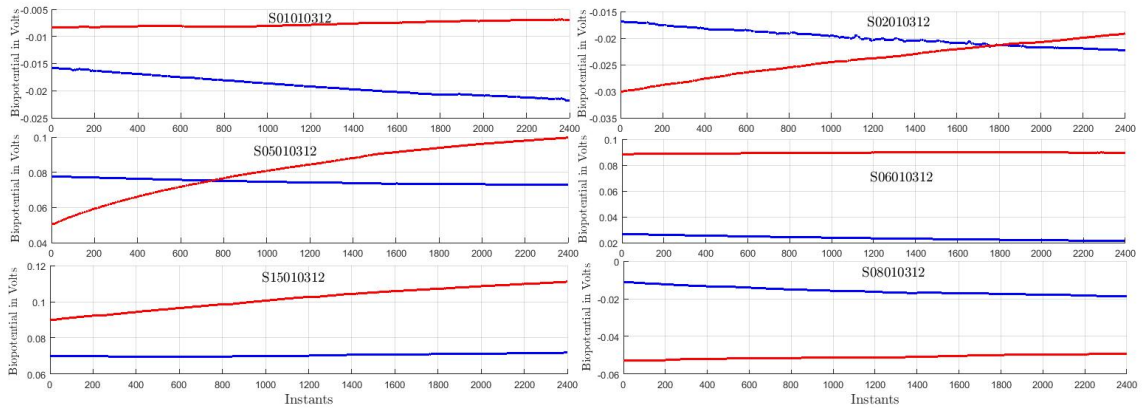


Figure 3.5: Representative time series plots of different subjects on same date

Figure 3.6 shows some representative LH and RH plots for a single subject S03 on different dates namely, 30Jan2012, 08Feb2012, 20Feb2012, 01Mar2012, 20Mar2012 and 26Mar2012. The figure shows that the biopotentials are different even for same subject when recorded in different sessions.

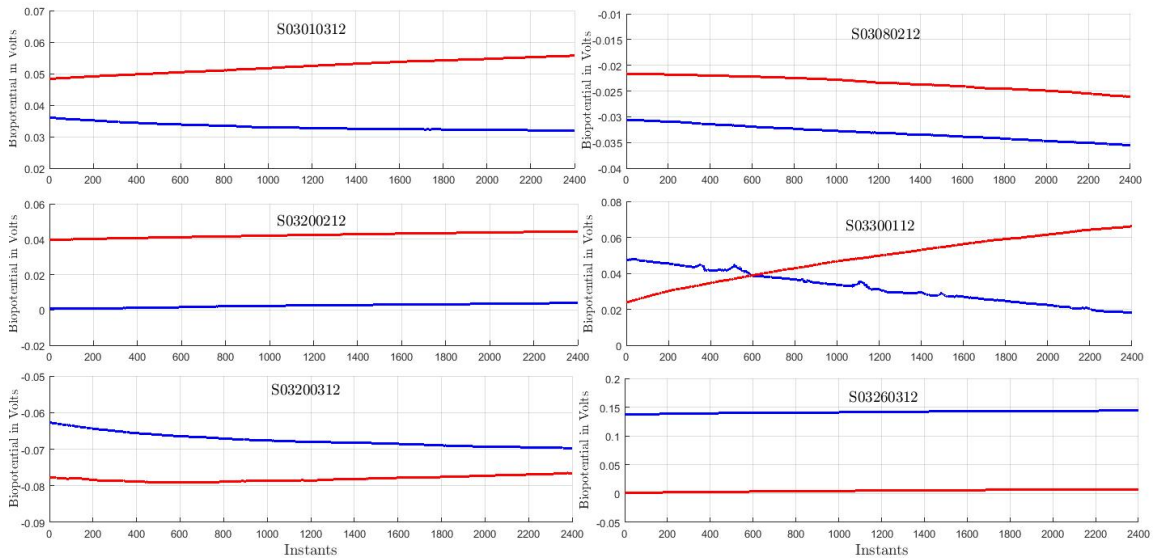


Figure 3.6: Representative time series plots of same subject on different dates

It has been found that the potentials measured across the two fingers of each

hand of the human subject:

- 1) vary from person to person, even on same dates as shown in Figure 3.5.
- 2) vary with time of the day and also from day to day, even for the same subject as shown in Figure 3.6.
- 3) vary continuously with time, as evident in all cases shown in Figure 3.4 and are different for each hand of a subject.
- 4) show positive as well as negative polarity for both the hands, as evident from the plots shown in Figure 3.4.
- 5) may show same or different trends for each hand, even in a set of recorded data shown in Figure 3.9.

Thus, variability, in all senses of the term, is an essential feature of these LH and RH biopotentials recorded from human subjects.

3.2.2 Classifying the left and right hand (LH and RH) signals:

In view of the general characteristics observed for these signals, the LH and RH biopotentials recorded in the various sets in Phase1 and Phase2, considering all 16 subjects for Phase1 and all 14 subjects for Phase2, are studied in terms of their polarity and trends.

Signal polarity: The wholly positive data sets, the wholly negative data sets and the data sets in which the signal value may transit from positive to negative or vice versa once or multiple number of times have been segregated into three categories. These are henceforth referred to as Positive, Negative and Transitive data sets respectively. The criteria chosen to classify the signals as positive, negative or transitive polarity is given below:

Let x_i denote the biopotential at the i -th instant.

For any particular dataset $\{x_i\}$, $i \in [1,2400]$,

If $x_i \geq +0.01\text{mV}$ for all $i \in [1,2400]$, then the data set is Positive;

If $x_i \leq -0.01\text{mV}$ for all $i \in [1,2400]$, then the data set is Negative;

else, it is Transitive.

The counts, in percentages, of the LH and RH datasets in the two phases are tabulated in Table 3.1 and the corresponding bar graph is shown in Figure 3.7.

Table 3.1: Occurrence of signals with specific polarity

Values	%count	
	Phase1	Phase2
Positive LH	68.8	8.8
Negative LH	28.7	89.7
Transitive LH	2.6	1.5
Positive RH	40.6	25.9
Negative RH	52.9	68.2
Transitive RH	6.5	5.9

It is observed from Table 3.1 and Figure 3.7 that in Phase1, the count of Positive LH biopotentials (68.8%) are more than that of Positive RH biopotentials (40.6%), whereas the reverse is more typical for the Negative polarity with 28.7% LH signals as compared to 52.9% RH signals being Negative. This finding is reversed in the case of Phase2 measurements, where the number of Positive LH biopotentials are lesser (8.8%) than Positive RH biopotentials (25.9%), while more LH signals (89.7%) are of Negative Polarity as compared to RH biopotentials (68.2%).

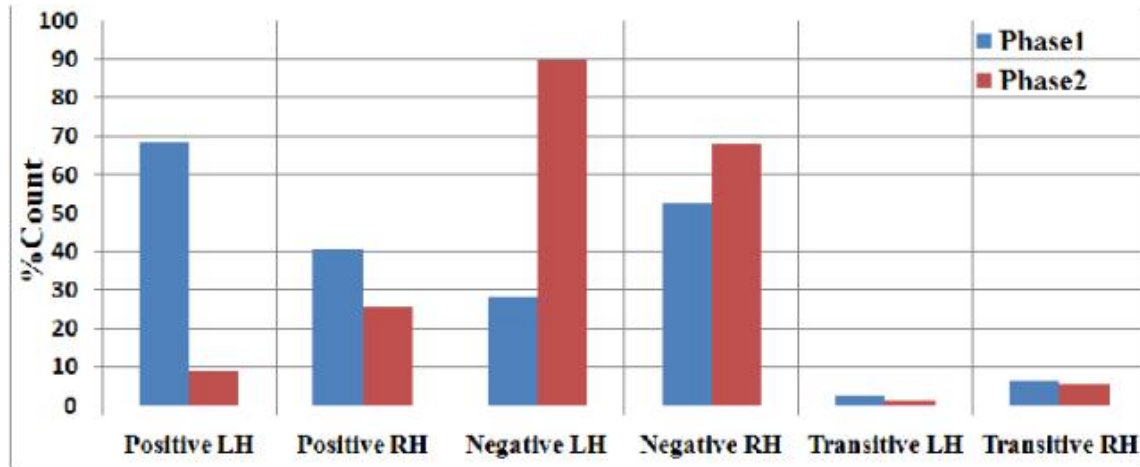


Figure 3.7: Bar graph depicting polarity counts of the LH and RH biopotentials in Phase1(blue) and Phase2(red)

In general, it is observed that the biopotentials obtained in Phase2 are mostly of Negative polarity, where the subjects may be considered to be more relaxed owing to the recording of data for a longer duration. A similar finding by some researchers states that negative or low basal skin potential levels (SPL) have been recorded in relaxed human subjects and it has been proposed that this may be related to sodium ion reabsorption and available epidermal potassium ion concentrations [108], [109], [28]p26.

In both phases of measurement in the present study, there is a low count of cases, less than 3% of LH signals and less than 7% of RH signals, where one or more Transitions took place during a 2 minute recording of data. A further analysis of Phase2 measurements, where the data sets were recorded multiple times in a day from the subjects, showed that Transitive data typically occurred once a day, usually during the midday. Similar findings are not readily available in literature for endosomatic EDA recordings.

Signal Trend: As mentioned earlier, it is observed from Figure 3.4 that the slowly varying LH and RH signals display all possible types of trends at different times

for the same as well as for different subjects. It has also been observed that in any pair of measured data, the signals may individually show the same trend or different trends. Consequently, an analysis has been done to study whether any particular trend is dominant for a particular hand in a particular phase. For this purpose, the difference of the biopotential recorded at the first instant from that at the last instant, that is 2400th instant, in a set was used to classify the signals in terms of their trends. These have been referred to henceforth as Increasing, Decreasing and Constant trends. The criteria used to classify the signals into these categories is referred below:

For any particular dataset $\{x_i\}$, $i \in [1,2400]$,

let $\text{Diff} = (x_{2400} - x_1)$.

If $\text{Diff} > +4\text{mV}$, then the data set is Increasing;

If $\text{Diff} < -4\text{mV}$, then the data set is Decreasing;

else, when $+4\text{mV} \geq \text{Diff} \geq -4\text{mV}$, then the data set is Constant.

The total count, in %, of occurrences of these trends have been assessed for both the phases, as shown in Figure 3.8 and tabulated in Table 3.2. The datasets have been classified into one of the three trends, namely, Increasing, Decreasing and Constant trends. The minimum and maximum values of the parameter Diff for each trend have been determined for LH and RH signals of Phase1 and Phase2 separately. The minimum and maximum values of the parameter Diff obtained for each of the three trends are named as minimum Diff and maximum Diff of the particular trend and are listed in Table 3.2. The overall Diff in a particular phase for the LH or RH signals is accordingly calculated as the difference between the maximum Diff of the Increasing Trend and the minimum Diff of the Decreasing Trend.

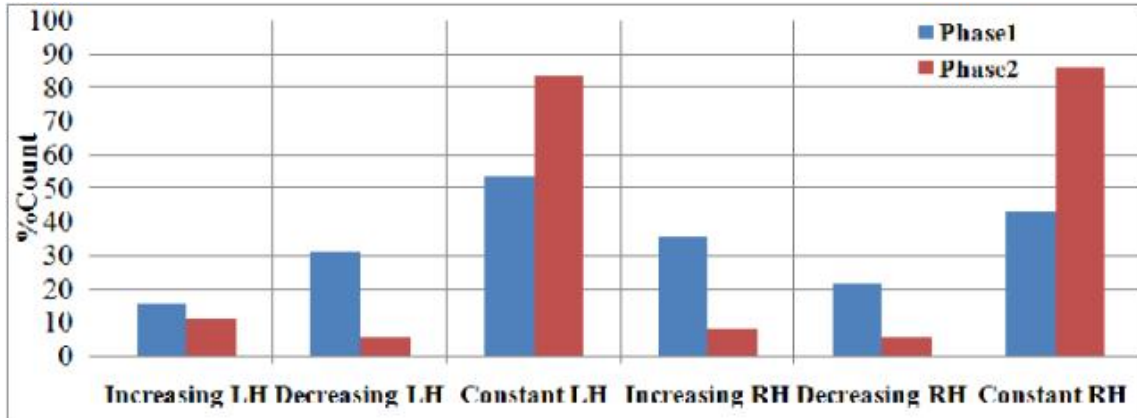


Figure 3.8: Bar graph depicting Trends of LH and RH biopotentials in Phase1 (blue) and Phase2 (red)

Certain general observations can be made from the bar plots in Figure 3.8 as well as the tabulated data in Table 3.2 as stated hereafter.

Table 3.2: Occurrence of trends and corresponding minimum Diff and maximum Diff of acquired biopotentials

Trend	%Count		Minimum Diff(mV)		Maximum Diff(mV)	
	Phase1	Phase2	Phase1	Phase2	Phase1	Phase2
Increasing LH	15.4	11.0	4.06	6.18	23.11	11.98
Decreasing LH	31.0	05.4	-29.52	-9.9	-4.19	-8.05
Constant LH	53.7	83.9	-3.98	-3.53	3.98	3.93
Increasing RH	35.7	08.1	4.12	6.14	49.48	10.04
Decreasing RH	21.6	05.7	-21.42	-15.59	-4.07	-11.46
Constant RH	42.7	86.3	-3.83	-3.97	3.92	4.00

- i) The occurrence of Constant trend is more than both Increasing and Decreasing trends for both the phases and for both hands. Furthermore, as might be expected, the minimum Diff and maximum Diff are very close to -4mV and +4mV respectively in both phases for both hands.

- ii) Between the Increasing and Decreasing trends, Increasing trend is dominant over the Decreasing trend in both phases for both hands.
- iii) The values of minimum Diff of the Increasing LH and Increasing RH signals in Phase1 are almost close to -4mV, but their maximum Diff values are widely different, with the value for the RH signals (49.48mV) being more than twice that of the LH signals(23.11mV). This aspect indicates that for a short duration of rest, the Increasing RH signals exhibit a higher variability as compared to the corresponding Increasing LH signals.
- iv) The values of overall Diff of both LH and RH signals is significantly larger in Phase1 (52.63mV for LH and 70.9mV for RH) than in Phase2 (21.88mV for LH and 25.63mV for RH). An analysis of this phenomena shows that for both these signals, the minimum Diff in Phase1 (-29.52mV for LH and -21.42mV for RH) is much smaller than that in Phase2 (-9.9mV for LH and -15.59mV for RH) and also the maximum Diff in Phase1 (23.11mV for LH and 49.48mV for RH) is much larger than that in Phase2 (11.98mV for LH and 10.04mV for RH). So, this So, this phenomena is due to an overall increase in variability, both positive and negative, of the signals in Phase 1 as compared to those in Phase 2, where the subjects rest for longer durations.

Thus it is evident that a longer duration of rest typically causes the values of Diff of both LH and RH signals to decrease and also leads to an increase in the % occurrence of Constant trend for both these signals.

Trends seen as a pair Since the biopotentials have been acquired simultaneously from the left and right hands so, prior to characterizing the pair of signals, the occurrences of the 3 trends in the combination of the LH and RH signals have been presented in Table 3.3 and the observations are stated herewith.

It is observed that in both phases, the occurrence of the combination of Constant LH and Constant RH signals is the maximum. However, the effect of a longer

Table 3.3: Occurrence in % of trends in a pair of LH and RH signals

	Phase1		
Trend	Increasing RH	Decreasing RH	Constant RH
Increasing LH	5.47	2.60	7.29
Decreasing LH	11.72	8.33	10.94
Constant LH	18.49	10.68	24.48
	Phase2		
Trend	Increasing RH	Decreasing RH	Constant RH
Increasing LH	1.51	1.51	7.86
Decreasing LH	0.30	0.00	4.53
Constant LH	6.04	4.23	74.02

duration of rest is clearly evident in the fact that while close to 25% of the data sets in Phase1 are a combination of Constant LH and Constant RH signals, the fraction of data sets in this category goes up to almost 75% in case of Phase2. Furthermore, if all the combinations of a Constant trend in any one hand, LH and/or RH, with any of the other trends in the other hand are considered, then almost 72% of the data sets in Phase1 and 97% of the data sets in Phase2 fall in this category. Hence, the other combinations are quite less likely, typically only about 28% data sets in Phase1 and about 3% data sets in Phase2.

In view of these findings, it is important to study the occurrence and nature of the various patterns possibly exhibited by a pair of signals. For example, an Increasing LH and an Increasing RH pair of signals may seem to be parallel if their slopes are almost the same or may seem to be diverging or converging, in case their slopes are different. Similarly, a combination of one Increasing and the other Decreasing set of signals may give rise to diverging or converging patterns or the signals may even cross each other at some point in time depending on their slopes and actual potential values.

3.2.3 Classifying the pair of LH and RH signals:

The characteristics exhibited by a pair of LH and RH signals have been studied in this stage. A few representative time-series plots of the pairs of LH and RH signals measured from different subjects on different dates are shown in Figure 3.9, where blue colour is used to depict LH biopotentials and red colour is used for RH biopotentials.

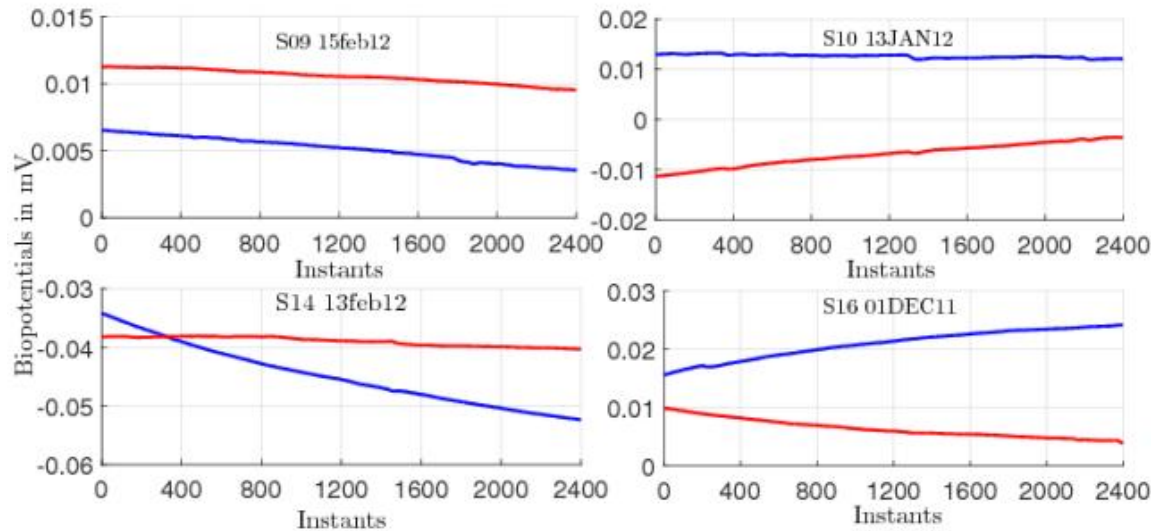


Figure 3.9: Representative time series plots of a pair of signals, LH in blue and RH in red, acquired from 4 different subjects at different times

It is observed that the pairs of signals form 4 different patterns. Similar patterns are observed for all subjects at various times. This is evident in Figure 3.10, where these different patterns, recorded at different times from 4 randomly selected subjects, are shown with 4 different colours for each subject.

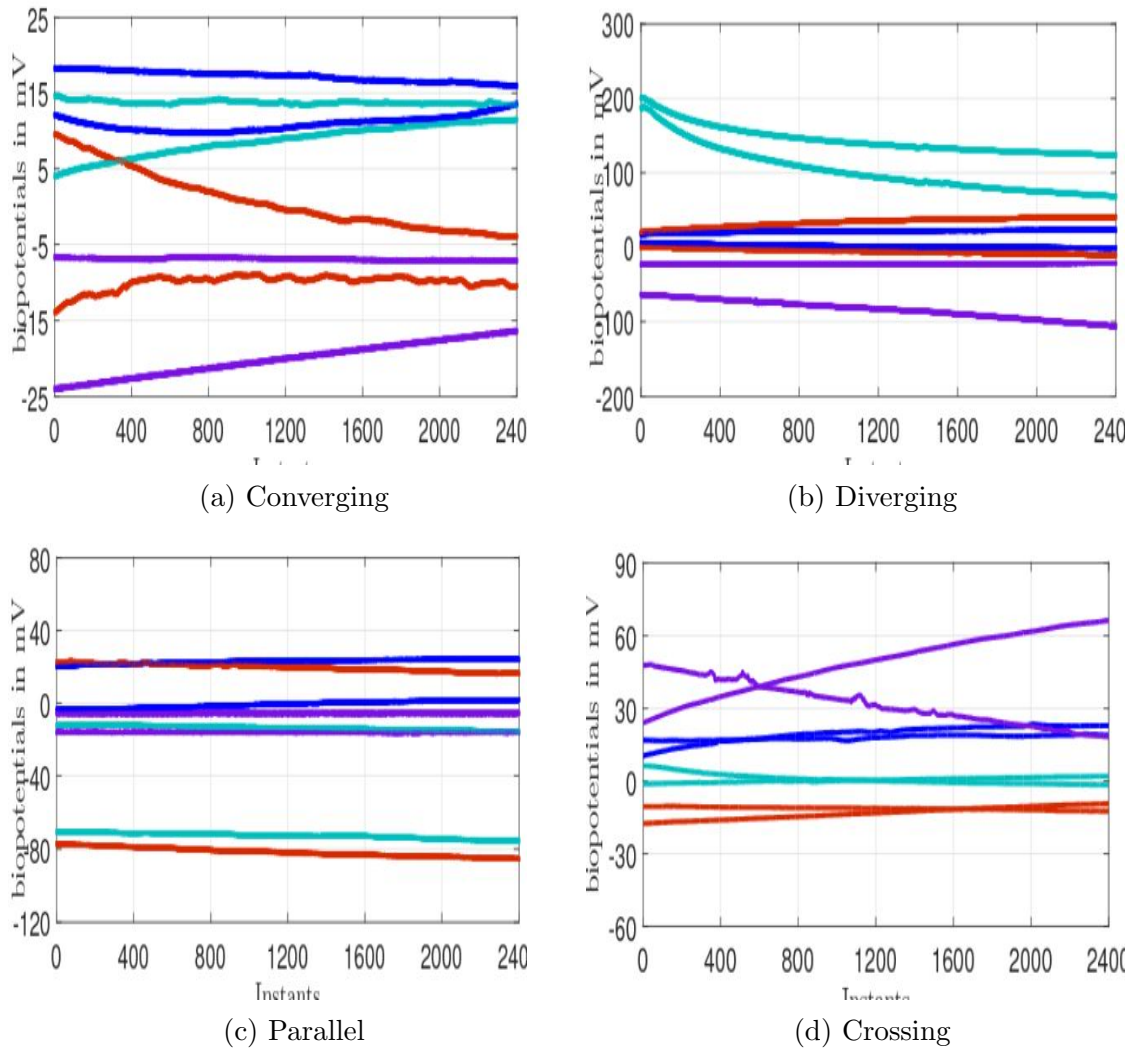


Figure 3.10: Typical patterns in pairs shown with different colors for each pair of four different subjects observed at different times

It is observed that the pairs of signals exhibit all four possible patterns, henceforth labelled as Converging, Diverging, Parallel and Crossing, as shown in Figure 3.10a, Figure 3.10b, Figure 3.10c and Figure 3.10d respectively. It must be noted that, in accordance with the earlier observations, the underlying individual LH and RH signals are mostly constant, and also increasing or decreasing in a few cases. Fur-

thermore, in the plots shown in Figure 3.9, the LH and RH signals are either positive or negative in polarity. However, similar pairwise patterns have been observed for transitive signals also, as shown in Figure 3.10.

It has been observed earlier that in most cases, the signals vary almost monotonically within a small range of 20mV. So, the pair of signals have been characterized in terms of the four possible patterns using the difference between the two initial values of a set of recorded LH and RH biopotentials and the difference of the two corresponding final values and then comparing them. Parallel signals are considered to have the initial and final differences within 4mV of each other, while corresponding differences more than +4mV and less than -4mV are used to label converging and diverging pair of signals. A crossing pair of signals is identified by the fact that the sign of the initial and final differences in such signals change. On this basis, the criteria for this classification is defined as follows:

For any particular pair of signals, let x_{LHi} and x_{RH_i} represent the i -th instant of the LH and RH signals.

Let the first difference be denoted as $d_1 = x_{LH1} - x_{RH1}$ and

the last difference be denoted as $d_{2400} = x_{LH2400} - x_{RH2400}$.

If $d_1 > 0\text{mV}$ and $d_{2400} < 0\text{mV}$ or viceversa, then the data set is Crossing;

else both d_1 and d_{2400} have same sign, and $d_1 - d_{2400}$ is evaluated.

If $(d_1 - d_{2400}) > +4\text{mV}$, then the data set is Converging;

else if $(d_1 - d_{2400}) < -4\text{mV}$, then the data set is Diverging;

else $-4\text{mV} \leq (d_1 - d_{2400}) \leq +4\text{mV}$, and the data set is Parallel.

Table 3.4: Occurrence of patterns in a pair of recorded biopotentials

Pattern	% Count	
	Phase1	Phase2
Converging	41.15	9.97
Diverging	21.09	14.80
Parallel	33.07	73.11
Crossing	4.69	2.11

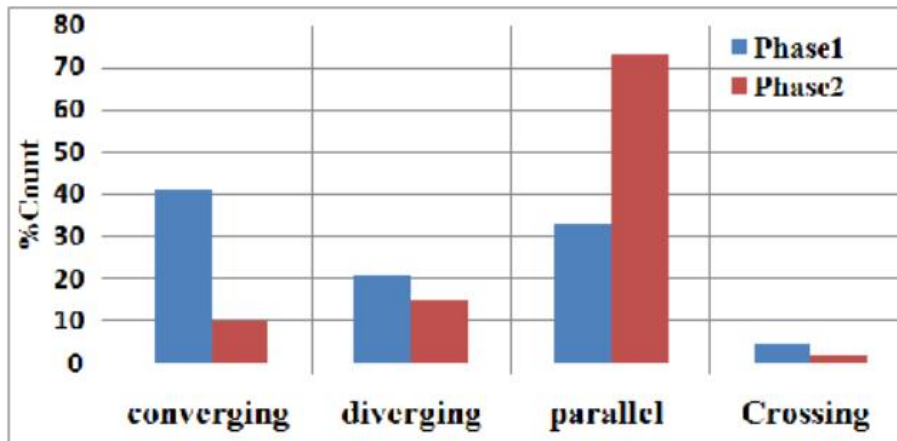


Figure 3.11: Bar graph depicting count of patterns in a pair of LH and RH biopotentials in Phase1(blue) and Phase2(red)

Subsequently, the proportion of occurrence of these patterns, in %, has been tabulated for Phase1 and Phase2 in Table 3.4, while the corresponding bar graph is shown in Figure 3.11. The observations have been listed hereafter.

- a) The Parallel pattern dominates in Phase2 in which the subject was in prolonged rest owing to multiple data recordings. Even in Phase1, this is the second most likely pattern.
- b) The Converging and Diverging patterns are more likely in the shorter duration of rest in Phase1 than in the longer duration of rest in Phase2. It is

further observed that in Phase 2, the Diverging pattern is more likely than the Converging pattern.

- c) As is to be expected, the Crossing pattern was observed to occur the minimum number of times in both the phases.

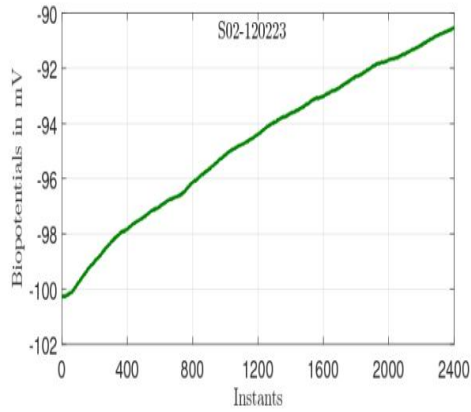
3.2.4 Two New Proposed Signals: Gap and Pair Sum (PS):

It has been observed that both the acquired signals are time-varying in nature. Yet, all the LH and the RH signals acquired from same or different individuals at same or different times remain within certain ranges. Hence, there seems to be an interdependence between the signals, though they are not identical over any two acquired set of 2 minutes.

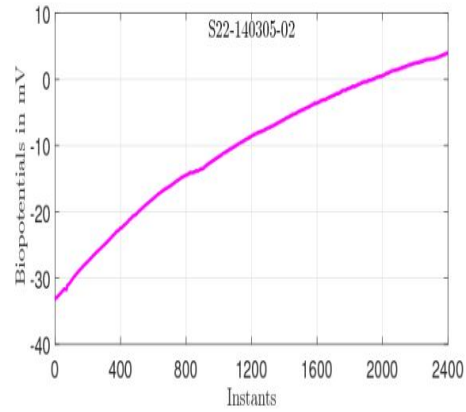
In order to explore this interdependence, sets of data containing the instantaneous difference and instantaneous sum of the LH and RH signals recorded in a data set have been determined. On this basis, two types of derived signals are proposed as follows:

- a) **Gap signal**-The data set resulting from the instantaneous difference between the respective LH and RH biopotentials, that is, $\{x_{LHi} - x_{RH_i}\}$, for $i \in [1,2400]$, has been termed and denoted as the *Gap* signal.
- b) **Pair Sum signal**-The corresponding data set resulting from the instantaneous sum of the acquired pair of signals, that is, $\{x_{LHi} + x_{RH_i}\}$, for $i \in [1,2400]$, has been termed as the *Pair Sum* signal, henceforth denoted as PS signal.

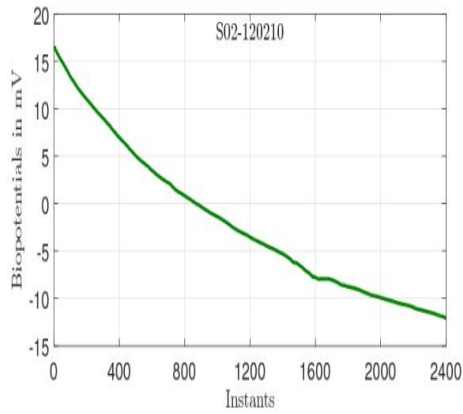
Representative plots of these derived signals are shown in Figure 3.12. From a comparison of Figure 3.12 with Figure 3.4, it can be stated that both these derived signals show all possible variations in terms of polarity, trend as well as range of variation, as have been observed in case of the individual LH and/or RH signals. In view of this, the occurrence of the different polarities and trends in these signals have been analysed hereafter.



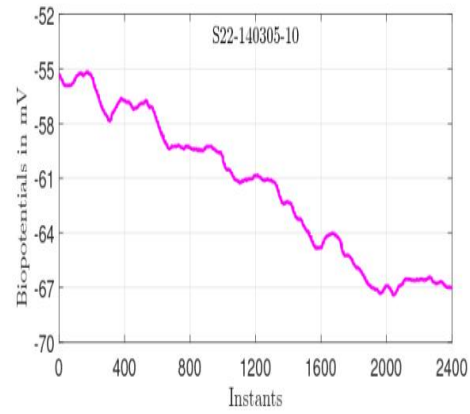
(a) Increasing Negative:Gap



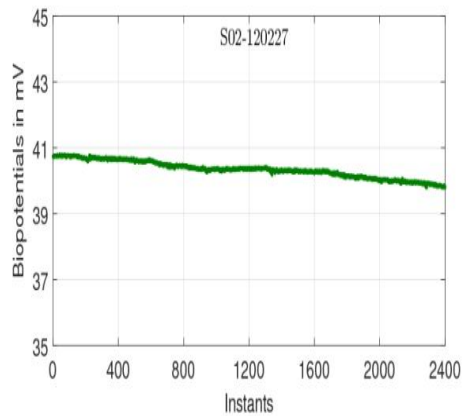
(b) Increasing Transitive:PS



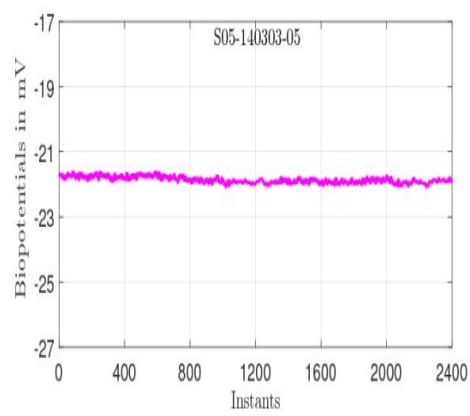
(c) Decreasing Transitive:Gap



(d) Decreasing Negative:PS



(e) Constant Positive:Gap



(f) Constant Negative:PS

Figure 3.12: Representative plots of observed trends and polarities in Gap and PS signals

Polarity of Derived Signals: As in the cases of the individual LH and RH signals, the possibility of occurrence of Positive, Negative or Transitive signals have been determined for the Gap and PS signals also using the same criterion as stated in Section 3.2.2. The counts, in %, of the corresponding cases are tabulated in Table 3.5 and the corresponding bar graph is shown in Figure 3.13. The signals are named PositiveGap, NegativeGap and TransitiveGap and PositivePS, NegativePS and TransitivePS accordingly.

Table 3.5: Occurrence of derived signals with specific polarity

Values	% count	
	Phase1	Phase2
PositiveGap	61.7	43.2
NegativeGap	10.7	51.1
TransitiveGap	27.6	5.7
PositivePS	47.9	3.3
NegativePS	21.1	94.0
TransitivePS	31.0	2.7

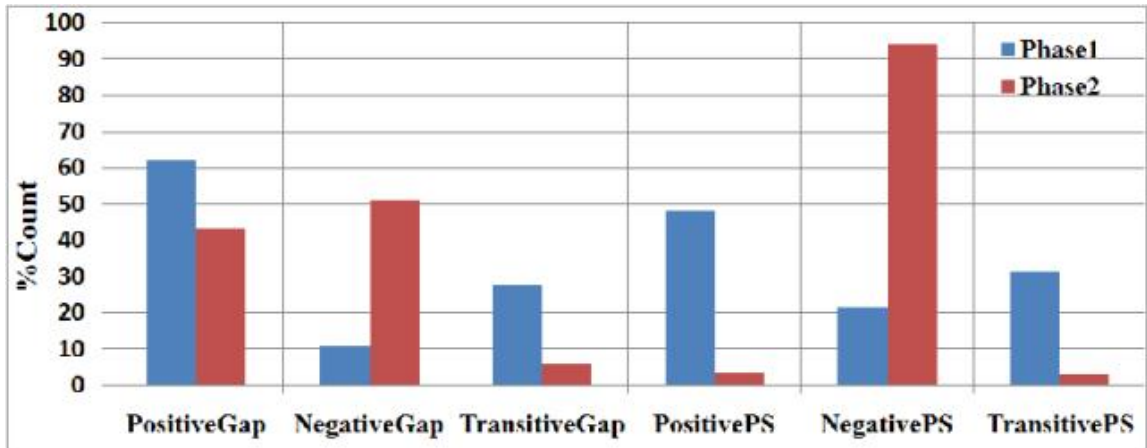


Figure 3.13: Bar graph depicting polarity counts of the Gap and PS biopotentials in Phase1(blue) and Phase2(red)

The observations and inferences can be summarized as follows.

- i) In Phase1, most Gap and PS signals are Positive, while Negative signals are fewer. This indicates that the most likely pairing in Phase1 is that of PositiveLH signals with less PositiveRH signals. However, unlike the case for the LH and RH signals, the Transitive nature is the second most likely for both Gap and PS signals.

- ii) In Phase2, the Transitive signals are very few for both Gap and PS, as also for the individual LH and RH signals. Both Gap and PS signals are most likely to be Negative. This has also been observed for both LH and RH signals.

- iii) In Phase2, the PositiveGap signals are almost as likely as the NegativeGap signals, but PositivePS signals are almost unlikely in Phase2. This is despite the fact that both PositiveLH and PositiveRH signals occur significantly in Phase2. This indicates that a PositiveLH (RH) signal is more likely to be paired with a more NegativeRH (LH) signal in Phase2.

- iv) In Phase2, 94% of the data sets combine to yield NegativePS signals. This is supportive of the findings by earlier researchers as well as the findings of the present study on the polarity of the individual signals, as stated in Section 3.2.2, that the basal SPL or the endosomatic EDA potentials are mostly negative in case of relaxed subjects.

Trends of Derived Signals: These signals, so derived from the recorded biopotentials for each set, have also been analyzed in terms of their trends. The same criteria, as stated in Section 3.2.2 for individual LH and RH signals, has been considered for finding the trends of the derived signals also.

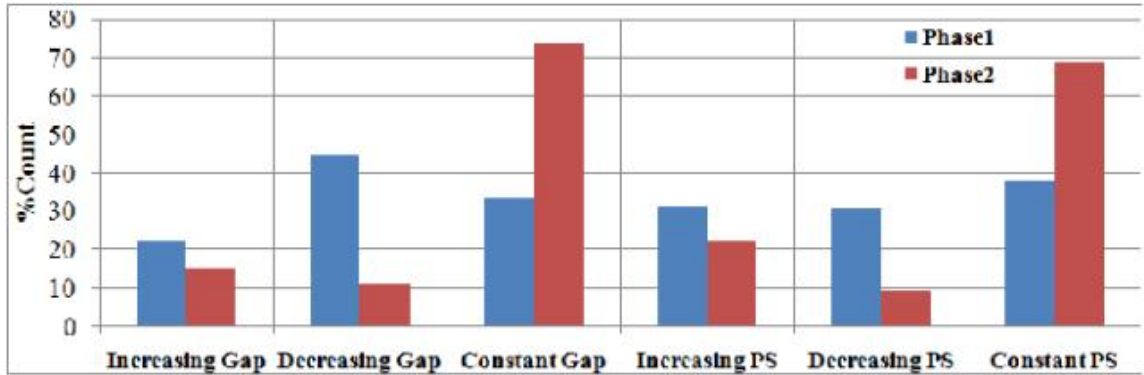


Figure 3.14: Bar graph depicting Trends for Gap and PS signals in Phase1 (blue) and Phase2 (red)

Table 3.6: Occurrence of trends and corresponding minimum Diff and maximum Diff of derived signals

Trend	% Count		Minimum Diff(mV)		Maximum Diff(mV)	
	Phase1	Phase2	Phase1	Phase2	Phase1	Phase2
Increasing Gap	22.14	15.11	4.05	4.12	20.89	44.51
Decreasing Gap	44.53	11.18	-71.77	-25.58	-4.01	-4.04
Constant Gap	33.33	73.72	-3.91	-3.99	3.86	3.76
Increasing PS	31.25	22.05	4.21	4.02	44.8	40.31
Decreasing PS	30.73	09.06	-32.90	-40.51	-4.09	-4.01
Constant PS	38.02	68.88	-3.96	-3.67	3.89	3.93

As in the case of the LH and RH signals, it is relevant to observe the prevalence or absence of a particular trend in comparison to the others for these derived signals also. This has been represented in Figure 3.14 for both phases, while the total count, in %, of the occurrences of these trends for the Gap and PS signals have been stated in Table 3.6. Table 3.6 also lists the values of minimum Diff and maximum Diff of the Gap and PS signals, as earlier defined in Section 3.2.2. The observations can be summarized as follows.

- i) In these cases also, the Constant trend is the most likely for both the phases, except for the Gap signals in Phase1. In this case, the Decreasing trend is the

most likely (44.53%), although the % of occurrence of the Constant trend is also quite large (33.33%). This nature is observed to be identical to the nature of the underlying LH and RH signals.

- ii) In Phase1, the Decreasing trend dominates for the Gap signals, with the Constant and Increasing trends being less and least likely respectively. However, in case of the corresponding Pair Sum (PS) signals in Phase1, it is observed that all the three trends are almost equally likely. No similar finding has been observed for the underlying LH and RH signals.
- iii) In case of Phase2, both the Gap and the PS signals show disparities in likelihood of occurrence of the three trends. In both cases, the Constant trend is significantly most likely, the Increasing trend is quite less likely while the Decreasing trend is the least likely. The dominance of the Constant trend is supported by the finding in Section 3.2.2 that the combinations of a constant trend in one hand with any of the other trends in the other hand is a dominant feature in a pair of signals.
- iv) The overall Diff of the derived signals, as evident from the minimum Diff of the Decreasing trend and the maximum Diff of the Increasing trend, exhibit two different characteristics for the Gap and PS signals.

A comparison of these values for the Gap and PS signals in the two phases show that these are quite similar in case of PS signals, although the overall Diff of Gap signals in Phase1 is significantly larger than that in Phase2.

This is due to the fact that for the Gap signals, the minimum Diff in Phase1 is much smaller than that in Phase2, being almost three times smaller, although the maximum Diff in Phase1 is almost twice smaller than that in Phase2.

So, it can be inferred that in case of Phase2, the acquisition of data over a longer duration expectedly maximizes the Constant trend for the individual signals as well

as these derived signals. Thus, both the Gap and the PS signals depict the nature of interdependence of the LH and RH signals.

The effect of a longer duration of rest is evident in the overall Diff of the Gap signal as well as the prevalence of the Constant trend in both the Gap and PS signals. The overall Diff for the Gap signal is significantly smaller in Phase2 than in Phase1. As in the case of the acquired signals, the effect of the duration of rest is also evident from the increased likelihood of the Constant trend for both these signals in Phase2, as compared to Phase1.

It can further be inferred that the natures of the interdependence vary in the two derived signals. In Phase1, where data was acquired for short duration of rest, the likelihood of occurrences of the three trends as well as the overall Diff differ in case of Gap signals. Contrarily, the PS signals in Phase1 show an almost equal likelihood of all three possible trends and also the overall Diff and hence, are more representative of the baseline nature of the interdependence of the passively acquired LH and RH signals.

3.3 Quantitative analysis of the signals:

The next study involves the quantitative analysis of the recorded (LH and RH) as well as the derived (Gap and PS) signals with the objective of identifying some additional representative features and parameters. In the first stage, all the available data recorded in the two phases are considered for statistical analysis. In order to identify subject-wise features, if any, a subject-wise analysis of the data is then performed by considering the total data recorded for a particular subject in a particular phase. Thereafter, the data are analyzed setwise for identifying some overall characteristic features or parameters of these 4 signals.

3.3.1 Overall analysis:

In this study, the statistical characterization of the overall corpus of data recorded in Phase1 and Phase2 for all sets of all subjects has been done by evaluating the frequency distribution of the data and the data range, span, central tendencies and dispersion.

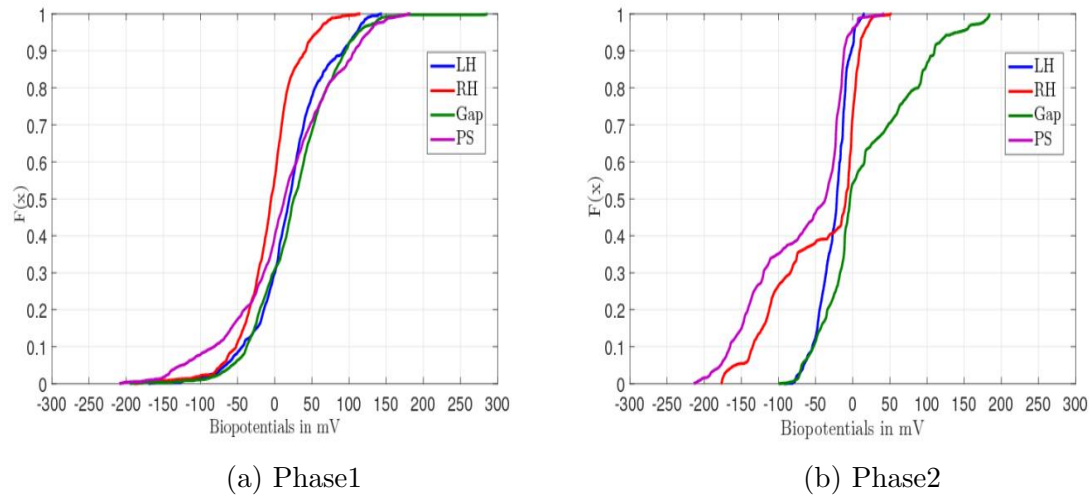


Figure 3.15: Cdf plots of LH, RH, Gap and PS biopotentials recorded in Phase1 and Phase2

In order to infer the variation of the recorded data, the cumulative distribution functions (cdf) have been plotted in Figure 3.15 for LH, RH, Gap and PS signals in both the phases. All four signal types have been considered since it has been observed in Section 3.2 that the overall characteristics displayed by the derived signals are similar to those of the individual biopotentials obtained from each hand.

The basic statistical parameters, namely range, span, two relevant central tendencies, namely median and mean, and the conventional measure of dispersion, namely standard deviation (SD), of the individual signals and the derived signals have been determined for both phases and these are tabulated in Table 3.7. These have been calculated considering all the sets of the 16 subjects for Phase1 and 14 subjects in

Phase2 separately. It is reiterated that for each type of signal, there are 384 sets of data for Phase1 and 331 sets for Phase2 and each set is a record of 2400 number of instantaneous biopotentials.

Table 3.7: Basic statistical parameters of biopotentials

Parameters	Range (mV)		Span mV	Median mV	$Mean_{overall}$ mV	$SD_{overall}$ mV
	Min	Max				
Phase1						
LH	-169.68	144.29	313.97	19.74	19.83	49.71
RH	-189.64	115.31	304.95	-4.72	-7.06	39.13
Gap	-195.09	286.47	481.56	25.78	26.90	54.10
PS	-208.98	182.92	391.90	13.10	12.77	71.26
Phase2						
LH	-93.03	15.26	108.29	-21.31	-25.83	20.27
RH	-177.23	52.29	229.52	-9.26	-44.48	59.69
Gap	-99.72	184.61	284.33	-3.50	18.65	63.28
PS	-213.71	42.43	256.14	-36.69	-70.31	62.79

In this study, two terms, namely the overall mean and overall SD, have been used to denote the mean and SD of all data in all sets in a particular phase and are denoted henceforth as $Mean_{overall}$ and $SD_{overall}$ respectively. These are defined using the standard notions as follows:

$$Mean_{overall} = \frac{1}{N} \sum_{i=1}^N (x_i) \quad (3.1)$$

$$SD_{overall} = \sqrt{\frac{1}{N} \sum_{i=1}^N (x_i - Mean_{overall})^2} \quad (3.2)$$

where N denotes the total number of data, that is 384×2400 for Phase1 and 331×2400 for Phase2.

The observations from the cdf plots in Figure 3.15 as well as the statistical parameters stated in Table 3.7 for the 4 signals are stated hereafter.

- (i) It is observed that the overall span in Phase1 is much larger than that in Phase2 for all 4 signal types. The spans of the Gap and PS signals are larger than LH and RH signals in both phases. The span of LH biopotentials in Phase2 is the least, although the corresponding RH signals exhibit a wide variation. However, in Phase1, the spans of LH and RH biopotentials are almost identical.
- (ii) It is observed from the cdf plots that, as expected, the biopotentials recorded in Phase2 are mostly negative for both the hands, and this is evident from their median values also. The corresponding median values of the Gap and PS signals are also negative.
- (iii) From Figure 3.15a, it can be interpreted that the RH biopotentials are more likely to have smaller values as compared to the LH biopotentials in Phase1. However, such a unimodal trend is not evident in Phase2, as shown in Figure 3.15b. In this case, about 40% of the recorded instantaneous RH biopotentials are smaller than the overall recorded LH biopotentials, while the remaining RH biopotentials are significantly larger than the LH biopotentials.

Since the Gap and the PS signals have negative and positive contributions respectively from the RH signals, hence their natures in this case are antisimilar and similar respectively to that of the RH signal.

- (iv) There is an observed lack of symmetry about the median of the RH data in Phase2. This is reflected in the much larger SD as compared to that of the corresponding LH data. The mean and median values of the RH data in this phase are also far apart while the corresponding LH values are nearer to each other. As expected, the mean and median values for LH and RH data of Phase1 are close to each other.
- (v) The ranges of both LH and RH are within $\pm 200\text{mV}$ and spans are within 320mV . The corresponding ranges and spans of the derived signals are larger, but are well within the maximum possible factor of 2. This reconfirms the

interdependence between the LH and RH signals while the difference in the mean of both hands and also for both phases is characteristic of the bilaterality of the human system.

- (vi) It is seen that the overall ranges of the Gap signal is much more than those of the LH, RH and PS signals for both the phases. Also, the SD is largest for Gap signals for both the phases.
- (vii) As expected from the nature of the cdf plots in Figure 3.15, both LH and RH signals, and hence the derived Gap and PS signals, fail the Chi-square goodness of fit tests for normality at 5% significance levels for both the phases.

3.3.2 Subject-wise analysis:

From the previous analysis considering the data recorded from all the subjects in a phase, it may be inferred that though the variation of the data in a single set of 2 minutes duration is not much, yet the overall statistical parameters show significant variations. It is thus necessary to ascertain whether this variation is an essential characteristic of the biopotentials or is it related to the presence of different subjects.

The next step involves the quantification of these variations in individual subjects. For this, the subject-wise mean and span of the acquired LH and RH biopotentials have been tabulated in Table 3.8 for Phase1 and Phase2.

The detailed statistics of the overall raw data have been stated earlier in Table 3.7 in Section 3.3.1. It can be inferred from the $Mean_{overall}$ and $SD_{overall}$ stated for LH and RH signals in the Table that for a confidence interval of 95% [110], the respective mean values should lie in the interval of

- 1) 14.86mV and 24.80mV for Phase1 and -28.01mV and -23.65mV for Phase2 for LH,
- 2) -10.97mV and -3.15mV for Phase1 and -50.91mV and -38.05mV for Phase2 for RH.

However, it is observed from Table 3.8 that the subject-wise mean values differ

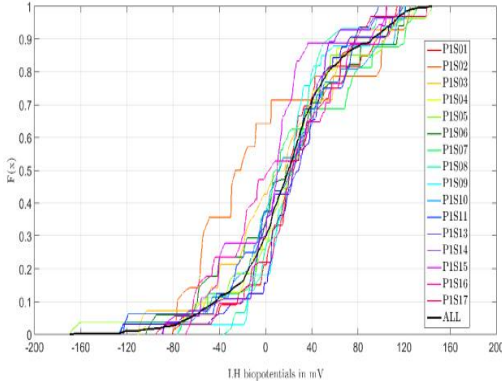
considerably from this range. Even so, the subject-wise mean values are more likely to be within this range in case of Phase1, specifically in the case of 9 and 5 out of 16 subjects respectively for LH and RH signals. In case of Phase2, this does not hold true in general as evident from the fact that out of 14 subjects, none of the subjects have mean values within the range for LH signals and only 2 subjects within it for RH signals.

Table 3.8: Subject-wise mean and span

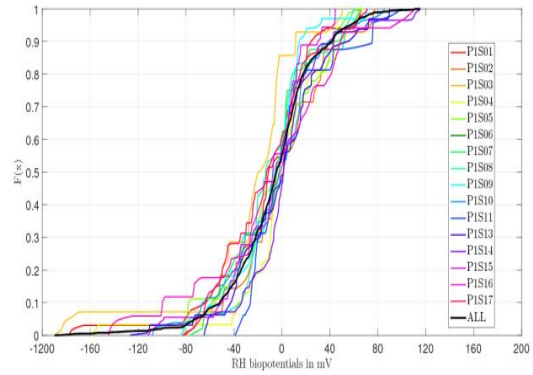
Phase1					Phase2				
Sub. no.	mean(mV)		span(mV)		Sub. no.	mean(mV)		span(mV)	
	LH	RH	LH	RH		LH	RH	LH	RH
S01	24.83	-13.79	195.60	243.70	S02	-40.76	-84.66	45.68	133.50
S02	-1.37	-1.14	206.70	159.50	S04	-12.38	-46.51	52.06	161.40
S03	11.04	-27.64	227.80	240.30	S05	-14.53	-53.97	26.51	208.70
S04	20.13	0.37	241.60	226.10	S10	-21.21	-97.47	103.90	56.55
S05	19.53	-7.16	314.00	148.50	S11	-2.72	-153.52	56.77	64.14
S06	17.02	-12.51	225.80	163.50	S12	-30.56	16.75	50.88	42.73
S07	25.92	-8.28	207.70	141.80	S13	-17.31	-6.63	14.59	57.73
S08	23.60	-6.49	161.90	125.90	S18	-46.23	-40.21	36.92	119.30
S09	24.58	-10.39	195.50	155.90	S19	-29.43	-30.59	42.37	99.31
S10	20.61	-6.94	248.00	194.00	S20	-22.89	-57.27	40.13	117.70
S11	15.66	5.08	221.50	138.80	S21	-21.58	6.56	76.83	61.40
S13	26.20	-1.14	242.60	216.30	S22	-45.47	-2.80	72.56	62.33
S14	18.27	3.45	208.10	180.00	S23	-19.57	-20.31	58.13	119.40
S15	4.88	-11.87	194.80	157.00	S24	-44.03	-127.20	68.24	38.52
S16	12.99	-9.32	174.70	255.60	O/all	-25.83	-44.48	200.35	229.52
S17	26.29	-12.30	234.80	153.90					
O/all	19.83	-7.06	313.97	304.95					

In contrast, it is observed that in general, the span of the subject-wise data in both phases are much smaller than the overall span for both LH and RH signals. More specifically, for 15 out of 16 subjects in Phase1, the LH and RH potentials are limited to less than 85% of the overall span while 13 of 14 subjects in Phase2 have their LH and RH potentials within 75% of the overall span. This reduced spread in

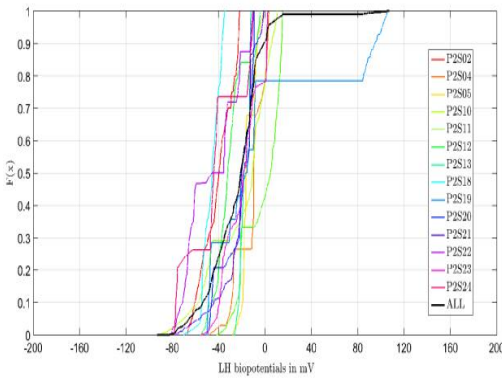
the recorded biopotentials for the individual subjects in Phase2 may also be ascribed to the longer duration of rest.



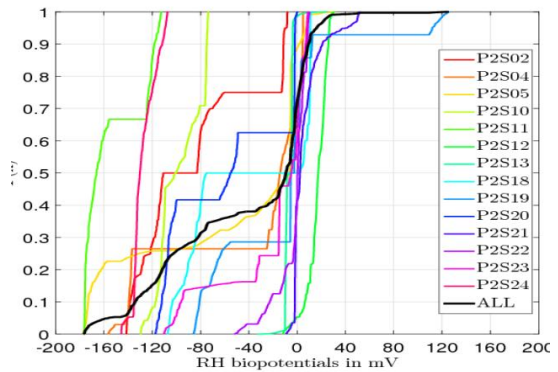
(a) Phase1:LH



(b) Phase1:RH



(c) Phase2:LH



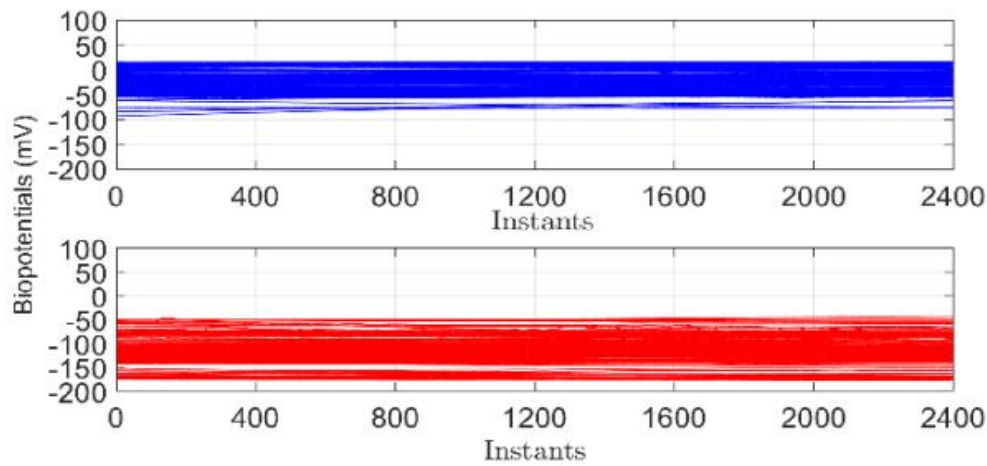
(d) Phase2:RH

Figure 3.16: Subject-wise and overall cdf of LH and RH biopotentials recorded in Phase1 and Phase2

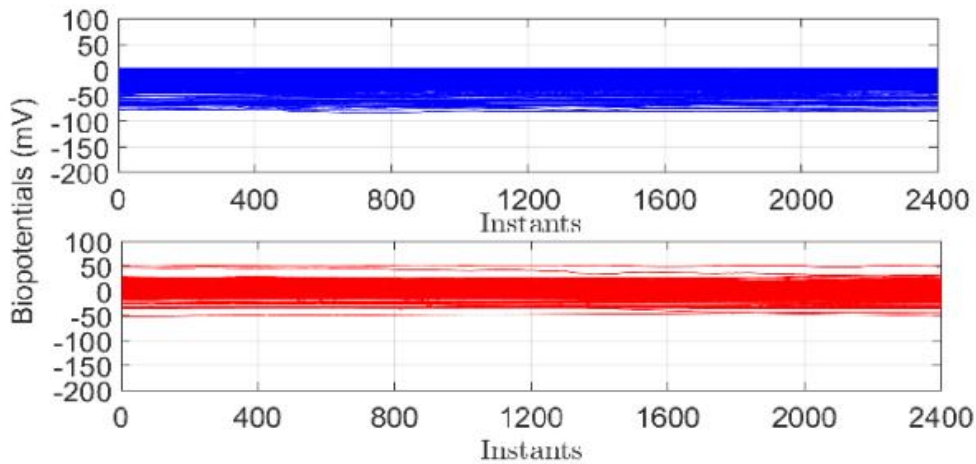
The cdf of the LH and RH biopotentials recorded for 16 subjects in Phase1 and 14 subjects in Phase2 have been plotted in Figure 3.16 along with their corresponding overall cdf plots. From Figure 3.16a and Figure 3.16b of the cdfs of LH and RH biopotentials in Phase1, it is clear that though the variations and ranges of the subject-wise cdfs are not the same, yet most of them appear to be close to the overall cdf except for those of 2 or 3 subjects. This is almost always true for the LH signals in Phase2 also, as evident from Figure 3.16c. However, from Figure 3.16d,

it is clear that this is not so for the RH signals in Phase2, where the variations of individual subjects are widely different as compared to the overall cdf.

3.3.3 Analysis of the anomaly in Phase2 RH signals



(a) Biopotentials on Specific dates; blue- LH, red-RH



(b) Biopotentials on Other dates; blue- LH, red-RH

Figure 3.17: LH and RH biopotentials recorded in Phase2 on specific and other dates

In the previous study, an anomaly is observed in the overall cdf of the RH potentials in Phase2, which cannot be ascribed to one or two specific subjects, as evident in Figure 3.16d. This led to a setwise analysis of the RH potentials recorded for all subjects on various dates.

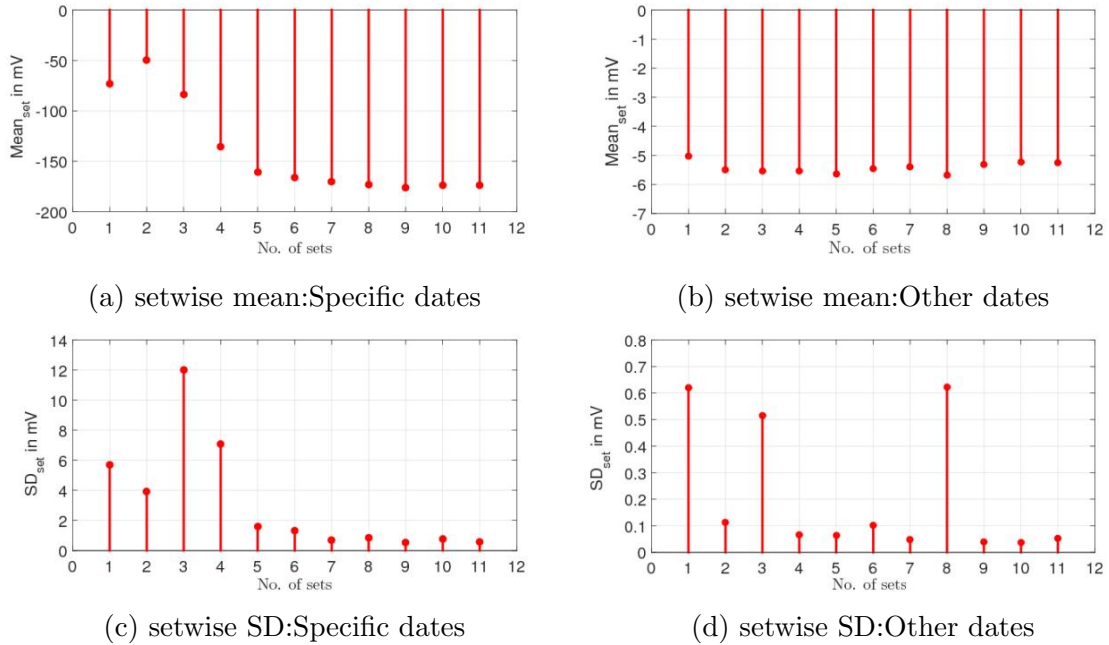


Figure 3.18: Typical setwise mean and SD of Phase2 RH potentials for one subject

It is observed that the RH potentials in Phase2 showed distributed values lower than approximately -50mV for 128 sets of data recorded on 5 specific dates, out of the total 331 sets recorded over 15 days. Figure 3.17a and Figure 3.17b depict the variations of LH and RH potentials on the specific dates and on the other dates respectively. It is also evident from the figures that the corresponding LH potentials do not show such variations. It has been observed that the LH potentials lie within -93.03 to 15.24mV on the specific dates and within -82.92 to 3.26mV on the other dates.

In the next step, the RH potentials recorded in Phase2 were classified into two groups- one for the specific dates and the other for the other dates. A typical plot of

setwise mean and setwise SD of the RH potentials of a subject, whose records were also taken on those specific dates, are given in Figure 3.18.

It is evident that while the setwise mean values of the RH signals are expectedly different for these two groups, the same cannot be clearly said for the setwise SD of these signals. In order to study this further, the setwise statistics of all the Phase2 RH potentials, as well as those for the Specific dates and Other dates, are tabulated in Table 3.9 and the corresponding cdf plots are shown in Figure 3.19.

Table 3.9: Statistical parameters of Phase2 RH biopotentials

Parameters for	Range (mV)		Span mV	Median mV	Mean mV	SD mV
	Min	Max				
All dates	-177.23	52.29	229.52	-9.26	-44.48	59.69
Specific dates	-177.23	-43.02	134.21	-79.89	-70.10	60.98
Other dates	-52.04	52.29	104.33	0.00	0.57	10.24

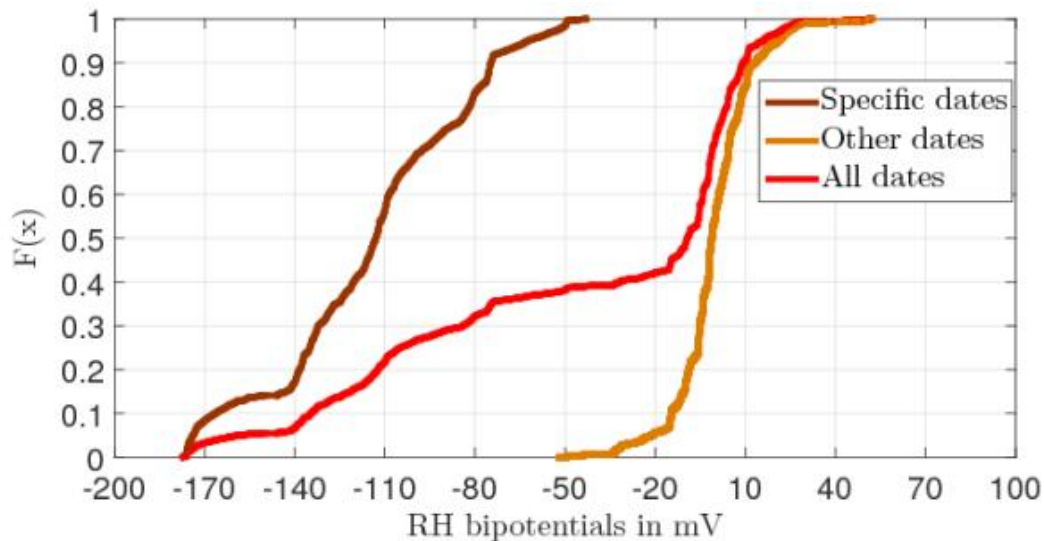


Figure 3.19: Cdf plots of Phase2 RH biopotentials

It can be inferred from the plots as well as the statistics that while the overall or even the subject-wise RH potentials in Phase2 might seem distributed over a wide

range yet, unlike those recorded on the specific dates, the variations in the setwise RH potentials are significantly smaller for the Other dates. For those specific dates, the SD is almost 6 times of that for the other dates. In view of this, the nature of changes in the biopotentials in a set acquired randomly and in consecutively acquired sets have been investigated.

3.3.4 Setwise analysis

The previous study leads to the quantitative study of the setwise data recorded for all the four types of signals in both phases. For this study, the mean of each set of data, henceforth referred as the setwise mean, $Mean_{set}$, of the recorded potentials as well as their standard deviations, henceforth referred to as setwise SD, SD_{set} , have been calculated for all the signals of all subjects in both phases as follows:

$$Mean_{set} = \frac{1}{2400} \sum_{i=1}^{2400} (x_i) \quad (3.3)$$

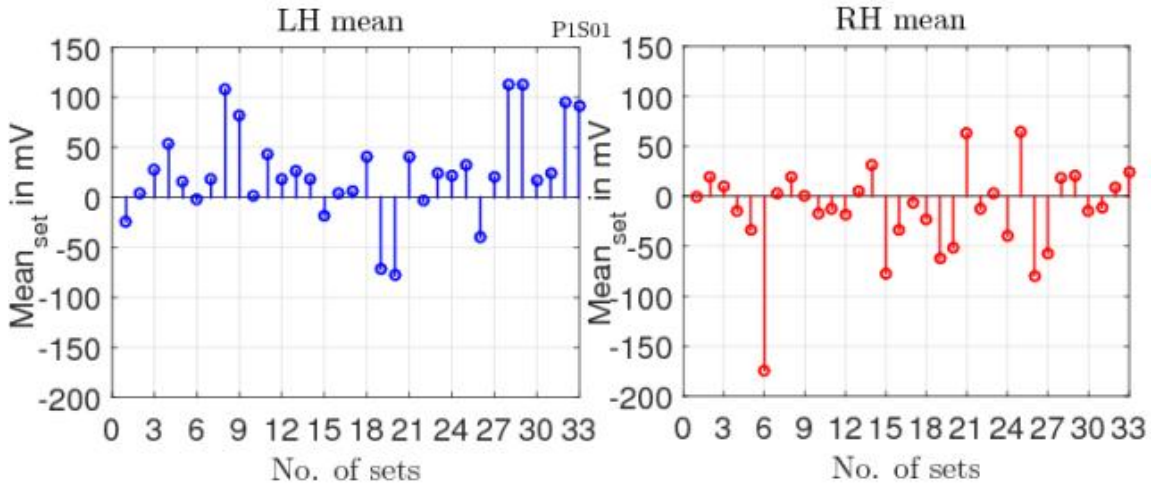
$$SD_{set} = \sqrt{\frac{1}{2400} \sum_{i=1}^{2400} (x_i - Mean_{set})^2} \quad (3.4)$$

It is to be noted that the mean and SD of all the setwise mean values, considering all subjects, have henceforth been referred to as the $Mean_{Mean_{set}}$ and $SD_{Mean_{set}}$ of the respective signal. Denoting the setwise mean of a particular set as $Mean_{set-i}$, the $Mean_{Mean_{set}}$ and $SD_{Mean_{set}}$ are defined as follows:

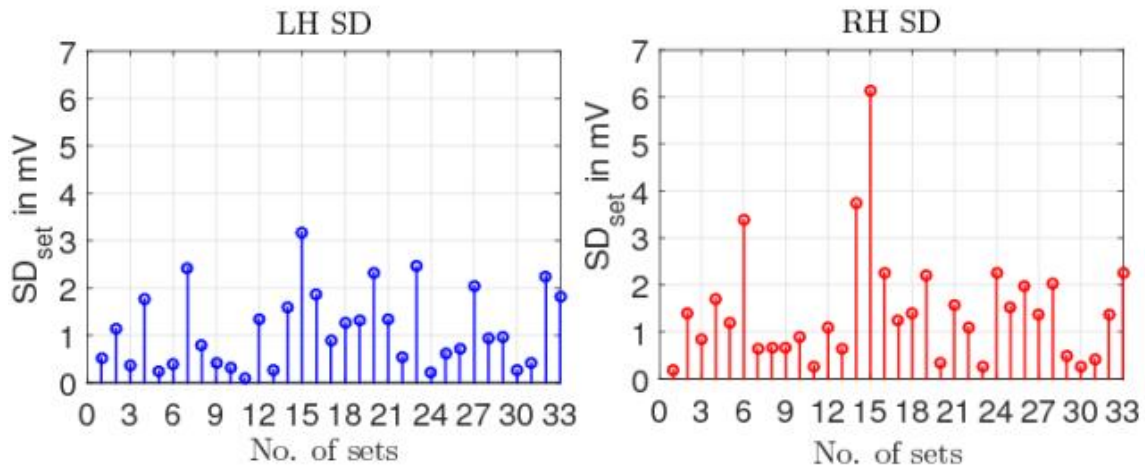
$$Mean_{Mean_{set}} = \frac{1}{N} \sum_{i=1}^N (Mean_{set-i}) \quad (3.5)$$

$$SD_{Mean_{set}} = \sqrt{\frac{1}{N} \sum_{i=1}^N (Mean_{set-i} - Mean_{Mean_{set}})^2} \quad (3.6)$$

where $N=384$ for Phase1 and $N=331$ for Phase2.



(a) $Mean_{set}$

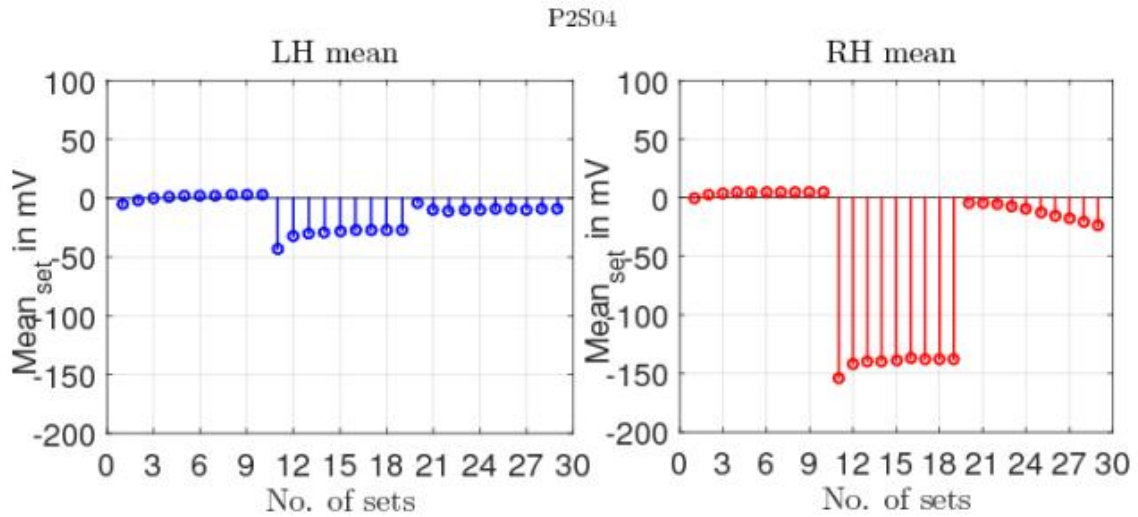


(b) SD_{set}

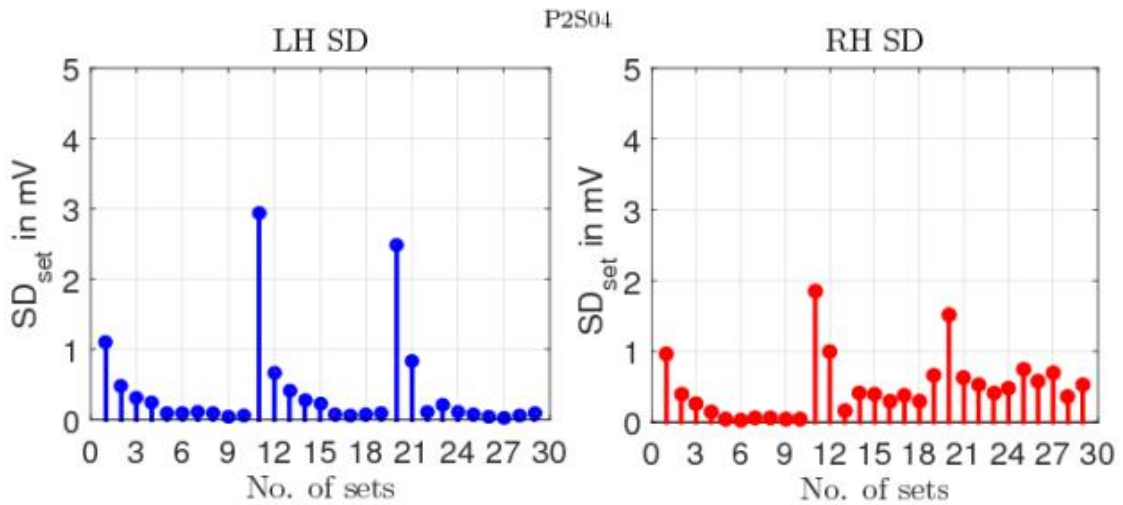
Figure 3.20: Typical plot of $Mean_{set}$ and SD_{set} for one subject:Phase1

A representative plot of the $Mean_{set}$ and the corresponding SD_{set} values of LH and RH potentials from Phase1 of a single subject, where one set of data was recorded

in a day, are shown in Figure 3.20. The corresponding plots in Phase2 of a single subject, with 10 sets of data recorded everyday for 3 days, are shown in Figure 3.21.



(a) $Mean_{set}$



(b) SD_{set}

Figure 3.21: Typical plot of $Mean_{set}$ and SD_{set} for one subject:Phase2

It is observed that in both phases, the natures are similar for the LH and RH

signals. Specifically, in Phase1, the $Mean_{set}$ and SD_{set} values are different and vary randomly. In case of Phase2, the mean values are close in the bunches of the 10 sets recorded consecutively in a single session. However, random variations similar to that observed in Phase1 are evident when groups of 10 consecutive sets are compared with each other.

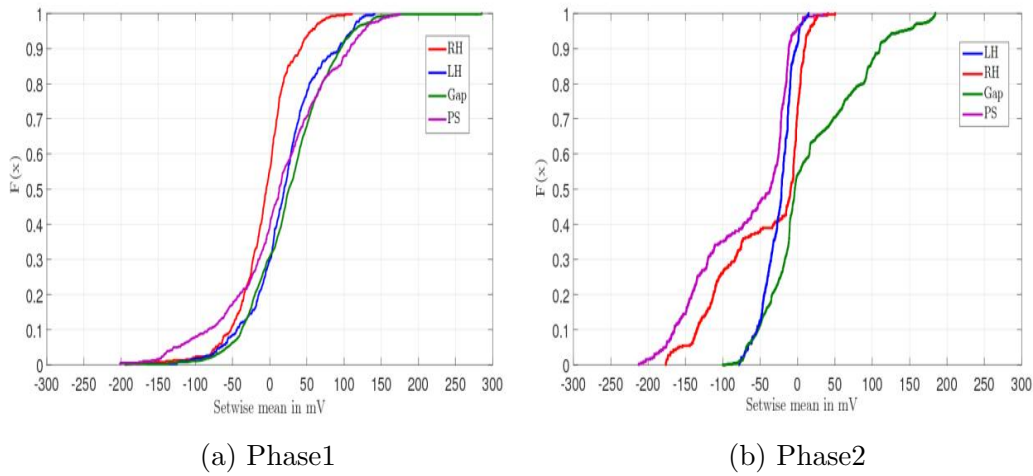


Figure 3.22: Cdf plots of $Mean_{set}$ of all 4 signals in Phase1 and Phase2

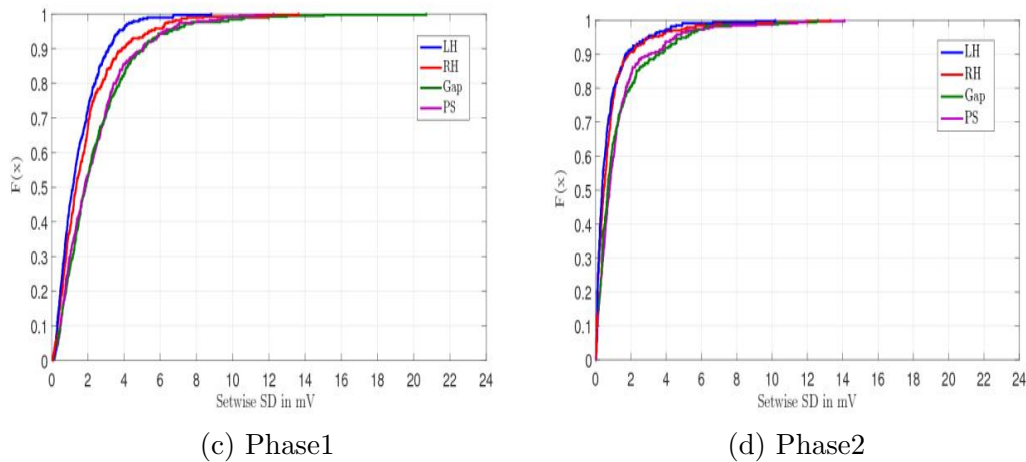


Figure 3.23: Cdf plots of SD_{set} of all 4 signals in Phase1 and Phase2

Another remarkable feature is that the SD_{set} values for Phase1 are typically larger

than the SD_{set} values for Phase2. In order to interpret this, the SD_{set} s of the first sets of each group of 10 consecutive sets in Phase2 are compared to the SD_{set} s of the sets in Phase1. The natures are similar. It can thus be hypothesized that the SD values for the first sets are all high followed by gradually decreasing values, showing that the variability of both the LH and RH potentials decreases with rest.

In order to validate these findings, the $Mean_{set}$ and SD_{set} for all the sets of data in both phases for all four types of signals of all subjects have been studied. The number of $Mean_{set}$ and SD_{set} values thus generated for the signals are 384 and 331 in Phase1 and Phase2 respectively. The cdf plots of the $Mean_{set}$ and the SD_{set} are plotted in Figure 3.22 and Figure 3.23 respectively.

Table 3.10: Chi-square test for ($Mean_{set}$) values

Hypothesis	H_0 : signal is normally distributed H_A : signal is not normally distributed				
Theoretical χ^2					
df	3	4	5	6	7
$\chi^2_{0.05}$	7.815	9.488	11.070	12.592	14.067
$\chi^2_{0.95}$: 0.352 for df=3					
Calculated χ^2					
Signal type	LH	RH	Gap	PS	
Phase1	25.779 (df=7)	23.676 (df=4)	2.407 (df=3)	26.731 (df=6)	
Phase2	50.588 (df=7)	383.981 (df=7)	67.436 (df=6)	336.213 (df=7)	
Conclusion	H_0 rejected for all except Gap signals in Phase1 at 5% significance level				

From the cdf plots of the $Mean_{set}$ of all 4 signal types, in Figure 3.22, it is not clear whether the signals are normally distributed. So, the normality of the $Mean_{set}$ values of all 4 signals for both phases was tested using Chi-square goodness of fit tests, which were performed at 5% significance levels as shown in Table 3.10. The

theoretical χ^2 values with corresponding degrees of freedom (df) are taken from a standard table and are provided for ready reference. The proposed null hypothesis is that the setwise mean values of LH, RH, Gap and PS signals for both the phases follow a normal distribution against the alternative hypothesis that the data are not normally distributed. The test results indicate that the $Mean_{set}$ values, and so also the original acquired signals, are not normally distributed, except for the Gap signals in Phase1.

It is further obvious from Figure 3.23 that the setwise SD in both phases are typically low, within few tens of mV. This corroborates the earlier observations regarding the daily variations in the signals.

Table 3.11: Statistical characteristics of setwise mean, $Mean_{set}$ of LH, RH, Gap and PS signals

Parameters	Range (mV)		Span mV	Median mV	$Mean_{Mean_{set}}$ mV	$SD_{Mean_{set}}$ mV
	Min	Max				
Phase1						
LH	-165.59	141.50	307.09	19.53	19.83	49.74
RH	-180.58	111.06	291.64	-4.60	-7.06	39.09
Gap	-189.05	284.37	473.42	26.49	26.90	54.07
PS	-201.78	176.52	378.3	12.81	12.77	71.28
Phase2						
LH	-78.04	14.95	92.99	-21.30	-25.83	20.25
RH	-176.24	50.31	226.55	-9.22	-44.48	59.76
Gap	-89.78	184.18	273.96	-3.39	18.65	63.34
PS	-212.45	40.70	256.14	-36.74	-70.31	62.85

In order to study the various aspects of the $Mean_{set}$ and the SD_{set} of these signals in more detail, their statistics have been tabulated in Table 3.11 and Table 3.12 respectively and the overall observations and inferences are listed hereafter. It is to be noted that for this purpose, the cdf plots of the setwise mean in Figure 3.22 have been compared with those of the overall data in Figure 3.15, while their statistics in Table 3.11 and Table 3.7 respectively have also been compared.

Table 3.12: Statistical characteristics of setwise standard deviations, SD_{set} of LH, RH, Gap and PS signals

Parameters	Range (mV)		Span mV	Median mV	$Mean_{SD_{set}}$ mV	$SD_{SD_{set}}$ mV
	Min	Max				
Phase1						
LH	0.08	8.82	8.74	1.18	1.51	1.23
RH	0.06	13.64	13.58	1.36	1.86	1.80
Gap	0.08	20.69	20.61	1.87	2.48	2.30
PS	0.10	12.25	12.15	1.82	2.35	1.99
Phase2						
LH	0.02	9.06	10.20	0.37	0.77	1.18
RH	0.02	13.30	13.28	0.47	0.89	1.48
Gap	0.02	12.60	12.58	0.69	1.33	1.81
PS	0.02	14.10	14.08	0.79	1.31	1.78

- (i) A comparison of the cdf plots for the recorded and derived signals of all the subjects for both the phases shown in Figure 3.15 and the corresponding cdf plots for the corresponding setwise mean of all the signals shown in Figure 3.22 shows that the nature of variation of the overall signals and that of the corresponding setwise mean values are almost identical. A comparison of the corresponding ranges and statistics of the original signals and the setwise mean values, stated in Table 3.7 and Table 3.11 are also very close.
- (ii) The span of the overall data is slightly larger than the span of the corresponding $Mean_{set}$ values, except for PS signals in Phase2, and this is evident from the corresponding ranges also.
- (iii) It can be theoretically established that $Mean_{Mean_{set}} = Mean_{overall}$. However, it must be noted that $SD_{Mean_{set}} \neq SD_{overall}$, though they are very close. This is so since $SD_{Mean_{set}}$ denotes the dispersion of the setwise means, which are representative of each set of recorded data, while $SD_{overall}$ denotes the dispersion

of the total corpus of actual recorded data in a phase.

- (iv) The variability of the data in a set around its setwise mean, $Mean_{set}$, is indicated in its SD_{set} value. As evident from the range of the SD_{set} values in Table 3.12, this variability is very low for all the subjects, both in Phase1 and in Phase2.

As can be seen from the cdf plot for SD_{set} in Figure 3.23 also, 90% of the SD_{set} values lie within 5mV in Phase1 and 4mV in Phase2. This difference, though not very significant, is to be expected due to the extended period of rest in Phase2. This finding also validates the choice of $\pm 4mV$ as the limit for classification of the signal trends for both the phases.

- (v) A notable feature in the overall as well as the setwise statistics in both phases is the large difference in the mean and median of the overall RH signals, while that of the LH signals are almost identical. This is particularly remarkable in case of Phase2, where the anomaly in the RH signals was observed. However, a comparison of the large overall SD (59.69mV) with the significantly smaller setwise SD, with $Mean_{SD_{set}} = 1.86mV$ and $SD_{SD_{set}} = 1.80mV$, of the Phase2 RH signals confirms that this is primarily due to a shift in the setwise means of the RH signals in Phase2 for some specific dates and not due to large variations in the signals per se.

As expected, this characteristic affects the corresponding values of the setwise mean of the derived signals also. However, as noted earlier, the corresponding values in the overall and setwise statistics, though very close, are not identical for the LH, RH, Gap as well as PS signals.

- (vi) As in case of the mean of the overall signals, a comparison of the ranges of the $Mean_{set}$ values of all 4 signal types also shows that the span for derived signals are more than those for the acquired signals for both the phases.
- (vii) It is to be noted from Table 3.12 that the overall spans of the SD_{set} values

are typically an order smaller than that of the $Mean_{set}$ values. Even so, the spans and maximum values of SD_{set} are smaller for LH signals than RH signals in both phases indicating a likelihood of larger variability in case of the RH signals in the class of subjects whose data have been acquired.

It is also noted that in case of SD_{set} values, there is not much difference in the mean or median of any of the 4 signal types in any of the phases. Additionally, the SD of these setwise SDs, $SD_{SD_{set}}$ is typically within 2mV for all signals in both phases, except for the Gap signals in Phase1.

3.4 Discussions

In this chapter, the qualitative and quantitative features of endosomatic EDA potentials acquired from the left hand (LH) and the right hand (RH) of human subjects have been studied. These signals, which may be considered as slowly changing baseline biopotentials of these human subjects, were recorded in two phases, Phase1 and Phase2, with short 2 minute and much longer durations of rest respectively. The study has been performed for a total of 715 pairs of biopotentials, specifically 384 pairs of biopotentials recorded in Phase1 and 331 pairs recorded in Phase2.

The primary qualitative observation regarding the acquired data is that in both phases, the LH, as well as the RH, potentials lie within a limited range, typically $\pm 300\text{mV}$ with variability being an essential feature. Both LH and RH biopotentials vary continuously with time, with different values and trends exhibited for each hand, even for the same person on different dates or for different persons on the same date. However, they vary within few tens of mV only in a span of 2 minutes, which is equivalent to 2400 instants at a sampling rate of 50ms.

These biopotentials have thereafter been classified in terms of their polarities as well as trends and their prevalence in a particular phase have been studied in terms of % occurrence. The data sets have been segregated into three categories in terms of their polarities, namely Positive, Negative and Transitive data sets, and in

three categories in terms of their trends, namely Increasing, Decreasing and Constant trends.

In the next stage, the pairs of LH and RH signals recorded simultaneously in a data set have been classified in terms of their patterns. The pair of signals have been characterized in terms of the four possible patterns, namely Parallel, Converging, Diverging and Crossing signals.

A major observation is that LH and RH biopotentials remain bounded in a limited range despite their inherent variability over the large duration for which the data was recorded for all the subjects. This indicates an interdependence between the LH and RH signals. This aspect has been explored by defining two derived signals in terms of the instantaneous difference and instantaneous sum of the pairs of LH and RH signals acquired in a set. These are termed respectively as the Gap and Pair Sum (PS) signals.

It is observed that the four acquired and derived signals are mostly Positive or Negative in Phase1, though they are mostly Negative in Phase2, where the data was acquired over longer durations of rest. This is consistent with findings and conjectures in reported literature [108], [109], [111], [28]p26. The Transitive signals were found to be minimal for both hands and for both phases and typically occurred during midday. In Phase2, the overall variability of RH as well as Gap signals is quite high as compared to the corresponding PS signals in both phases. A special feature of the Gap and PS signals in Phase1 is that the Transitive polarity is the second most likely, which is unlike the natures of the underlying LH or RH signals.

Among the signal trends, it is noted that the Constant trend typically dominates in all signals in both phases. It is also observed that if all the combinations of a Constant trend in any one hand, LH and/or RH, with any of the other trends in the other hand are considered, then almost 72% of the data sets in Phase1 and 97% of the data sets in Phase2 fall in this category. Thus, increased duration of rest has a tendency to stabilize the baseline biopotentials.

However, it is observed that the natures of the interdependence vary in the two

derived signals. In Phase1, where data was acquired for short duration of rest, the likelihood of occurrences of the three trends differ in case of Gap signals. Contrarily, the PS signals in Phase1 show an almost equal likelihood of all three possible trends.

In the pair of signals, it is observed that the Parallel pattern dominates in Phase2, in which data was recorded over prolonged duration of rest. Even in Phase1, this is the second most likely pattern. As is to be expected, the Crossing pattern was observed to occur the minimum number of times in both the phases.

In general, it is observed from the data recorded over both phases for both hands that all three polarities and all three trends of the 4 signals as well as all four patterns of a pair of signals are a common feature for every individual and that these may occur at various times. It has also been observed that the polarities, trends as well as patterns often repeat for an individual, but there is no definite interval of time for this to occur.

In the next stage, the quantitative analysis of the acquired as well as derived set of signals, namely LH, RH, Gap and PS signals, has been performed. From the cumulative distribution function (cdf) plots of all these signals and Chi-square goodness of fit tests, it is evident that these signals do not follow a normal distribution, as might be expected for biological signals [112].

The basic statistical parameters, namely range, span, two relevant central tendencies, namely median and mean, and the conventional measure of dispersion, namely standard deviation (SD), of the individual signals and the derived signals have also been determined for both phases. While the individual sets of these signals, as recorded/determined in a set of 2 minutes, show limited variation, yet the statistical parameters determined for the overall collected data in both phases show significant variability.

In order to determine whether this variation is related to the presence of different subjects, the LH and RH data recorded from individual subjects over the total duration in both Phase1 and Phase2 have been analyzed. The study does not show any apparent subject-wise characteristics, except the expected reduction in the span of

the data recorded subject-wise, as compared to the overall data, in both the phases for both LH and RH signals.

Another general observation from the cdf plots of the signals shows that while all signals in Phase1 as well as LH signals in Phase2 exhibit an unimodal distribution as expected, the RH signals and the associated Gap and PS signals in Phase2 do not follow this nature. In order to study this phenomena, the individual sets of RH signals in Phase2 have been analyzed. It is clearly seen that the RH signals recorded for different subjects in Phase2 on certain specific dates show mean values in different ranges, while the RH signals recorded on all other dates follow the expected unimodal distribution. Also, while the SD of the data recorded on the specific dates are higher, yet the individual sets do not seem to show much variation. It is also observed that the corresponding LH potentials do not show such variations.

This leads to the quantitative study of the setwise data recorded for LH and RH potentials and also for the corresponding Gap and PS potentials in both phases. It is observed that the setwise mean values, $Mean_{set}$ of all the signals show similar natures of variation as seen for the overall signals. Also, in accordance with the findings for the overall data, all four signals in Phase2, and their median values, are mostly negative for both the hands.

The associated setwise SD values, SD_{set} show low variations for both the phases. In fact, 90% of the SD_{set} values lie within 5mV in Phase1 and 4mV in Phase2. This finding validates the choice of $\pm 4mV$ as the limit for classification of the signal trends for both the phases. Even so, the spans and maximum values of SD_{set} are smaller for LH signals than RH signals in both phases indicating a likelihood of larger variability in case of the RH signals in the class of subjects whose data have been acquired.

It is also noted that in case of SD_{set} values, there is not much difference in the mean or median of any of the four signal types in any of the phases. Additionally, the SD of these setwise SDs, $SD_{SD_{set}}$ is typically within 2mV for all signals in both phases, except for the Gap signals in Phase1.

It is notable that in case of the Phase2 RH signals also, the large overall SD

(59.69mV) contrasts with the significantly smaller setwise SD, with $Mean_{SD_{set}}$ and $SD_{SD_{set}}$ both within 2mV, to confirm that this is primarily due to a shift in the setwise means of the RH signals in Phase2 for some specific dates and not due to large variations in the signals per se.

Based on the aforementioned findings, it may be said that the setwise mean, $Mean_{set}$, values of LH and RH signals are representative of the LH and RH biopotentials in a set of data acquired from the human subjects. It follows that the $Mean_{set}$ of the Gap and PS signals are also representative of the derived Gap and PS signals in any set.

Furthermore, among the two derived signals, while the Gap signals show more variability, the PS signals show remarkable consistency across both the phases and for both the overall and the setwise analysis and hence, are more representative of the baseline nature of the interdependence of the passively acquired LH and RH signals..

Chapter 4

Characterisation of the Deviation Signals

4.1 Introduction

In Chapter 3, the biopotentials that have been passively acquired from various human subjects have been characterized qualitatively as well as quantitatively. It is to be noted that physical inference of the particular subjects have not been presented in this study, although the effects of the quantum of rest on all the subjects and also the biopotentials of all those subjects whose data were acquired on some particular dates of measurement have been inferred from both the qualitative and the quantitative aspects.

The individual natures of the signals have been qualitatively studied in terms of trend and polarity, and their pairwise nature has been studied in terms of exhibited patterns. The occurrence of these aforementioned qualitative features have then been quantified by interpreting the standard statistical parameters like mean, SD, skewness, kurtosis and cdf plots. It is observed that in both phases of measurement involving different quantum of rest, the statistical characteristics of the respective overall LH, RH, Gap and PS signals and their setwise means show great similar-

ity. Hence, the setwise mean of an individual acquired, or derived, signal has been considered as an attribute for the signal.

A subsequent analysis is now required to characterise the time-series nature of the signals, both acquired and derived. In order to provide a common basis for all four types of signals, the setwise mean is removed from the signals and then these *deviation* signals are characterised.

The chapter is organised as follows. The general characteristics of the Deviation signals and their statistical characteristics are studied and described in Section 4.2. The trends of the Deviation signals are seen in Section 4.2.1. This is followed by the classification of the Deviation signals as pairs in Section 4.2.2. The modelling of the Deviation signals and the identification of certain signal attributes have been detailed in Section 4.3 and the analysis of the model is discussed in Section 4.4. This is followed by a study of the interrelationship between the two regression model parameters, Zero Crossing Instant (ZCI) and slope m in Section 4.5. The overall discussions are stated in Section 4.6.

4.2 General Characteristics:

In Chapter 3, the acquired LH and RH signals, as well as the derived Gap and PS signals have been observed to be time-series plots with a small variability about their respective setwise mean, $Mean_{set}$. In order to study this variation in the signals, the corresponding Deviation signals, henceforth denoted as LHdev, RHdev, Gapdev and PSdev, have been derived using standard notions [104] by removing the corresponding signal bias, $Mean_{set}$, from the respective signal. Hence, the four Deviation signals in Phase1 as well as Phase2 corresponding to the four acquired and derived signals have been obtained as

$$LHdev = LH - Mean_{set}(LH) \quad (4.1)$$

$$RHdev = RH - Mean_{set}(RH) \quad (4.2)$$

$$Gapdev = Gap - Mean_{set}(Gap) \quad (4.3)$$

$$PSdev = PS - Mean_{set}(PS). \quad (4.4)$$

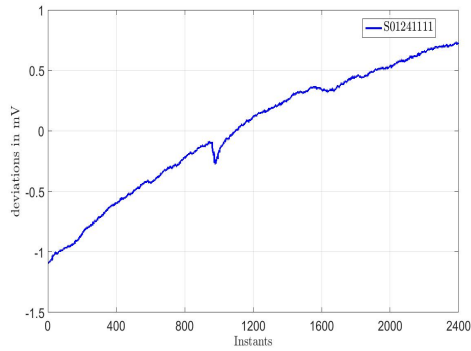
It is to be noted that in case of Phase2, where the subjects were in prolonged durations of rest, the setwise mean values were considered for each individual set of 2 minutes duration.

In order to visualize the effect of varying durations of rest on the signals, representative LHdev and RHdev signals from Phase1 as well as the initial set, namely set1, and the last recorded set, specifically set8 in this case, from a sample recorded in Phase2 are shown in Figure 4.1.

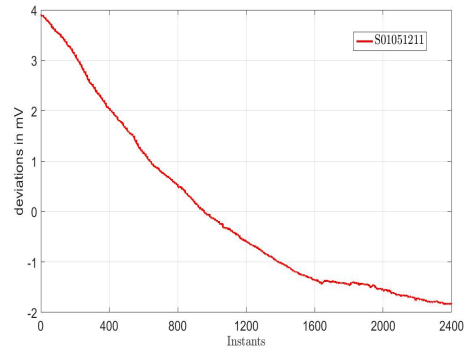
It is observed that, in general, the Deviation signals in Phase1 and in set1 of Phase2 show monotonic variations. However, in case of the LHdev and RHdev signals recorded for the particular subject in set8 of Phase2, when the subject is in a deeply relaxed condition, the signal variations are not smooth and the overall range of signal variation has also decreased significantly. This is in accordance with the findings reported in literature [28], [113].

In order to study these signals further, the actual recorded LH and corresponding LHdev signals as well as the recorded RH and corresponding RHdev signals for all subjects in both Phase1 and Phase2 are shown in Figure 4.2, while the corresponding derived signals and their deviations, namely Gap and Gapdev as well as PS and PSdev signals, are shown in Figure 4.3.

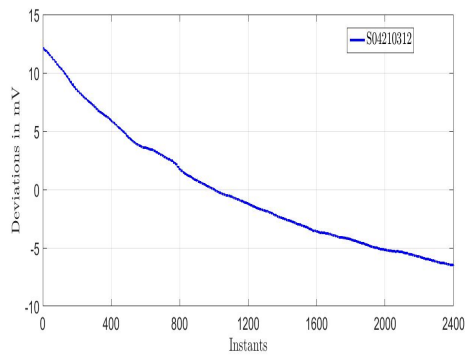
Thereafter, the nature of the distributions of all the four Deviation signals have been studied. For this, their cdfs have been plotted in Figure 4.4 for both the phases and it is observed that in all cases 90% of the instantaneous deviations lie within ± 10 mV. So, the cdf plots are further elaborated for the region ± 10 mV in Figure 4.5.



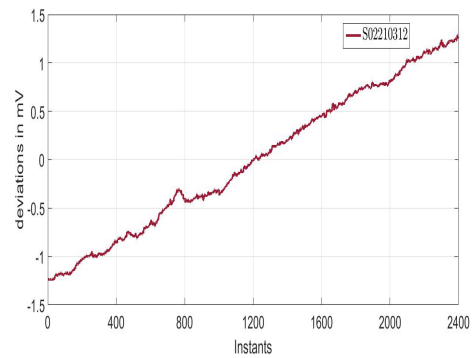
(a) LHdev: Phase1



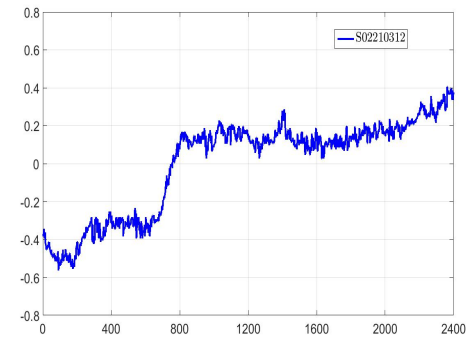
(b) RHdev: Phase1



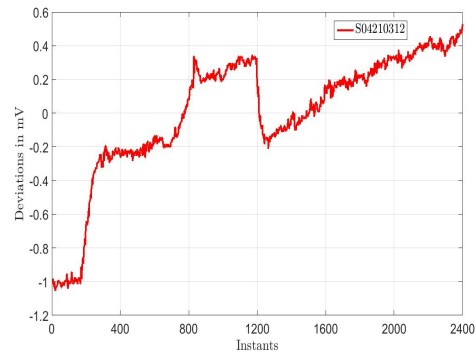
(c) LHdev: Phase2, set1



(d) RHdev: Phase2, set1



(e) LHdev: Phase2, set8



(f) RHdev: Phase2, set8

Figure 4.1: Sample time-series plots of LH and RH Deviation signals in sets of Phase1 and initial and final sets of Phase2

The statistical parameters of the four Deviation signals in both phases are tab-

ulated in Table 4.1. In this case, the skewness and kurtosis of the signals are also evaluated in order to interpret the nature of these signals in more detail.

The observations from the time-series plots in Figure 4.2 and Figure 4.3, the cdf plots in Figure 4.4 and Figure 4.5 as well as the tabulated statistical parameters of all these four Deviation signals in Table 4.1 are listed hereafter.

For this analysis, the values in Table 4.1 for the Deviation signals have also been compared with those of the actual acquired and derived signals stated in Table 3.7 in Section 3.3, as relevant.

1. It is observed in Figure 4.2 and Figure 4.3 that, as expected, the LH and RH deviations, as well as the Gap and PS deviations, vary with time for both the phases for all subjects and for all sets for both hands.
2. The removal of the respective $Mean_{set}$ from a signal leads to a common basis for comparing the various signals, since all the Deviation signals vary within a much narrower range of ± 30 mV, unlike the overall signal variations within ± 300 mV.

It is obvious that the mean of all the signals are 0mV. It is observed from Table 4.1 that the median values of all four Deviation signals in both phases are also very close to 0mV. Furthermore, these signals are in general neither left nor right skewed.

3. It is further observed from Table 4.1 that the variation in LHdev is significantly smaller, within ± 20 mV in both Phase1 and Phase2, as compared to that in RHdev. The larger variability of RHdev leads to corresponding variations in Gapdev and PSdev signals.

This is also reflected in the smaller values of SD for LHdev signals, 1.94mV and 1.40mV, as compared to those for the RHdev signals, 2.58mV and 1.73mV, in Phase1 and Phase2 respectively. This finding is comparable with the setwise SD, SD_{set} , values of the acquired biopotential ranges mentioned in Table 3.12.

It is observed that the mean of the setwise SDs, $Mean_{SD_{set}}$, are 1.51mV and 0.77mV for LH signals in Phase1 and Phase2, while the corresponding values for RH signals are 1.86mV and 0.89mV respectively.

4. It is observed from Figure 4.2 that for both Phase1 and Phase2, the LHdev and RHdev signals seem to vary in an overall monotonic manner, albeit very gradually, with time in the limited duration of typically 2 to 10 minutes. Most of these signals cross zero in the middle epoch of the time-series plot and this indicates the time at which the setwise mean occurs in a data set.

It is further observed that this smooth nature of the variations are lost in certain cases, particularly in case of RHdev signals in Phase2, as also in certain cases in LHdev in Phase2. This occurs typically when the subjects are in the later stages of the extended periods of rest. During this stage, some of the supine subjects enter a sleep state with associated small motor movements and/or snoring. It has been observed that in the signals that have been recorded, this feature is more evident in the RHdev signals. In the corresponding LHdev signals, they may not be evident at all or else, may be present in much reduced orders.

However, irrespective of this phenomena, all LHdev, RHdev, Gapdev and PSdev signals are Transitive in nature and typically, at least one zero crossing occurs near the middle epoch.

5. It is seen from Figure 4.2 as well as a comparison of the spans in Table 4.1 and Table 3.7 that for Phase1, the overall span of the deviations are approximately 10 times smaller than that of the actual recorded data for LH signals and is about 6 times smaller for RH signals. On the other hand, for Phase2, this characteristic reverses and the span of the deviations are only 3 and 4 times smaller than those of the actual recorded LH and RH signals respectively, although the overall span is still smaller for the LH Deviation signals.

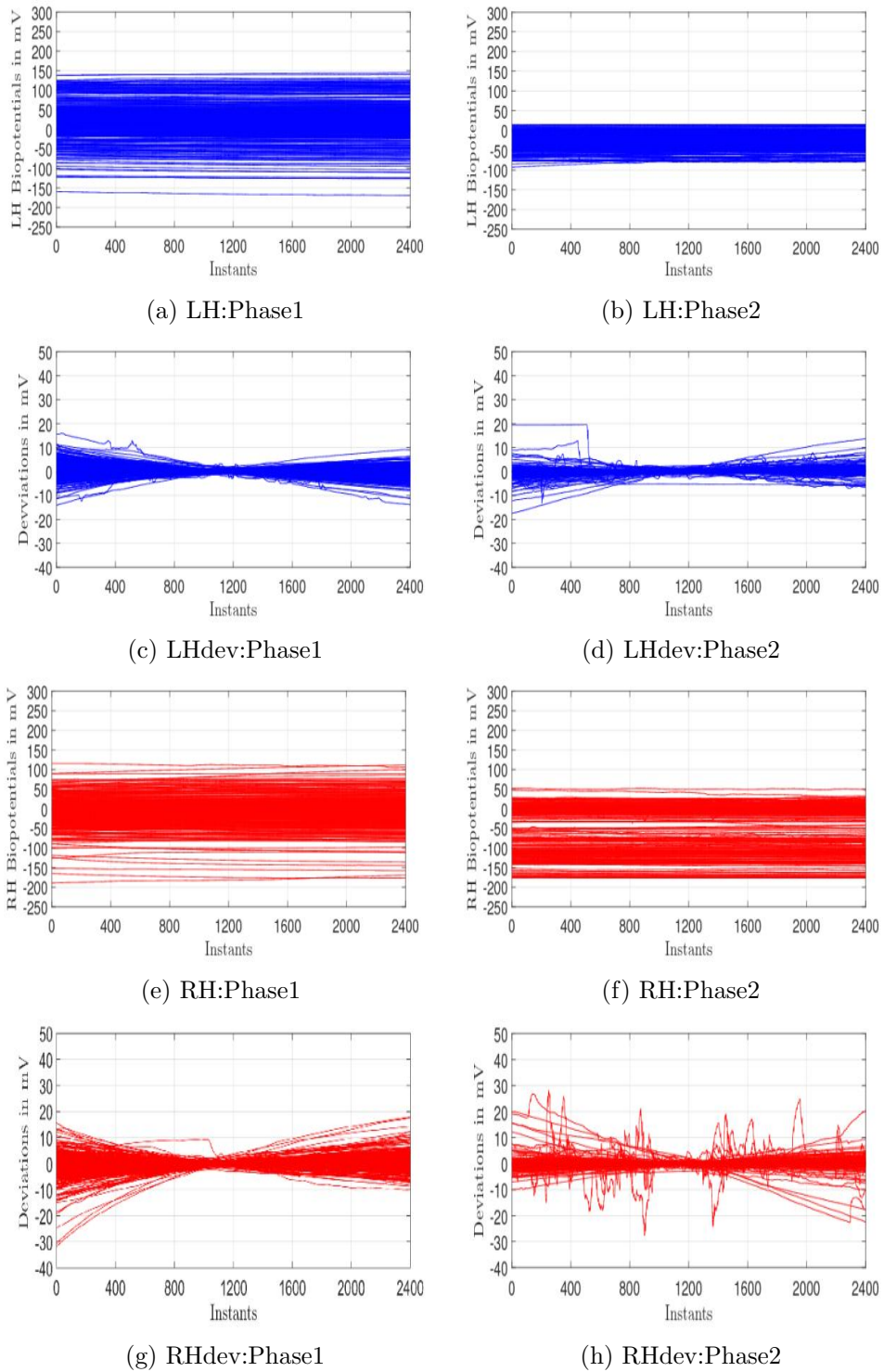
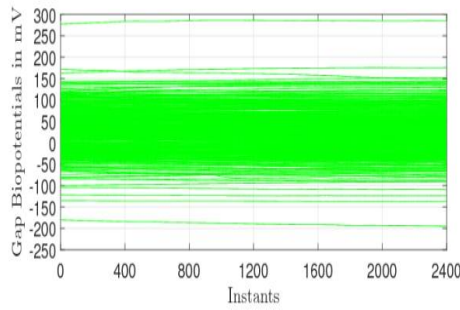
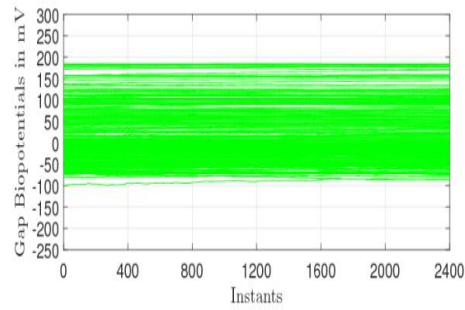


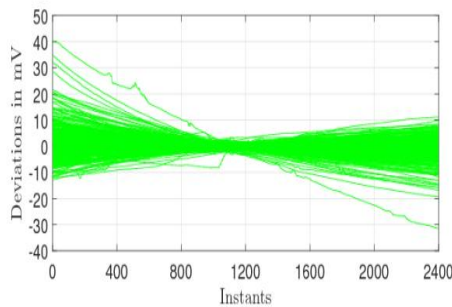
Figure 4.2: Time-series plots of all LH, LHdev, RH and RHdev signals in Phase1 and Phase2



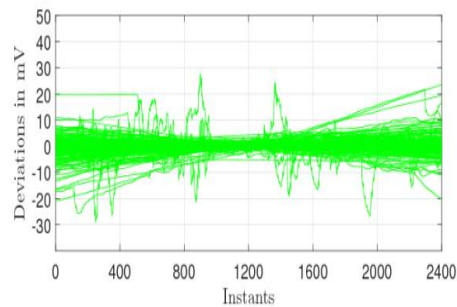
(a) Gap:Phase1



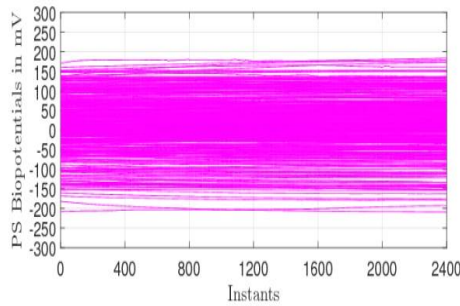
(b) Gap:Phase2



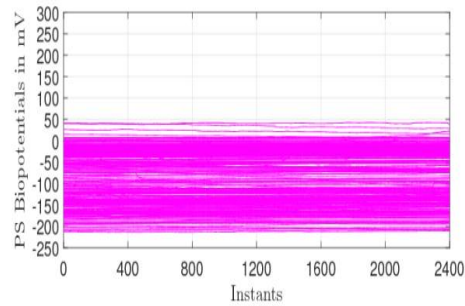
(c) Gapdev:Phase1



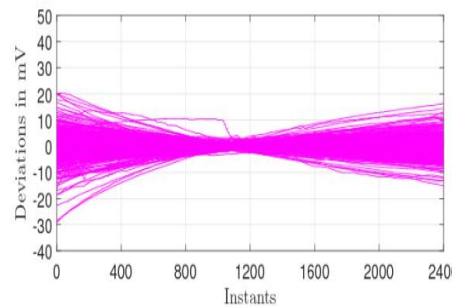
(d) Gapdev:Phase2



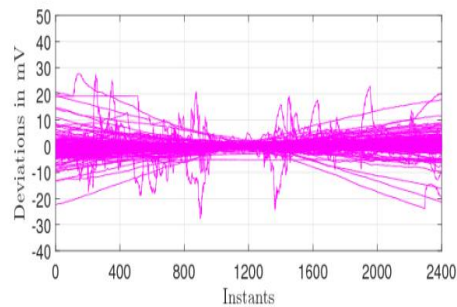
(e) PS:Phase1



(f) PS:Phase2



(g) PSdev:Phase1



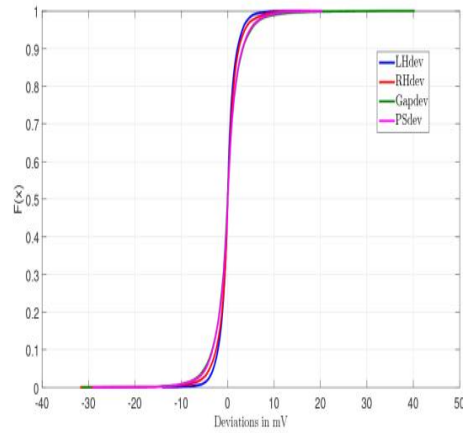
(h) PSdev:Phase2

Figure 4.3: Time-series plots of all Gap, Gapdev, PS and PSdev signals in Phase1 and Phase2

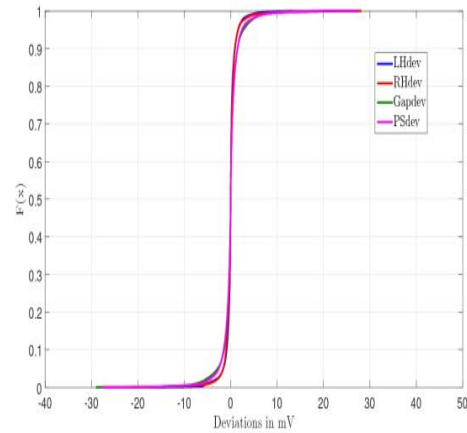
6. Another observation from Table 3.7 is that the span of acquired data in Phase1, specifically 313.97 mV and 304.95 mV for LH and RH signals respectively, is more than that in Phase2, specifically 108.29 mV and 229.52 mV for LH and RH signals respectively. However, in case of the Deviation signals, the case is reversed. The span of LHdev and RHdev in Phase1 are 30.02 mV and 49.59 mV as compared to 36.95 mV and 55.87 mV for Phase2 respectively.
7. It is observed from the cdf plots that the all the four Deviation signals for both the phases are clustered tightly around zero, leading to a highly peaked distribution. As a result, all the signals show a high kurtosis. Among Phase1 and Phase2, the kurtosis is higher for Phase2 than Phase1, which seems to indicate a reduction in signal variability due to elongated periods of rest. This is corroborated by the smaller values of SD in Phase2 as compared to Phase1.
8. It is seen from the zoomed plot in Figure4.5 that 80% of the Deviation signals lie within $\pm 3\text{mV}$ for Phase1 and within $\pm 2\text{mV}$ for Phase2. It is further seen that in all cases, the Deviation signals show a single peak distribution. This is unlike the variant nature of the cdf observed for the RH biopotentials in Phase2 in Figure 3.15 in Section 3.3.1.

In order to study any subject dependence in this aspect, the cdf plots of the SDs of the LH and RH signals recorded over all data sets for each subject of Phase1 and Phase2 are shown in Figure 4.6 and Figure 4.7. It is observed that the variability in the Deviation signals is obtained for all subjects in both phases of measurement. Furthermore, considering all 16 and 14 subjects in Phase1 and Phase2, 70% of the individual SD values for all subjects lie within $\pm 2\text{ mV}$ for both the phases.

9. As expected, the Gapdev and the PSdev signals also show the same nature of variations as shown by LHdev and RHdev signals.

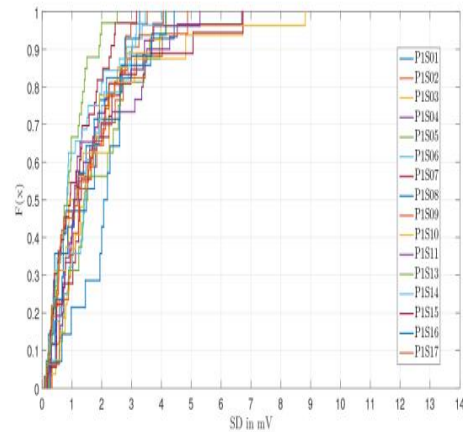


(a) Phase1

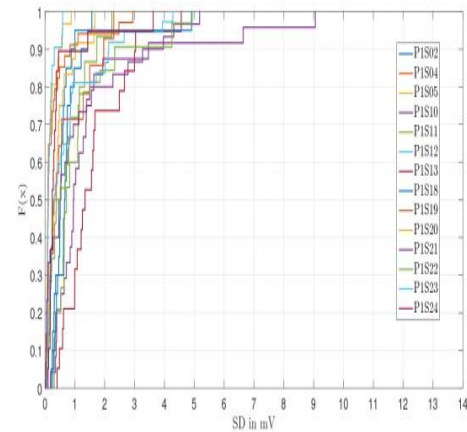


(b) Phase2

Figure 4.4: Cdf plots of LH, RH, Gap and PS Deviation signals in Phase1 and Phase2

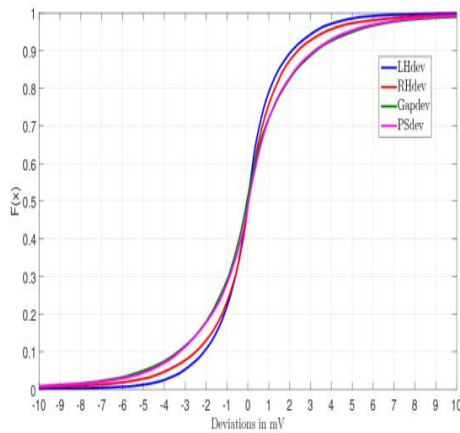


(a) Phase1

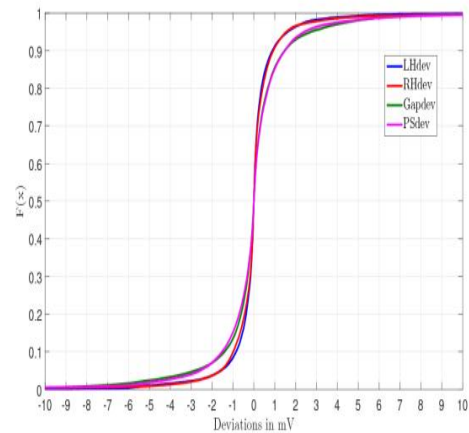


(b) Phase2

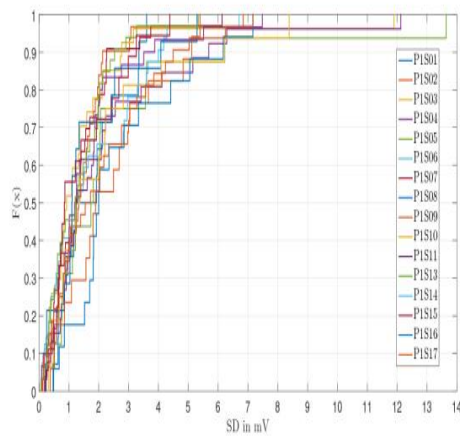
Figure 4.6: Cdf plots of SD of LH signals for all subjects



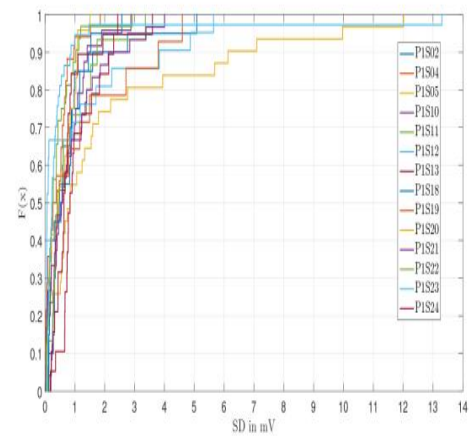
(a) Phase1



(b) Phase2

Figure 4.5: Zoomed plots of cdf of Deviation signals within ± 10 mV

(a) Phase1



(b) Phase2

Figure 4.7: Cdf plots of SD of RH signals for all subjects

4.2.1 Trends in Deviation Signals:

In the next stage of analysis, the trends of the Deviation signals have been determined, as has been done in the case of the acquired and derived signals. It is to

Table 4.1: Statistical characteristics of Deviation signals

Parameters	Range (<i>mV</i>)		Span (<i>mV</i>)	SD (<i>mV</i>)	Median (<i>mV</i>)	Skewness	Kurtosis
	Min	Max					
Phase1							
LHdev	-14.14	15.88	30.02	1.94	-0.00	0.07	8.41
RHdev	-31.78	17.81	49.59	2.58	0.03	-0.72	15.67
Gapdev	-14.72	21.49	36.21	3.58	-0.04	0.71	16.11
PSdev	-29.27	20.33	49.60	3.08	0.04	-0.21	9.31
Phase2							
LHdev	-17.51	19.44	36.95	1.40	-0.00	1.24	44.08
RHdev	-27.68	28.19	55.87	1.73	-0.00	0.36	55.62
Gapdev	-25.74	21.64	47.38	2.38	-0.00	0.13	27.29
PSdev	-27.75	27.58	55.33	2.21	0.00	0.37	31.32

be expected that like the recorded signals, these Deviation signals may also exhibit any one of the three possible trends, namely Decreasing trend, Increasing trend or Constant trend, over the duration of 2 minutes. However, in view of the fact that the Deviation signals vary over a much smaller range, the criterion for classifying the trends has been altered suitably.

As mentioned earlier, it is seen in Table 4.1 that the SD for the LH and RH Deviation signals are approximately within 2 mV, considering both the phases. Furthermore, in this case also, the difference of the potentials at the first instant from that at the last instant in a set is used to classify the Deviation signals in terms of their trends. When the difference is found to be less (or more) than -2mV (or +2mV) of the first instant potential, the signal is categorized to have a Decreasing (Increasing) trend. Changes within ± 2 mV have been labelled to belong to Constant trend. This can be mathematically expressed as follows:

For any particular dataset $\{x_i\}$, $i \in [1, 2400]$,

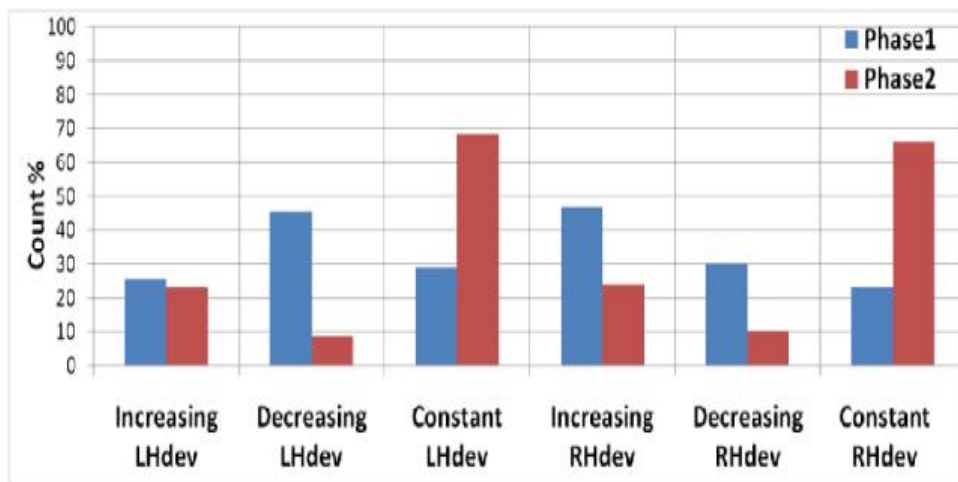
let $\text{DiffDev} = (x_{2400} - x_1)$.

If $\text{DiffDev} > +2\text{mV}$, then the Deviation data set is Increasing;

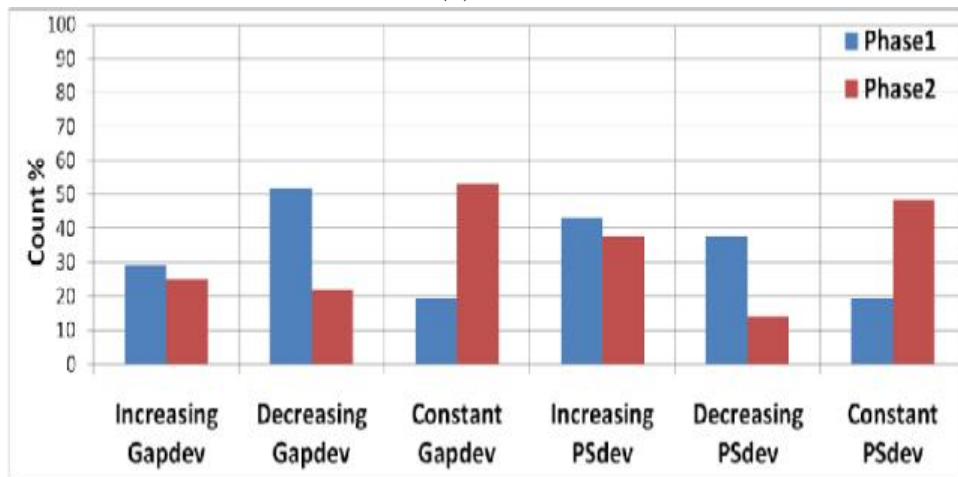
If $\text{DiffDev} < -2\text{mV}$, then the Deviation data set is Decreasing;

else, when $+2\text{mV} \geq \text{DiffDev} \geq -2\text{mV}$, then the Deviation data set is Constant.

The % count of the trends are shown in Figure 4.8 and are tabulated in Table 4.2.



(a) LHdev and RHdev



(b) Gapdev and PSdev

Figure 4.8: Observed Trends in all 4 types of Deviation signals

Table 4.2: Trends in Deviation signals

For	%count		
	Increasing	Decreasing	Constant
Phase1			
LHdev	25.52	45.31	29.17
RHdev	46.88	29.95	23.18
Gapdev	28.91	51.82	19.27
PSdev	42.97	37.76	19.27
Phase2			
LHdev	23.26	8.46	68.28
RHdev	23.87	9.97	66.16
Gapdev	25.08	21.75	53.17
PSdev	37.46	14.20	48.34

The observations on the % count, from Table 4.2 and Figure 4.8, are summarized hereafter.

- i) The increasing trend for LHdev signals is less in comparison to that for RHdev, Gapdev and PSdev of Phase1. In comparison, the increasing trend for PSdev is maximum, while that for LHdev, RHdev and Gapdev are almost the same for Phase2.
- ii) In case of RHdev, the increasing trend dominates the other trends in Phase1. This nature is replicated in the derived PSdev signal too.
- iii) In Phase2, the dominant trend is the constant trend, while the non-dominant trend is the decreasing trend for all four Deviation signals.
- iv) The constant trend dominates the nature of all Deviation signals in Phase2 as compared to that in Phase1. This phenomena can also be ascribed to the prolonged rest of the subjects in Phase2.

4.2.2 Pairs of LHdev and RHdev Signals:

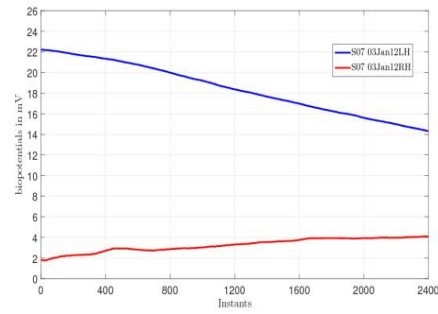
In order to analyse the time-series nature of the signals, it is relevant to compare the patterns observed in the pairs of the original acquired LH and RH signals with those observed in the corresponding pairs of LHdev and RHdev signals. Representative plots are shown in Figure 4.9 and Figure 4.10 for Phase1 and Phase2 respectively for all 4 patterns of pairs of acquired LH and RH signals. It is observed that in both phases, when the original signal pairs are Converging, Diverging or Crossing in nature, the Deviation signals are typically Crossing in nature.

On the other hand, when the signal pairs are Parallel, then the deviation signal pairs are very close to each other as expected and it is difficult to classify them. These Deviation signals seem almost overlapping in nature and typically exhibit multiple crossings. Thus the only pattern in the pair of Deviation signals is the Crossing pattern, whether once or multiple times.

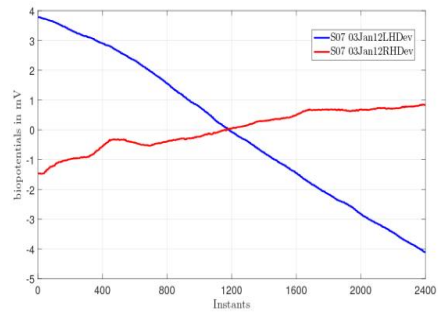
Table 4.3: Occurrence, in % count, of Trends in LHdev and RHdev signals

	Phase1		
Trend	Increasing RHdev	Decreasing RHdev	Constant RHdev
Increasing LHdev	10.94	7.29	7.29
Decreasing LHdev	21.88	14.84	8.59
Constant LHdev	14.06	7.81	7.29
	Phase2		
Trend	Increasing RHdev	Decreasing RHdev	Constant RHdev
Increasing LHdev	6.04	4.83	12.39
Decreasing LHdev	2.72	0.30	5.44
Constant LHdev	15.10	4.83	48.34

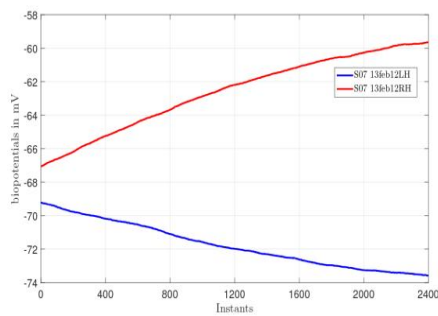
The occurrence of the various combinations of the trends of LHdev and RHdev signals in a set, which contribute to this pattern in a pair of Deviation signals, have been tabulated in Table 4.3.



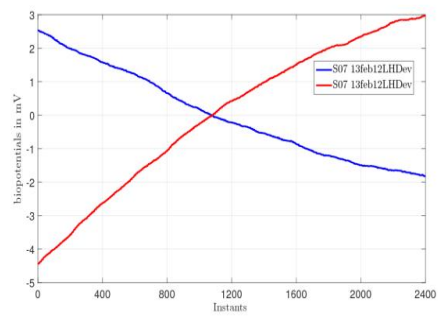
(a) Acquired Signals:Converging



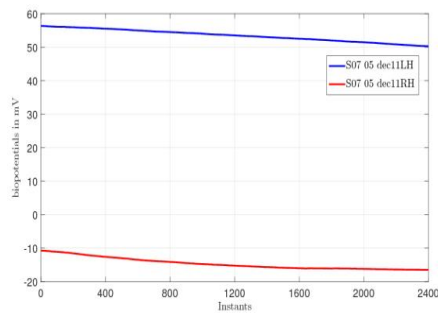
(b) Corresponding Deviations:Crossing



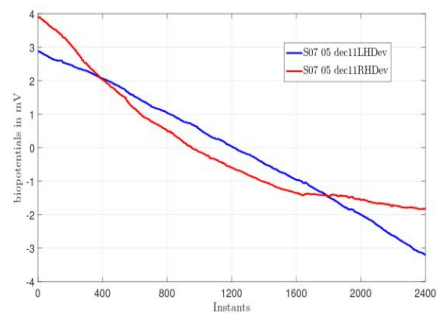
(c) Acquired Signals:Diverging



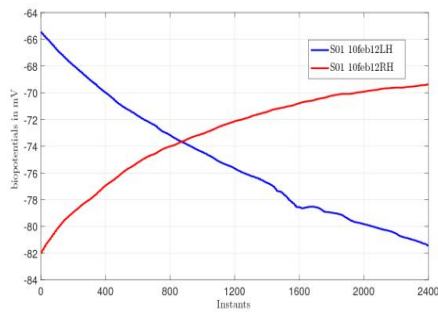
(d) Corresponding Deviations:Crossing



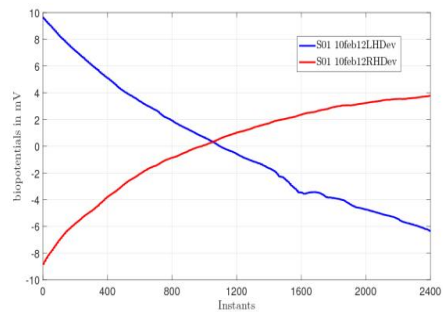
(e) Acquired Signals:Parallel



(f) Corresponding Deviations:Crossing

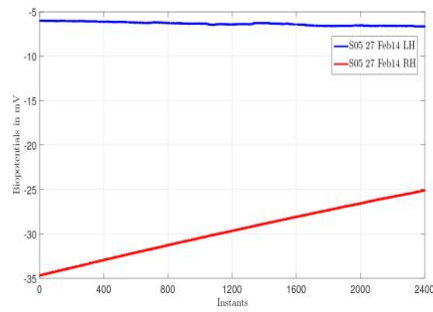


(g) Acquired Signals:Crossing

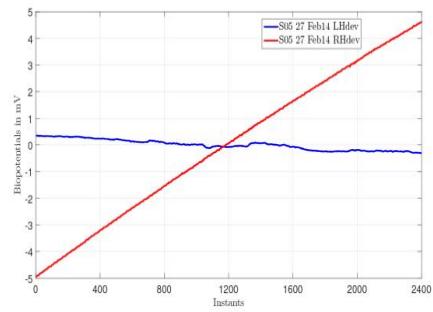


(h) Corresponding Deviations:Crossing

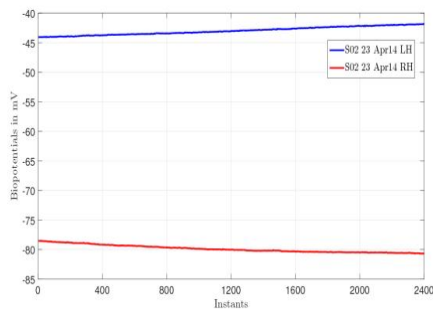
Figure 4.9: Sample LH and RH signal patterns and their corresponding Deviation signal pairs:Phase1



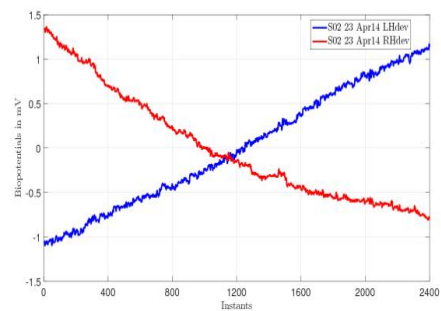
(a) Acquired Signals:Converging



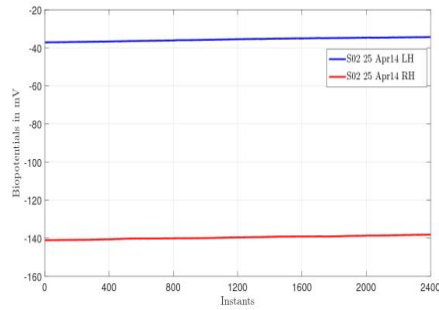
(b) Corresponding Deviations:Crossing



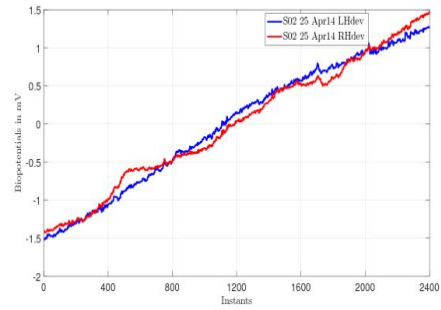
(c) Acquired Signals:Diverging



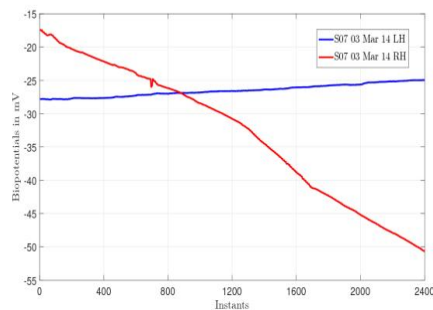
(d) Corresponding Deviations:Crossing



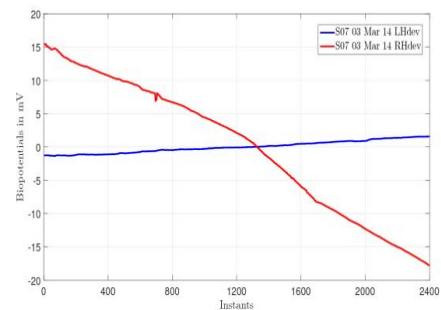
(e) Acquired Signals:Parallel



(f) Corresponding Deviations:Crossing



(g) Acquired Signals:Crossing



(h) Corresponding Deviations:Crossing

Figure 4.10: Sample LH and RH signal patterns and their corresponding Deviation signal pairs:Phase2

It is observed that in Phase1, as expected, all possible combinations of trends for the individual Deviation signals are observed in significant numbers, as is the case for the underlying acquired signals. However, it must be noted that all these combinations lead to the most dominant pattern being the crossing nature for the LHdev and RHdev signals. This is quite unlike the nature of a pair of acquired signals. The primary cause for this is that the setwise mean in most cases occurs in the middle epoch and hence, both the Deviation signals cross zero during that period of time. This is true for all possible combinations of LHdev and RHdev even when both LHdev and RHdev follow the same trend. That is to say that even when both Deviation signals are increasing, decreasing or of constant trend, they are inclined differently since their slopes are necessarily not the same and hence, the pair shows a crossing pattern near the middle epoch.

The same argument is valid for the Deviation signals in Phase2 also. Additionally, in case of Phase2, almost 50% of the deviation pair signals comprise of the combination of constant LHdev signal with constant RHdev signal but this only leads to overlapping or multiply crossing pairs of Deviation signals.

4.3 Modelling the Deviation Signals:

The next task is to model the acquired as well as derived signals. It is observed that while the acquired as well as derived signals may differ significantly in their setwise mean values, yet the Deviation signals are essentially of the same nature. Some typical plots for the LHdev and RHdev signals obtained for a randomly selected subject are shown in Figure 4.11. It is evident from earlier observations that the natures of the corresponding Gapdev and PSdev signals are also similar.

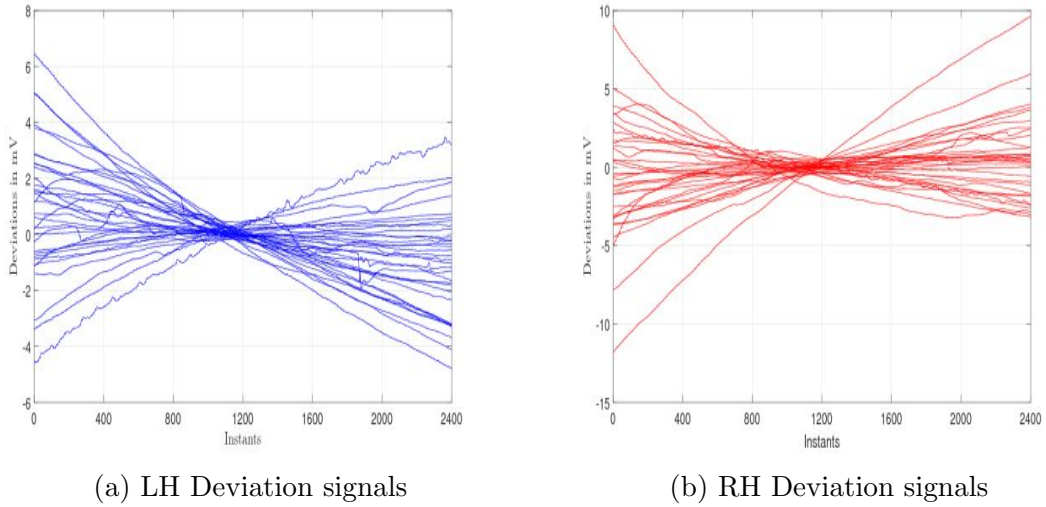


Figure 4.11: LH and RH Deviation signals of a typical subject

It is evident from Figure 4.11, as well as earlier observations, that the plots show a butterfly like variation and in most cases, the $Mean_{set}$ occurs in the middle epoch of the total duration of 2 minutes, or 2400 instants, in a set of data. In view of this, the time duration of a data set has been subdivided into 3 epochs, which are labelled as initial epoch from the 1st till 800th instant, middle epoch from 801th till 1600th instant and final epoch from 1601th till 2400th instant.

The individual Deviation signals mostly follow a regular pattern. They typically start from a maximum positive (or minimum negative) value, then they decrease (or increase) almost linearly, cross zero near the 1200th instant in the middle epoch and then end at certain negative (or positive) value in the last (2400th) instant. This feature is obtained for almost all the cases and therefore, these signals have been modeled as straight lines.

4.3.1 Zero Crossing Instant (ZCI):

The $Mean_{set}$ is a representative feature of all four signal types. Since this typically occurs in the middle epoch of any acquired or derived signal, so the time instant

where the corresponding Deviation signals cross zero closest to the 1200th instant is considered to be a point on the fitted line. These time instants are referred hereafter as the zero crossing instant (ZCI) for each set. The $Mean_{set}$ of the acquired and the derived signals occur at the ZCI of the corresponding Deviation signals. The ZCI values have been determined for all sets of LHdev, RHdev, Gapdev and PSdev signals for both the phases and the standard regression fit is computed in terms of ZCI.

4.3.2 Slope m of the Trendline:

The other parameter used to characterise the fitted straight line is its slope, m . It has already been observed that all the Deviation signals vary almost monotonically within ± 30 mV in 2400 instants, which is typically 1/10th of the range of the corresponding acquired and derived signals. Furthermore, from Figure4.5, it has been noted that 80% of the Deviation signals lie within ± 3 mV for Phase1 and within ± 2 mV for Phase2. Hence, it is to be expected that the slope of the fitted trendline will be very tightly clustered in most cases.

The straight line is considered to pass through the ZCI of the Deviation signal. The slope, m , of the trendline can thus be expressed in terms of the corresponding ZCI as follows.

Let y_k be the value of the deviation signal at the k -th instant, where $k \in [1, 2400]$. Then, the bias, c , of the trendline can be defined in terms of the ZCI and the equation for the trendline can be formulated accordingly.

$$\text{Hence, } c = (-m) \times ZCI \quad (4.5)$$

$$\text{and, } y_k = m \times k + c = m \times (k - ZCI) \quad (4.6)$$

The slope, m , is determined from the Deviation data set by minimising the square of the error between the deviation signal and the fitted trendline which passes through

the ZCI. So, the objective is to minimize

$$p = \sum_{k=1}^{2400} [y_k - m(k - ZCI)]^2 \quad (4.7)$$

$$\begin{aligned} &= \sum_{k=1}^{2400} y_k^2 - \sum_{k=1}^{2400} 2m(k - ZCI)y_k + \sum_{k=1}^{2400} m^2(k - ZCI)^2 \\ &= m^2 \sum_{k=1}^{2400} (k - ZCI)^2 - 2m \sum_{k=1}^{2400} (k - ZCI)y_k + \sum_{k=1}^{2400} y_k^2. \end{aligned} \quad (4.8)$$

$$\text{Hence, } \frac{\partial p}{\partial m} = 2m \sum_{k=1}^{2400} (k - ZCI)^2 - 2 \sum_{k=1}^{2400} (k - ZCI)y_k = 0 \quad (4.9)$$

$$\text{or, } m \sum_{k=1}^{2400} (k - ZCI)^2 = \sum_{k=1}^{2400} (k - ZCI)y_k$$

$$\text{So, } m = \frac{\sum_{k=1}^{2400} (k - ZCI)y_k}{\sum_{k=1}^{2400} (k - ZCI)^2} \quad (4.10)$$

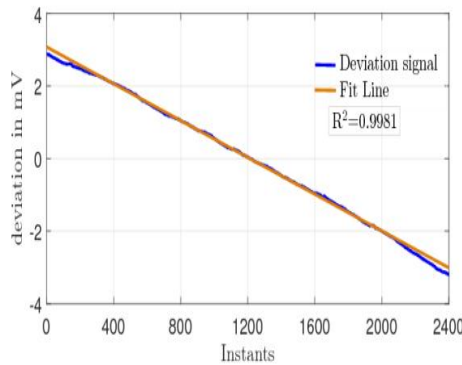
The values of the slope, m , for all sets of LHdev, RHdev, Gapdev and PSdev signals in both phases have been calculated using the ZCI determined for each Deviation signal and equation (4.10).

4.3.3 Instantaneous Residuals:

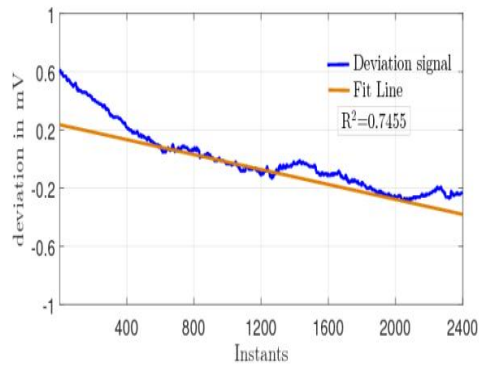
In order to validate this proposed linear model, the residuals have been determined at each instant for each data set of all 4 types of Deviation signals.

For this, the residuals have been defined as follows. Let the value of the actual Deviation signal at a particular instant k be denoted as y_{actual_k} , while the value predicted at that instant from the fitted straight line is y_k . Then, the instantaneous Residuals, henceforth also referred simply as Residuals, have been determined for all the Deviation signals as the difference $\{y_{actual_k} - y_k\}$ for $k \in [1, 2400]$.

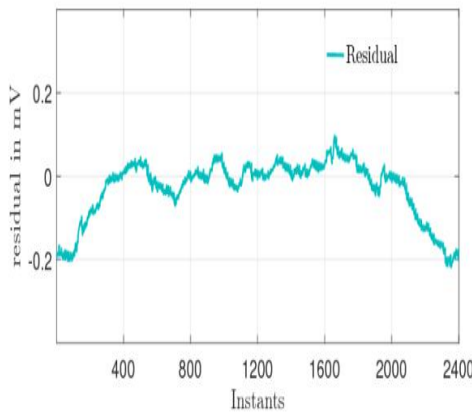
Two sample Deviation signals along with the fitted trendlines and the corresponding Residuals are shown as time-series plots in Figure 4.12. In Figure 4.12a and Figure 4.12b, the Deviation signal is shown in blue and the corresponding fit line obtained from the regression model is shown in brown colour and the respective fit factors have also been stated. The time-series plots of the corresponding Residuals are shown in Figure 4.12c and Figure 4.12d.



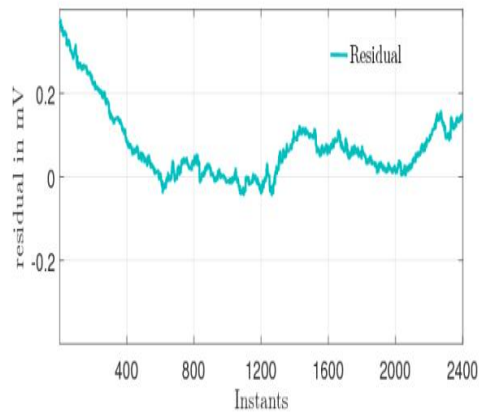
(a) SampleFit1



(b) SampleFit2



(c) Residual1



(d) Residual2

Figure 4.12: Sample fit plots and their Residuals

It is observed that the Residuals vary randomly in both cases, but within a very narrow range of approximately $\pm 0.2\text{mV}$. However, the nature of the Residuals are

widely different in the two cases. Also, since the Deviation signal in Figure 4.12b is almost constant while that in Figure 4.12a varies over a much larger range, so the corresponding fit factors of the trendlines are quite different in the two cases, affecting the efficacy of the regression model.

4.4 Analysis of the regression model

In view of the aforementioned aspects, the characteristics of the observed ZCI, the determined m as well as the calculated Residuals for all Deviation signals in both phases for all four types of Deviation signals have been studied in this Section.

4.4.1 Characteristics of ZCI

The cdf plots for the ZCI evaluated for all sets of data in both phases and their zoomed plots in the middle epoch are shown in Figure 4.13 and Figure 4.14, while their corresponding statistical characteristics have been tabulated in Table 4.4.

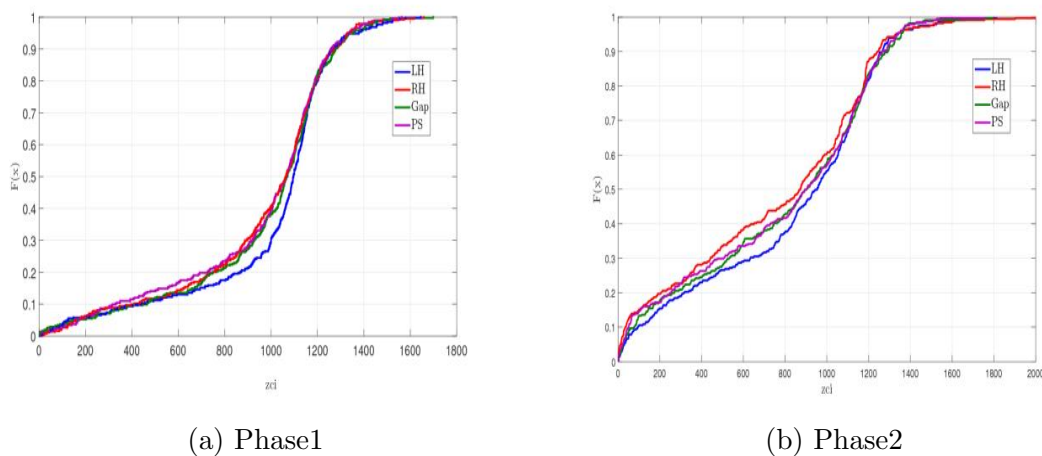
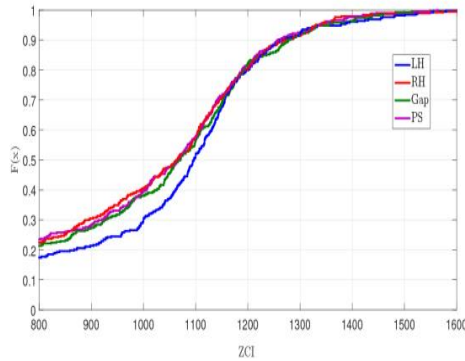
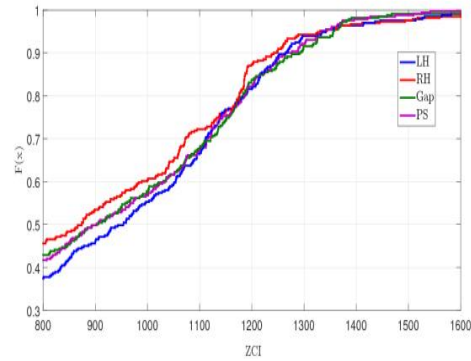


Figure 4.13: Cdf plots of Zero Crossing Instants (ZCI) of Deviation signals



(a) Phase1



(b) Phase2

Figure 4.14: Zoomed cdf plots of ZCI of Deviation signals in the middle epoch

Table 4.4: Statistical characteristics of Zero Crossing Instant (ZCI)

Parameters	Range		Span	Median	Mean	SD
	Min	Max				
Phase1						
LHdev	6	1646	1640	1096	997	332
RHdev	15	1659	1644	1064	957	334
Gapdev	1	1699	1698	1069	971	334
PSdev	2	1564	1562	1066	949	344
Phase2						
LHdev	2	1813	1811	954	820	432
RHdev	1	1999	1998	874	746	461
Gapdev	1	1793	1792	903	786	446
PSdev	2	1758	1756	902	776	452

The observations from Figure 4.13, Figure 4.14 and Table 4.4 are listed hereafter.

1. As is evident from the cdf plots in Figure 4.13, the ZCI values do not follow a normal distribution for any of the signal types. This has been verified using a Chi-square goodness of fit test with the null hypothesis that the ZCI values comes from a normal distribution. It has been found that the test rejects the

null hypothesis at the 5% significance level. Furthermore, it is observed in Figure 4.14 that more than 75% and more than 50% of all data sets of all 4 signal types in Phase1 and Phase2 respectively have their ZCI in the middle epoch.

2. From the overall statistics, it is seen that in Phase1, the spans of ZCI for LHdev and RHdev are almost the same, while in case of Phase2, the ZCI of RHdev signals are spread over a larger span.
3. In Phase1 as well as in Phase2, the spans of ZCI for PSdev are the minimum, indicating a tighter clustering of the ZCI in these signals.

As expected, the contrasting observation is noted in case of Gapdev signals in Phase1, where the span of ZCI is maximum. However, in Phase2, the span of Gapdev signals is significantly smaller than those of the LHdev and RHdev signals, and is closer to that of the PSdev signals.

4. Despite the discrepancy in the spans, the mean, median and SD values of the ZCI for all four signal types are very close to each other in Phase1. However, due to the lack of normality, there exists a wide gap between the median and mean of ZCI in each case.
5. The gap between mean and median values of ZCI exists for all the signal types in Phase2 also. Additionally, the values of mean, median and SD of the ZCI for all the four signal types are not as close as those in Phase1. The values of SD of the ZCI are also larger in Phase2 than in Phase1. All these features characterise the larger variety of variations that are observed in Deviation signals when the data is acquired over a prolonged period of rest.

On the basis of this analysis, the ZCI is considered as one of the parameters characterizing the straight lines that fit the Deviation signals of all four types of signals.

4.4.2 Characteristics of slope m

The cdf plots of m of all the data sets in Phase1 as well as Phase2 for all types of signals are shown in Figure 4.15, while the corresponding zoomed plots in the range ± 0.01 mV/instant are shown in Figure 4.16. The statistical characteristics of the parameter m are tabulated in Table 4.5.

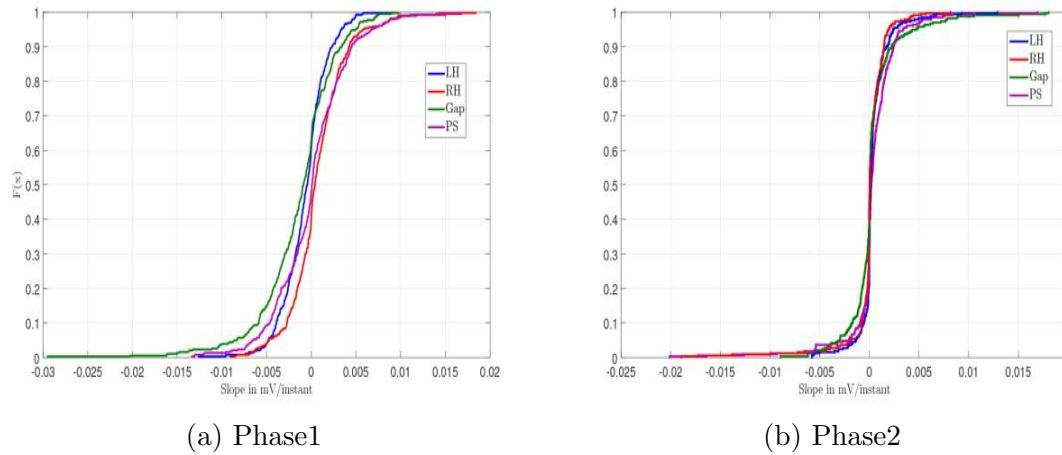


Figure 4.15: Cdf plots of slopes, m , of trendlines fitted to Deviation signals

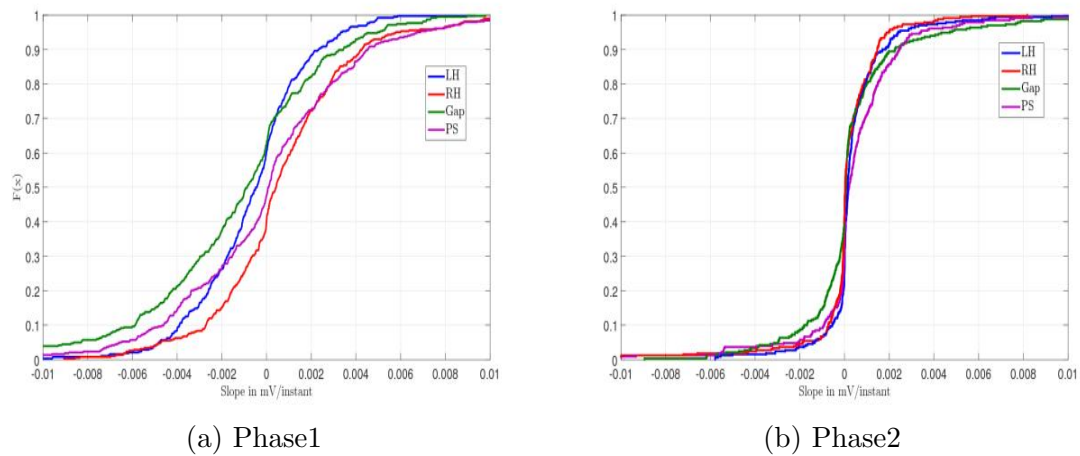


Figure 4.16: Zoomed cdf plots of slopes, m , within ± 0.01 mV/instant

Table 4.5: Slopes m , in mV/instant, of fitted trendlines

Parameters	Range		Span	Median	Mean	SD
	Min	Max				
Phase1						
LHdev	-0.0126	0.0093	0.0219	0.0005	-0.0007	0.0025
RHdev	-0.0091	0.0184	0.0275	0.0004	0.0007	0.0033
Gapdev	-0.0295	0.0098	0.0393	0.0009	-0.0014	0.0043
PSdev	-0.0134	0.0167	0.0301	0.0001	-0.0000	0.0041
Phase2						
LHdev	-0.0058	0.0129	0.0187	0.0001	0.0004	0.0016
RHdev	-0.0189	0.0082	0.0271	0.0000	0.0001	0.0022
Gapdev	-0.0089	0.0181	0.0270	0.0000	0.0003	0.0027
PSdev	-0.0201	0.0169	0.0370	-0.0002	-0.0004	0.0027

The observations from Figure 4.15, Figure 4.16 and Table 4.5 are listed hereafter.

1. It is observed that the slopes, m , of the trendlines for all the 4 types of Deviation signals may be positive or negative and they lie within a narrow range of -0.030mV/instant to $+0.020\text{mV/instant}$. In both phases, the SD of the slopes are less than 0.005mV/instant for the trendlines of all 4 types of Deviation signals.

From the zoomed plot in Figure 4.16, it is observed that even within this small range, 80% of the slope values in Phase1 fall within -0.006 mV/instant to $+0.004\text{ mV/instant}$. The range of m in case of Phase2 trendlines is even smaller, where 80% of the slope values lie within $\pm 0.002\text{ mV/instant}$ for all the signal types, indicating the stabilizing effect of rest on the trendline.

2. From a visual inspection of the slopes for all the signal types, it is difficult to ascertain the normality of the distributions of m for all the signal types. So, the slopes for all the 4 signal types in both phases were checked using the Chi-square goodness of fit test for the null hypothesis that the slope comes from a normal distribution.

It has been observed that the test rejects the null hypothesis at the 5% significance level for the slopes of RHdev, Gapdev and PSdev signals of Phase1 as well as the slopes of all four signal types of Phase2. However, m for the LHdev signals in Phase1 accepts the null hypothesis with $p=0.132$ at the 5% significance level.

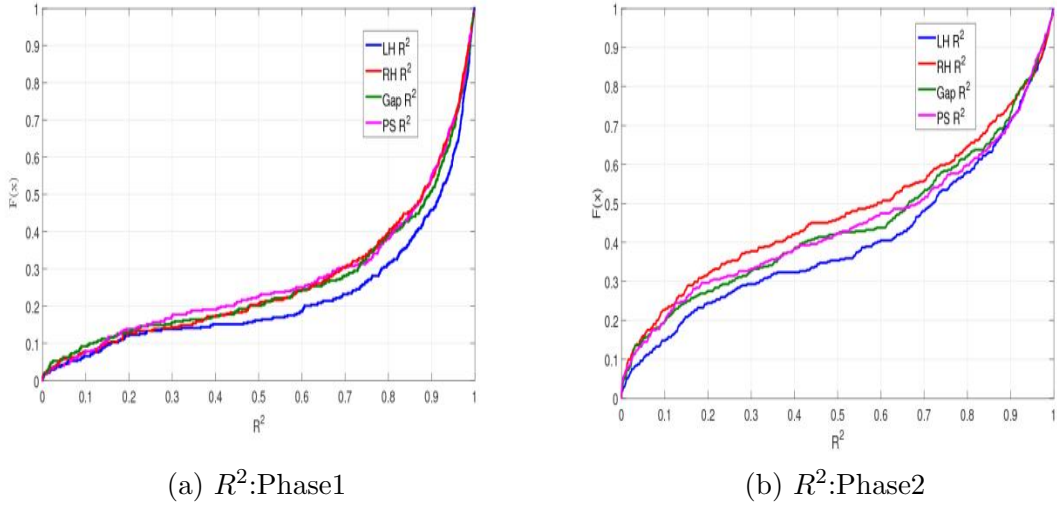
3. In Phase1, the mean as well as the median of the calculated m values are very close to 0, typically within $\pm 0.001\text{mV/instant}$. In case of Phase2, with subjects under prolonged periods of rest, these values are consistently smaller, typically less than $\pm 0.0005\text{mV/instant}$.

Hence, it is observed that the trendline that fits all four types of Deviation signals can be characterised using the zero crossing instant, ZCI and the slope, m and these parameters of the trendlines for all 4 types of Deviation signals lie within definite ranges in most cases.

4.4.3 Characteristics of Residuals:

As mentioned earlier, the efficacy of this linear model can be ascertained from an analysis of the goodness of fit of the trendlines and the statistical analysis of the instantaneous Residuals. Both these aspects have been studied herewith.

The cdf plots of the R^2 values obtained for the trendlines fitted to all 4 types of Deviation signals in both the phases are shown in Figure 4.17 while their mean, median and SD values in the two phases are tabulated in Table 4.6.

Figure 4.17: Cdf plots of R^2 values obtained for trendlines of all 4 Deviation signalsTable 4.6: Mean, Median and SD of the fit factor (R^2) for trendlines of all 4 Deviation signals

Parameters	Median	Mean	SD	Median	Mean	SD
	Phase1			Phase2		
LHdev	0.92	0.78	0.30	0.72	0.60	0.35
RHdev	0.88	0.74	0.30	0.59	0.52	0.37
Gapdev	0.89	0.74	0.31	0.66	0.56	0.37
PSdev	0.88	0.73	0.31	0.69	0.56	0.37

It has been observed that almost 80% or more of the R^2 values for all the Deviation signals in Phase1 and more than 50% for those in Phase2 are greater than 0.5. Furthermore, the medians of the R^2 values for all the Deviation signals in Phase1 are quite high, typically 0.88 or more, but in case of Phase2, while the median is 0.72 for the LH signals, it is reduced to 0.59 for RH signals. In both phases, the fit factors of the Gapdev and PSdev signals are similar and lie between those of the LHdev and RHdev signals. These indicate that the signals in Phase1 are more quasi-linear than those in Phase2, which is in line with all earlier findings.

In order to correlate this with the actual values of the underlying instantaneous Residuals, a quantitative analysis is done of the Residuals obtained for all the sets of data of all 4 types of Deviation signals for both the phases.

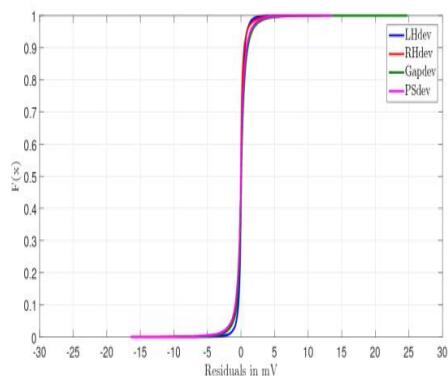
The cdf plots of the overall corpus of Residuals obtained for LHdev, RHdev, Gapdev and PSdev signals in both phases are shown in Figure 4.18, along with a zoomed cdf plot of the Residuals within $\pm 4\text{mV}$ in Figure 4.19. Their statistical characteristics are tabulated in Table 4.7.

Table 4.7: Instantaneous Residuals in mV

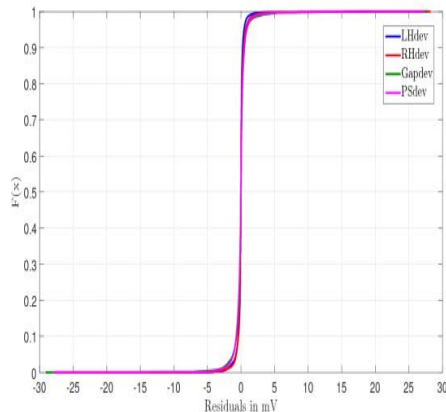
Parameters	Range		Span	Median	Mean	SD	Skewness	Kurtosis
	Min	Max						
Phase1								
LHdev	-9.64	6.92	16.56	0.02	0.05	0.60	-0.82	27.23
RHdev	-16.29	11.59	27.88	-0.03	-0.10	0.88	-1.90	38.86
Gapdev	-9.91	24.79	34.70	0.05	0.14	1.06	1.43	28.34
PSdev	-16.45	13.60	30.05	-0.02	-0.04	1.06	-0.90	24.37
Phase2								
LHdev	-13.50	19.31	32.81	-0.02	-0.05	0.72	10.72	272.14
RHdev	-27.87	28.23	56.10	-0.01	-0.01	0.82	2.80	208.72
Gapdev	-29.10	27.77	56.87	-0.01	-0.04	1.14	1.65	110.40
PSdev	-27.97	27.32	55.29	-0.03	-0.06	1.07	3.99	122.75

The observations from Figure 4.18, Figure 4.19 and Table 4.7 are as follows:

1. The total corpus of instantaneous Residuals of all Deviation signals in both phases are centered around 0, as indicated from their mean and median values, which are close to each other and almost 0.

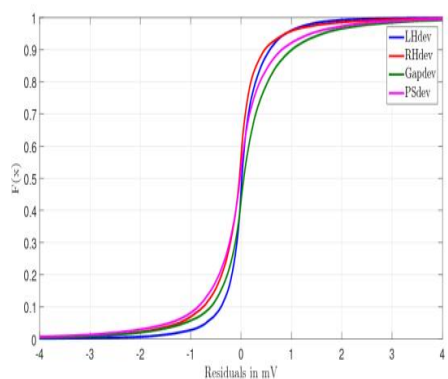


(a) Phase1

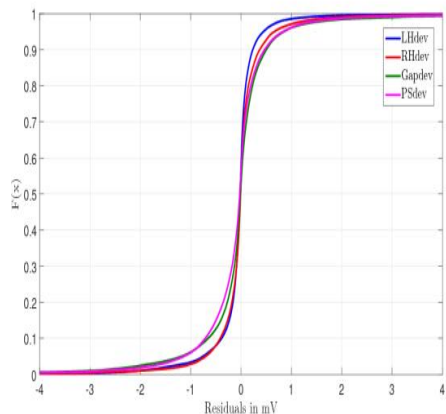


(b) Phase2

Figure 4.18: Cdf plots of instantaneous Residuals for all 4 Deviation signals



(a) Phase1



(b) Phase2

Figure 4.19: Zoomed cdf plots of instantaneous Residuals within $\pm 4\text{mV}$

2. A comparison of the span of Residuals of LHdev and RHdev signals in the two phases shows that the span in Phase2 is almost double that for Phase1.

The span of Residuals for RHdev signals is almost 1.5 times that for LHdev in both phases. The spans of Residuals in case of Gapdev are more than that of

RHdev signals in both phases. However, the spans of the Residuals of PSdev signals are slightly larger than those of the RHdev signals in case of Phase1, but are slightly smaller in case of Phase2.

3. A comparison of the SD of the Residuals of the various signals shows that it is almost identical for the RHdev signals in both phases, but the Residuals for the LHdev signals are observed to be more dispersed in Phase2 than in Phase1. A comparison of the SD values for the Residuals of LHdev and RHdev signals show that it is typically lesser for the LHdev signals in both Phases.

These indicate that in comparison to that for the RHdev signals, the trendline fit is better for LHdev signals in both phases.

4. No such remarkable result is evident for the Gapdev and PSdev signals, although the SD of the Residuals for PSdev in Phase2 are marginally better than those of the corresponding Gapdev signals. Also, the SD of the Residuals of Gapdev and PSdev signals are in general larger than those of the LHdev and RHdev signals, although within 1.2mV in both phases.
5. Although the cdfs of these Residuals are centered around 0, yet their distributions are not symmetric in any of the cases, but are left or right skewed. In Phase1, the Residuals of both LHdev and RHdev signals are slightly left skewed, but in Phase2, both are right skewed and particularly, the Residuals of LHdev signals are quite heavily right skewed. These long tails, as evident from the cdf plots also, lead to effectively higher values of kurtosis in Phase2 than in Phase1.
6. Each set of Residuals, generated for each set of Deviation signals, has been tested for types of Pearson distribution [114], [115], [116] using Matlab and the results in terms of their % occurrence are tabulated in Table 4.8.

It is observed that for more than 85% sets in Phase1 and more than 80% in Phase2 for all 4 types of Deviation signals, the Residuals of the Deviation

Table 4.8: Occurrence of types of Pearson distribution for Residuals

Parameters	Type with % count			Type with % count		
	Class1	Class4	Class6	Class1	Class4	Class6
	Phase1			Phase2		
LHdev	86.7	8.1	5.2	81.0	13.6	5.4
RHdev	90.1	7.8	2.1	86.4	10.3	3.3
Gapdev	91.1	5.5	3.4	80.1	13.6	6.3
PSdev	88.3	8.8	2.9	80.7	14.5	4.8
Class1:Four parameter Beta distribution Class4:Not related to any standard distribution Class6:F location-scale distribution						

signals follow a 4-parameter beta distribution. It is to be noted that in a 4 parameter beta distribution, two of the parameters are the minimum and maximum value, while the other two are shape parameters.

7. A further study of the zoomed cdf plots in Figure 4.19 shows that though the Residuals behave in a random manner, almost 99% of the total corpus lie within $\pm 4\text{mV}$ for all four types of Deviation signals for both the phases and the distribution also seems symmetric about 0mV .

These findings suggest that the linear model fits all four types of Deviation signals in both phases well, with most of the Residuals belonging to a 4 parameter beta distribution and almost 99% of them being restricted within $\pm 4\text{mV}$.

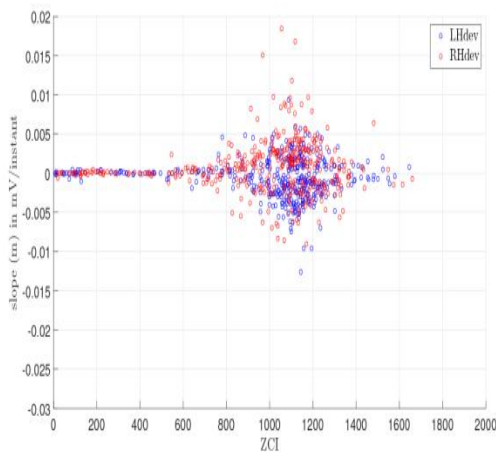
4.5 Interrelationship between ZCI and m:

It has been observed that both the parameters of the trendline fitted to the Deviation signals, namely ZCI and m, are highly clustered in nature. While most of the ZCI are in the middle epoch, the slopes are primarily limited in the range $\pm 0.01\text{mV}/\text{instant}$. Furthermore, most of the Residuals are clustered within $\pm 4\text{mV}$. In view of these observations, the interrelation between the two parameters, ZCI and m, have been

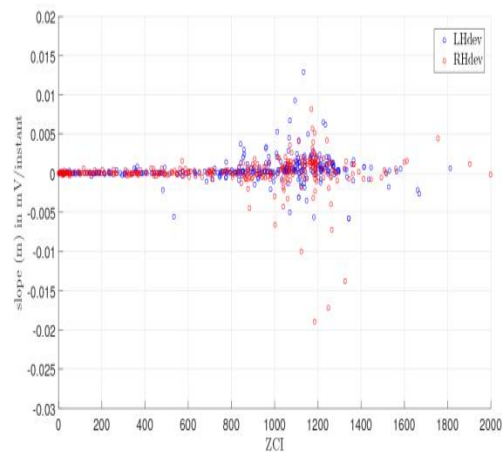
studied further in this Section with the objective of identifying the most probable ranges of these parameters.

Scatter plots of ZCI and m of all 4 types of Deviation signals for both the phases have been studied for this purpose. The scatter plots of m vs. ZCI for LHdev and RHdev signals for both phases have been shown in Figure 4.20, while those for the Gapdev and PSdev signals in both phases have been shown in Figure 4.21.

It is observed from all the scatter plots that a distinct cluster is seen near the middle portion of the plot, along with another sizable population in the initial epoch for ZCI with the slope values being even closer to 0. This seems to be true for all Deviation signals and for both phases.

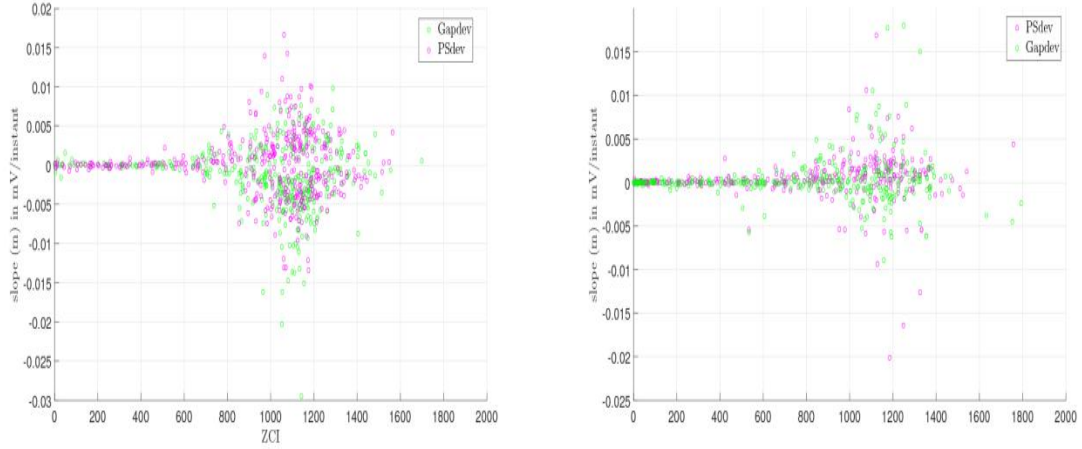


(a) LHdev and RHdev:Phase1



(b) LHdev and RHdev:Phase2

Figure 4.20: Scatter plots: m vs. ZCI for LHdev and RSdev signals



(a) Gapdev and PSdev:Phase1

(b) Gapdev and PSdev:Phase2

Figure 4.21: Scatter plots: m vs ZCI for Gapdev and PSdev signals

It is observed from all the scatter plots that a distinct cluster is seen near the middle portion of the plot, along with another sizable population in the initial epoch for ZCI with the slope values being even closer to 0. This seems to be true for all Deviation signals and for both phases.

In order to explore this further, the occurrence of data sets with corresponding values of ZCI in the initial, middle and final epochs, labelled as ZCI1, ZCI2 and ZCI3 respectively, and the slopes in the ranges $> 0.01\text{mV/instant}$, within $\pm 0.01\text{mV/instant}$ and $< -0.01\text{mV/instant}$, labelled as M1, M2 and M3 respectively, have been determined and stated in Table 4.9 for both the phases.

The following are the observations from the scatter plots in Figure 4.20 and Figure 4.21 as well as Table 4.9.

1. It is observed that for all four types of Deviation signals, most of the sets have a trendline with the slope m within $\pm 0.01\text{ mV/instant}$, M2, while the majority of the ZCI lie in the middle epoch, ZCI2. Typically, almost 75% and more of all 4 types of Phase1 Deviation signals and more than 50% of all 4 types of Phase2 Deviation signals lie in this combination class.

Table 4.9: % count of ZCI and m in the Deviation signals

Phase		Phase1			Phase2		
Type	Class	ZCI1	ZCI2	ZCI3	ZCI1	ZCI2	ZCI3
LHdev	M1	0	0.26	0	0	0	0
	M2	17.45	82.03	0.26	37.46	61.33	0.91
	M3	0	0	0	0	0.30	0
RHdev	M1	0	0	0	0	0.91	0
	M2	22.40	76.04	0.52	45.62	52.27	1.21
	M3	0	1.04	0	0	0	0
Gapdev	M1	0	3.91	0	0	0	0
	M2	21.35	74.48	0.26	42.90	54.99	0.91
	M3	0	0	0	0	1.21	0
PSdev	M1	0	1.30	0	0	0.91	0
	M2	23.44	73.70	0	41.69	56.50	0.30
	M3	0	1.50	0	0	0.60	0

ZCI1: $1 \leq \text{ZCI} \leq 800$, M1: $m < -0.01$ mV/instant,
ZCI2: $801 \leq \text{ZCI} \leq 1600$, M2: $-0.01 \leq m \leq 0.01$ mV/instant,
ZCI3: $1601 \leq \text{ZCI} \leq 2400$, M3: $m > 0.01$ mV/instant

It is also to be noted that in both phases, the largest proportion of LHdev signals belong to this combination class among all 4 types of Deviation signals.

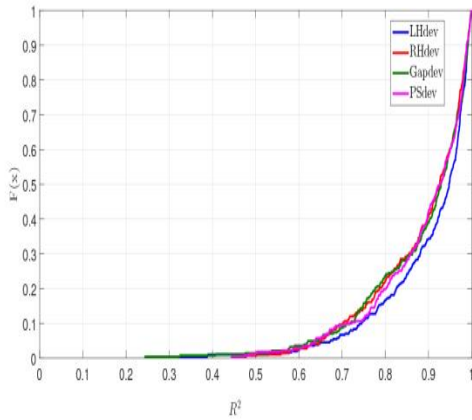
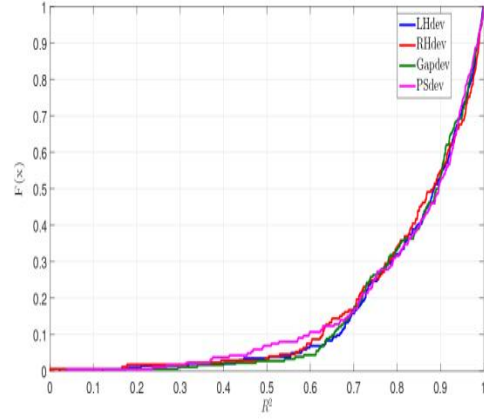
2. However, there are a significant number of sets for which the ZCI lies in the initial epoch, ZCI1, while the slopes m are well within M2 and are very close to 0, specifically almost 17% to 24% of Phase1 Deviation signals and almost 37% to 46% of Phase2 Deviation signals.

Thus, there exists a sizable proportion of signals that are almost constant in nature with consequently lower ZCI values and this proportion increases significantly with prolonged rest.

3. It is also observed that in case of Phase2, where the subjects are in prolonged periods of rest, the ZCI are almost equally likely to lie in the classes ZCI1 and ZCI2, within 1 to 1600, although no such finding is observed for the slope m.

Thus, there is a distinct predominance of the data sets that can be modelled using

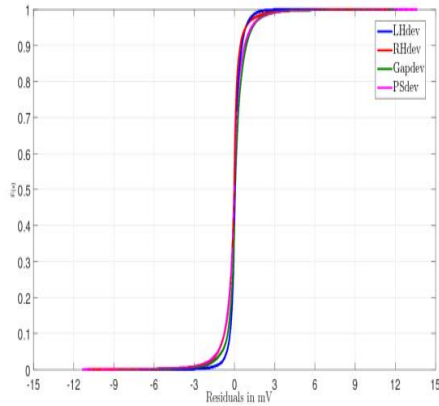
the trendline parameters in the range ZCI2 and M2, labelled henceforth as ZCI2M2. The goodness of fit for this class of Deviation signals has been termed as R^2_{ZCI2M2} . Their cdf plots for both the phases have been shown in Figure 4.22, while their statistical characteristics have been tabulated in Table 4.10.

(a) R^2_{ZCI2M2} :Phase1(b) R^2_{ZCI2M2} :Phase2Figure 4.22: Cdf plots of Fit factor R^2 of trendlines in the class ZCI2M2, R^2_{ZCI2M2} Table 4.10: Statistical characteristics of R^2_{ZCI2M2}

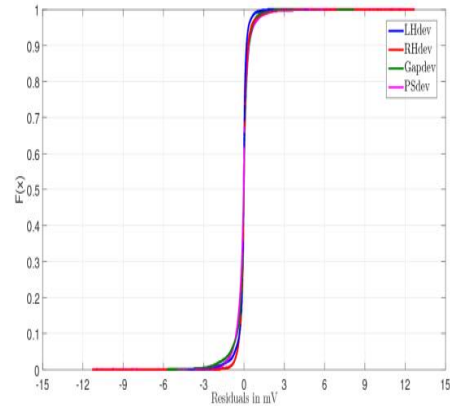
Parameters	Median	Mean	SD	Median	Mean	SD
	Phase1			Phase2		
LHdev	0.95	0.90	0.11	0.89	0.84	0.16
RHdev	0.92	0.88	0.12	0.88	0.83	0.17
Gapdev	0.93	0.88	0.13	0.89	0.84	0.15
PSdev	0.93	0.89	0.16	0.90	0.83	0.17

It is observed that in both Phase1 and Phase2, more than 95% of the data sets with trendlines belonging to the class ZCIM2 have R^2 values larger than 50%. Accordingly, the median values are also much higher, typically greater than 0.92 for the Phase1 ZCI2M2 data sets and greater than 0.88 for the corresponding Phase2 data sets.

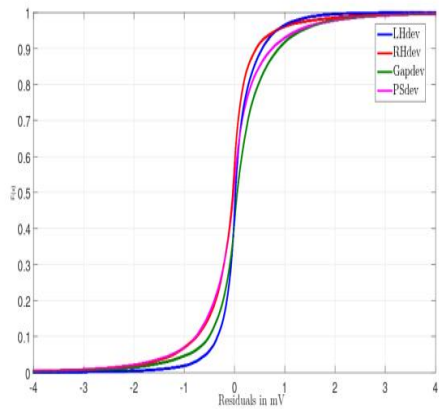
In view of these observations, the cdf plots of the corresponding Residuals, named as $\text{Residuals}_{ZCI2M2}$, are shown in Figure 4.23, along with the corresponding zoomed plots within $\pm 4\text{mV}$ in Figure 4.24. The statistical characteristics of $\text{Residuals}_{ZCI2M2}$ are tabulated in Table 4.11.



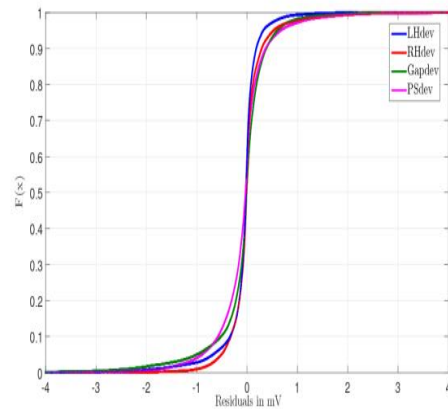
(a) Phase1



(b) Phase2

Figure 4.23: Cdf plots of Residuals for ZCI2M2 class ($\text{Residuals}_{ZCI2M2}$)

(a) Phase1



(b) Phase2

Figure 4.24: Zoomed cdf plots of $\text{Residuals}_{ZCI2M2}$ within $\pm 4\text{mV}$

Each set of these Residuals, generated from the corresponding Deviation signals

Table 4.11: Statistical characteristics of Residuals_{ZCI2M2}

Parameters	Range		Span	Median	Mean	SD	Skewness	Kurtosis
	Min	Max						
for Phase1 in mV								
LH	-7.32	6.92	14.24	0.02	0.06	0.50	-0.28	21.22
RH	-10.95	11.59	22.54	-0.03	-0.10	0.82	-0.27	28.15
Gap	-8.78	12.10	20.88	0.05	0.12	0.83	0.88	21.62
PS	-11.33	13.60	24.93	-0.02	-0.02	0.93	0.09	25.16
for Phase2 in mV								
LH	-4.33	4.72	9.05	0.02	-0.07	0.39	-2.41	22.47
RH	-11.26	12.64	23.90	-0.01	0.01	0.42	2.57	48.75
Gap	-5.70	8.10	13.80	-0.01	-0.06	0.57	-1.94	17.52
PS	-11.23	12.66	23.89	-0.03	-0.06	0.55	0.47	22.41

belonging to class ZCI2M2, has been tested for types of Pearson distribution using Matlab and the results in terms of their % occurrence are tabulated in Table 4.12.

Table 4.12: Type of Pearson distribution for Residuals_{ZCI2M2} with % count

Parameters	Type with % count			Type with % count		
	Class1	Class4	Class6	Class1	Class4	Class6
	Phase1			Phase2		
LHdev	85.7	7.9	6.4	80.8	14.3	4.9
RHdev	89.4	7.9	2.7	88.4	8.1	3.5
Gapdev	91.3	4.9	3.8	79.7	13.2	7.1
PSdev	90.1	8.1	1.8	78.6	16.6	4.8
Class1:Four parameter Beta distribution						
Class4:Not related to any standard distribution						
Class6:F location-scale distribution						

Observations from Figure 4.23, Figure 4.24, Table 4.11 and Table 4.12, along with relevant comparisons with the overall Residuals discussed earlier in Section 4.4.3 are stated hereafter as follows:

1. As in the case of the overall corpus of Residuals, in this case also, the total corpus of instantaneous Residuals of all Deviation signals in both phases are

centered around 0 and their mean and median values are close to each other and almost 0.

2. The factor of difference between the spans of Residuals for RHdev signals and LHdev signals are even larger in this combination class, with the RHdev Residual spans being 1.6 times and 2,7 times in Phase1 and Phase2 respectively.

The spans of Residuals in case of Gapdev are significantly less than those of RHdev signals in both phases. However, the spans of the Residuals of PSdev signals are almost equal or slightly larger than those of the RHdev signals in case of both phases.

Unlike the case of the overall corpus of Residuals, the span of Residuals of LHdev signals in Phase 2 are smaller than those of Phase1, while the corresponding spans for RHdev signals are similar. This finding is in tandem with the expected reduction in variability of the signals due to prolonged rest and hence, an increase in their quasi-linearity.

3. A comparison of the SD of the Residuals of the various signals shows that these are significantly lower in Phase2 for all signals than in Phase1. The values of the SD of Residuals $_{ZCI2M2}$ for all 4 types of signals are almost the same in a particular phase, except for that of LHdev signals in Phase1, with values much smaller than those of the other signals. In both phases, LHdev signals have the minimum SD for Residuals $_{ZCI2M2}$.

Thus in this class also, the trendline fit is better for LHdev signals in both phases in comparison to that for the RHdev signals, .

4. For this class, the distributions of Residuals $_{ZCI2M2}$ can be considered as symmetric for LHdev and RHdev in Phase1, since the values are within ± 0.5 . The corresponding distributions for the residuals of Gapdev and PSdev signals are not symmetric. In Phase2 however, only the distribution for PSdev Residuals $_{ZCI2M2}$ is symmetric, while the others are slightly left or right skewed.

The corresponding kurtosis values for all these cases are larger than those for a normal distribution, but are not too high, unlike the case for the overall Residuals.

5. In this case also, the Residuals_{ZCI2M2} mostly follow a 4 parameter beta distribution, typically more than 85% of the total data samples in Residuals_{ZCI2M2} in all 4 Phase1 signal types and more than 78% of data in all 4 Phase2 signal types.
6. The zoomed cdf plots in Figure 4.24 show that more than 99.2% of the total corpus of Residuals_{ZCI2M2} lie within $\pm 4\text{mV}$ for all four types of Deviation signals for both the phases and the distribution also seems symmetric about 0mV.

In view of these findings, it has been established that most of the Deviation signals can be well represented by trendlines with ZCI and m belonging to ZCI2 and M2 respectively and the Residuals from the fits belonging to this combination class typically lie within $\pm 4\text{mV}$. It is also evident that most of the sets of Residuals in this combination class belong to a 4 parameter beta distribution.

4.6 Discussions:

The variation of all 4 types of signals with respect to time have been studied on a common basis using Deviation signals. For this, the mean of each set, $Mean_{set}$, of all LH, RH, Gap and PS signals for both the phases has been subtracted from the corresponding recorded, or derived, set of biopotentials. These Deviation signals have been named as LHdev, RHdev, Gapdev and PSdev respectively. It is observed that all these signals cross zero typically in the middle epoch. This implies that in most cases, the setwise mean occurs in the middle epoch. This is seen for all subjects and for all sets for both hands.

In general, it is observed that the Deviation signals of the sets of Phase1 and signals of the first set, set1, of Phase2 show monotonic variations. It is further observed that this smooth nature of the variations are lost in certain cases, particularly in case of the later sets in Phase2, when the subjects are in extended periods of rest. This could be attributed to certain mechanical disturbances due to snoring or deep breathing caused by sleep induced in the subjects. In case of the acquired signals, it has been observed in Chapter 3 that the span of LH and RH signals is more for Phase1 than for Phase2. However, in case of the Deviation signals, the case is reversed. As expected, the Gapdev and the PSdev signals also show the same nature of variations as shown by LHdev and RHdev signals.

The statistical parameters of the Deviation signals in both the phases were compared with those of the corresponding signals. As expected, the Deviations are found to vary within a much narrower range of $\pm 30\text{mV}$ unlike the actual signal variations within $\pm 300\text{mV}$. A comparison of the SD values of the signals for both the phases shows that the SD values of LHdev (1.94mV and 1.40mV in Phase1 and Phase2 respectively) are lesser than those of RHdev (2.58mV and 1.73mV respectively) and also the variations of LHdev are within $\pm 20\text{mV}$, which is significantly smaller than those of RHdev. It is to be noted that these values are comparable with the SD values of the setwise SDs of the actual signals.

Since these are Deviation signals, the mean of all these signals are 0mV. It has been observed that the median values of all 4 Deviation signals in both phases are also very close to 0mV. Furthermore, these signals are in general neither left nor right skewed. However, all the signals show a high kurtosis, particularly in Phase2. Among Phase1 and Phase2, the kurtosis is higher for Phase2 than Phase1, which seems to indicate a reduction in signal variability due to elongated periods of rest. This is corroborated by the earlier observation that the SD values in Phase2 are smaller as compared to those in Phase1. It is further seen that that 80% of the Deviation signals lie within $\pm 3\text{mV}$ for Phase1 and within $\pm 2\text{mV}$ for Phase2. Furthermore, 70% of the individual SD values for all subjects lie within $\pm 2\text{mV}$ for both the phases.

It is thus inferred that while prolonged rest stabilizes the overall as well as the Deviation signals, yet induced sleep and other motor disturbances affect the RHdev signals more than the LHdev signals.

The pattern of variations of the Deviation signals have also been studied. Being Deviation signals, these signals are all Transitive in nature. However, like the recorded and derived signals, these Deviation signals also show Increasing, Decreasing and Constant trends when observed individually for both hands and at different times. It must be mentioned here that since the overall range of variation of these Deviations are approximately 1/10th of that for the acquired or derived signals, so the range of values considered for identifying the constant trend has been reduced to $\pm 2\text{mV}$ in place of $\pm 4\text{mV}$. It is to be noted that the SD values for these deviations is typically 2mV.

It is observed that in both phases, irrespective of whether the original LH and RH signal pairs are Converging, Diverging or Crossing in nature, the Deviation signal pairs, LHdev and RHdev, are typically Crossing in nature. On the other hand, when the signal pairs are Parallel, then the Deviation signal pairs are almost overlapping in nature and typically exhibit multiple Crossings.

In order to model all 4 types of Deviation signals, it is observed that these signals mostly follow an increasing, a decreasing or a constant linear pattern, which typically crosses through zero in the middle epoch at around 1200th instant, at the point of time when the $Mean_{set}$ occurs in the original signal. This instant of time closest to the 1200th instant, where the Deviation signal crosses zero, is denoted as the Zero Crossing Instant, ZCI, and the trendline is considered to pass through it. The slope, m , of the trendline has been determined accordingly using a linear regression model. The instantaneous error between the Deviation signal and its corresponding fitted trendline has been termed as Residuals. The characteristics of the ZCI, the slope m as well as the instantaneous Residuals generated due to the mismatch between the Deviation signal and its trendline have been studied.

It is observed that most of the ZCI as well as the slope m values are limited

within narrow ranges, while the Residuals are also tightly bound. The efficacy of the trendline fit is also established since the goodness of fit factor R^2 is typically better than 0.5 for all types of Deviation signals in both phases. These characteristics indicate that the model fits well with the Deviation signals, However, the span of Residuals for RHdev signals is almost 1.5times more than that for LHdev in both phases. This indicates that the non-determinism or stochasticity of RHdev, and hence RH signals, are more than that of LHdev and LH signals.

In view of the tight clustering of the ZCI and m values, their interrelationship has been studied by grouping the values in 3 classes and corresponding counts in each classes have been determined. It is seen that for all 4 types of Deviation signals, the slope m values of the Deviations lie within ± 0.01 mV/instant (Class M2), while the majority of the ZCI lie in the middle epoch, within 800 to 1600 (ZCI2). However, both in Phase1 and Phase2, there are a significant number of sets for which the ZCI lies in the start epoch, within 800 (ZCI1) for which the corresponding slopes are very close to 0. It has also been noted that in case of Phase2, where the subjects are in prolonged periods of rest, the ZCI are almost equally likely to lie in the classes ZCI1 and ZCI2, within 1 to 1600.

The R^2 values for this ZCI2M2 class of signals, R^2_{ZCI2M2} , were checked and it was found that the mean R^2_{ZCI2M2} values are about 0.9 for all four types of Deviation signals of Phase1 and are about 0.8 for Phase2. The instantaneous Residuals of this class, denoted as Residuals $_{ZCI2M2}$, were also studied. It is observed that the Residuals $_{ZCI2M2}$ also remain limited within ± 4 mV for more than 80% of all the LHdev and RHdev signals.

Hence, it can be inferred that most of the Deviation signals can be well represented by trendlines with ZCI within 800 to 1600 and slopes within ± 0.01 mV/instant. It is also evident that most of the Residuals in this combination class belong to a 4 parameter beta distribution.

Chapter 5

Synthesis of a pair of biopotential signals using representative features

5.1 Introduction

In Chapter3, the acquired LH and RH signals have been characterised in terms of their polarity, trend and pairwise natures. The interdependence of the pair of signals has also been inferred from the study. This led to the definition of two new derived signals, Gap and PS, which have also been characterized in terms of their polarity and trend. All four types of signals have also been analysed statistically.

In Chapter4, the identified setwise mean, $Mean_{set}$, of each signal has been deducted from the respective signal to obtain the respective Deviation signal. This led to a study of the time-series nature of these signals. The observation that these Deviations are typically small in magnitude and slowly, almost linearly, varying in nature led to the modelling of these signals using a simple linear regression fit. Based on the key observation that the $Mean_{set}$ typically occurs in the middle epoch of each signal, the parameter Zero Crossing Instant, ZCI, has been defined for the linear

model. A subsequent analysis showed that for all four types of Deviation signals, the ZCI and slope m of the fitted trendlines lie in a restricted zone and the corresponding Residuals for the signals are also limited within a certain range.

In this Chapter, these biopotentials have been synthesised on the basis of the aforementioned observations for the acquired and derived signals, as well as their Deviations. For this, a set of their essential characteristic features have been identified and then a procedure has been devised for the synthesis. This procedure has then been validated in terms of the variety of recorded signals for both the phases. The chapter is organised as follows. The characteristic features of the 4 types of signals that are required for synthesizing the pair of biopotentials are identified in Section 5.2 and the synthesis procedure is detailed in Section 5.3. The validation of this procedure has been stated both qualitatively and quantitatively by comparing them with the recorded pairs of biopotentials in Section 5.4. The overall discussions are stated in Section 5.5.

5.2 Identification of representative features

In order to synthesise a pair of biopotentials, it is essential to specify a minimal non-redundant set of key features and parameters. These have to be identified from the total corpus of features and parameters stated for the acquired LH, RH and derived Gap, PS signals in Chapter 3 as well as their corresponding Deviations, LHdev, RHdev, Gapdev and PSdev signals, in Chapter 4.

In Section 3.3.4, it has been inferred from a detailed quantitative analysis of the 4 types of signals that the setwise mean, $Mean_{set}$, of each signal is an essential parameter, which represents the particular set of acquired or derived signal. Since the signals to be generated are the LH and RH signals hence, out of the four possible choices, only the $Mean_{set}$ of the LH and RH signals are to be used for the synthesis.

The next task is to identify suitable Deviations and their parameters. The first choice for this would be the LHdev and RHdev signals. However, it has been observed

in Section 3.2.1 and Section 3.2.2 that the LH and RH signals, though not identical in any of the aspects, vary within $\pm 300\text{mV}$ for all the sets of data acquired for the same or different individuals at same or different times. This indicates an interdependence between the signals, which has been depicted using the derived Gap and PS signals. Hence, it is logical to use one of the acquired Deviations along with one of the derived Deviations in order to generate biopotentials.

Of the LH and RH signals, it is observed in Section 3.3.3 that prolonged duration of rest in Phase2 leads to an anomaly in the overall behaviour of the RH signals, while the LH signals are relatively unaffected. Furthermore, in Section 4.2, it is observed that the SD of the LHdev signals are in general lesser than those of the RHdev signals across both phases. Hence, the LHdev signal and its regression parameters, specifically its ZCI and slope, are considered suitable for the synthesis.

A similar analysis of the Gap, PS and Gapdev, PSdev signals is required to select the suitable interdependence feature. It has been observed in Section 3.2.4 that in comparison to the Gap signals, the PS signals in Phase1 show an almost equal likelihood of all three possible trends, indicating that these signals are more representative of the baseline nature of the interdependence of the passively acquired LH and RH signals. Furthermore, in Section 4.2.2, it is observed that irrespective of the original pattern of the pairs of LH and RH signals, their Deviations are typically Crossing in nature. It is also observed in Section 4.4 that although the range of values of the slopes of the fitted trendlines for the Gapdev and PSdev signals are quite similar, yet a tight clustering of the ZCI is noted for the PSdev signals in both phases. These aspects indicate that the PSdev signal is a more suitable candidate for representing the interdependence of the LH and RH signals.

Thus, the deterministic components required for the synthesis of the LH and RH pair of signals have been identified. But, it has been observed in Section 4.3 that each set of signals has a set of Residuals associated with it. It has also been established in Section 4.4.3 that these Residuals are essentially stochastic in nature and mostly follow a 4 parameter beta distribution. It must be noted that the Residuals

of the Deviations are the same as those for the corresponding acquired or derived signals. Since the signals to be synthesised are the LH and RH signals, hence their corresponding Residuals, or rather the Residuals of LHdev and RHdev signals, are chosen as suitable stochastic components.

On the basis of the aforementioned analysis, the following have been selected to form the minimal set of deterministic and stochastic parameters required for the synthesis of any realistic pair of LH and RH biopotentials:

- i) mean value of LH signal(LHmean)
- ii) mean value of RH signal(RHmean)
- iii) ZCI of the LH deviation(LHdevZCI)
- iv) slope value of the LH deviation(LHdev m)
- v) ZCI of the PS deviations(PSdevZCI)
- vi) slope of the PS deviations(PSdev m)
- vii) Residual of the LH deviation(LHdevRes)
- viii) Residual of the RH deviation(RHdevRes)

5.3 Synthesis of LH and RH biopotentials:

The synthesis of a pair of LH and RH signals is done in three stages as stated hereafter.

Firstly, the trendlines for the LHdev and PSdev signals are generated using suitable values of (LHdevZCI, LHdev m) and (PSdevZCI, PSdev m) respectively. These are termed as LHdevSim and PSdevSim respectively. The corresponding trendline for the RHdev signal, termed as RHdevSim, is generated by subtracting the LHdev

trendline from the PSdev trendline. It must be noted that the choices of (LHdevZCI, LHdev m) and (PSdevZCI, PSdev m) are critical in deciding the trends of the LHdevSim and RHdevSim signals.

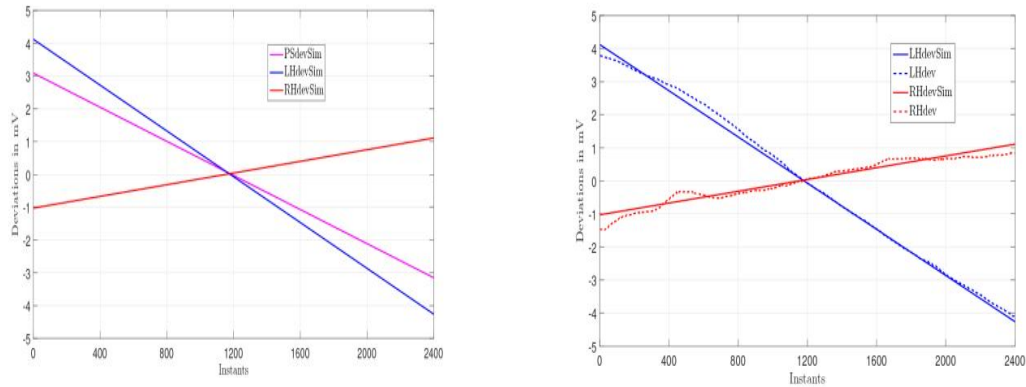
Thereafter, the deterministic components of the LH and RH signals, termed as LHSim and RHSim respectively, are generated by adding the LHmean and RHmean to the respective LHdev and RHdev trendlines. The values of LHmean and RHmean decide the polarities of the generated LHSim and RHSim trendlines.

In the final stage, the realistic biopotentials are generated by adding the instantaneous Residuals to the corresponding trendlines for the signals. Since these Residuals are stochastic in nature, so their values have to be randomly chosen from suitable 4 parameter distributions. Two such suitable sets of Residuals form the LHdevRes and RHdevRes sets and these are added to the respective LHSim and RHSim components to generate the realistic LH and RH pairs of signals, termed as LHRealistic and RHRealistic signals.

Considering that k denotes the time instant and using the relation for the trendline stated in Section 4.3.2, the algorithm for the synthesis of a pair of LH and RH signals can thus be stated as follows:

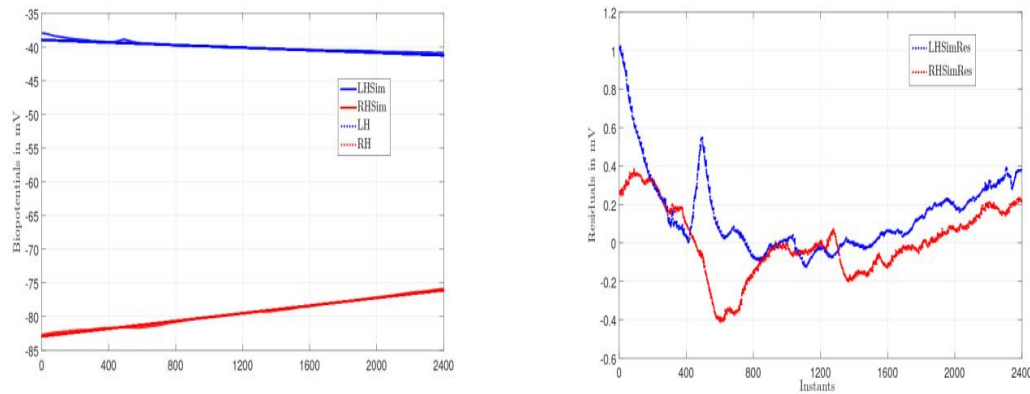
- i) Select LHdevZCI and LHdev m
Generate LHdevSim = LHdev m \times (k - LHdevZCI)
- ii) Select PSdevZCI and PSdev m
Generate PSdevSim = PSdev m \times (k - PSdevZCI)
- iii) Generate RHdevSim = (PSdevSim - LHdevSim)
- iv) Generate LHSim = (LHdevSim + LHmean)
- v) Generate RHSim = (RHdevSim + RHmean)
- vi) Generate a suitable set of LHdevRes from a 4 parameter beta distribution
Generate LHRealistic = LHdevRes + LHSim

- vii) Generate a suitable set of RHdevRes from a 4 parameter beta distribution
 Generate RHRealistic=RHdevRes + RHSim



(a) Synthesized LHdevSim, PSdevSim and (b) Synthesized trendlines and actual pair of RHdevSim trendlines
 Deviation signals

Figure 5.1: Synthesis of pair of Deviation trendlines



(a) Synthesized trendlines and actual pair of (b) Corresponding Residuals LHSimRes and LH and RH signals
 RHSimRes

Figure 5.2: Synthesised pair of signal trendlines and corresponding Residuals

The generation of the deterministic components LHSim and RHSim of a pair of biopotentials are shown in systematic stages in Figure 5.1 and Figure 5.2. For this,

the values of (LHdevZCI, LHdev m) and (PSdevZCI, PSdev m) are chosen from a pair of LHdev and PSdev signals in the ZCI2M2 class, as defined in Section 4.5. The corresponding values of the setwise means (LHmean, RHmean) are chosen to generate the LHSim and RHSim signals.

All simulated deviation signals, namely LHdevSim, PSdevSim and RHdevSim, for all 2400 instants are shown in Figure 5.1. In Figure 5.1a, the PSDevSim is shown in pink, LHdevSim is shown in blue and RHdevSim is shown with red color. Figure 5.1b provides a comparison of the synthesised LHdevSim and RHdevSim trendlines, shown in dotted lines, and the corresponding LHdev and RHdev signals, shown in solid lines.

In Figure 5.2, the synthesised pair of signal trendlines LHSim and RHSim are shown by adding the corresponding setwise mean values to the LHdevSim and RHdevSim signals. The synthesised LHSim and RHSim trendlines, shown in solid lines, can be compared with the corresponding LH and RH signals, shown in dotted lines in Figure 5.2a. The difference between the actual signal and the trendline is a stochastic Residual component. These Residuals for the LH and RH synthesis, termed here as LHSimRes and RHSimRes respectively, are shown in Figure 5.2b.

It is thus observed that the deterministic components of the biopotentials can be generated using the stated procedure and the Residuals generated are stochastic in nature and lie within -0.6mV to $+1.2\text{mV}$.

5.4 Validation of Synthesis Procedure

In this Section, the procedure for synthesis is validated for the ZCI2M2 class of signals. For this, a quantitative analysis has been performed in which the deterministic signal trendlines have been generated using available values of the deterministic parameters and the statistical characteristics of the corresponding Residuals have been verified. Thereafter, a qualitative study of the generated signals has been done to ascertain that the typical characteristics of the pair of LH and RH biopotentials can

be observed in the synthesised signals also.

5.4.1 Quantitative Analysis:

For the synthesis procedure, the deterministic parameters of ZCI and m for LHdev and PSdev signals need to be decided first. Since it has been established that the majority of Deviation signals in both phases belong to the ZCI2M2 class, so those pairs of LH and PS signals have been identified for which the LHdev as well as the PSdev signals belong to this class. This is done to ensure that the generated LH and RH signals can be compared with actual recorded pairs of LH and RH signals.

It is observed from Table 4.9 in Section 4.5 that individually 315 number of LHdev signals and 283 number PSdev signals in Phase1 and 203 number of LHdev signals and 187 number of PSdev signals in Phase2 belong to the ZCI2M2 class. Of these, there are 250 sets in Phase1 and 141 sets in Phase2 for which both LHdev and PSdev signals belong to the ZCI2M2 class. The exact ranges of the ZCI and m parameters for these selected LHdev and PSdev signals, as well as the setwise mean of the corresponding LH and RH signals are stated in Table 5.1 for both the phases.

Table 5.1: Parameter ranges for Trendline generation

Parameters	Phase1		Phase2	
	Min.	Max.	Min.	Max.
LHdevZCI	804	1580	801	1564
PSdevZCI	810	1564	814	1525
LHdev m	-0.0096	0.0057	-0.0058	0.0068
PSdev m	-0.0096	0.0098	-0.0093	0.0084
LHmean	-166.01	141.65	-76.45	14.20
RHmean	-180.58	111.06	-176.03	50.31
Slope(m) in mV/instant, ZCI in instant and mean in mV				

It is observed from Table 5.1 that in both the phases, the ZCI values for LHdev and PSdev span almost the total ZCI2 class (within 801 to 1600 instants) and

the corresponding slopes are also spread widely within the M2 class (within $\pm 0.01\text{mV/instant}$). As expected, the corresponding setwise means of the LH and RH signals in Phase1 are suitably spread within $\pm 300\text{mV}$ in Phase1, while the mean values in Phase2 are more tightly clustered and more so for the LHmean.

The instantaneous stochastic components required for synthesis of the LH and RH signals can be obtained in terms of the Residuals LHSimRes and RHSimRes respectively, as shown earlier in Figure 5.2b. The cdf plots of LHSimRes and RHSimRes for all the selected sets in both phases are shown in Figures 5.3(a) and (b), while their zoomed plots within $\pm 4\text{mV}$ are shown in Figures 5.3(c) and (d). Since the range $\pm 4\text{mV}$ is significant, hence the corresponding Residuals have been labelled as LHSimRes4 and RHSimRes4 respectively. The statistical characteristics of all these 4 classes of signals for both the phases are tabulated in Table 5.2.

For the validation of the synthesis procedure, the Residuals of the actual recorded pairs of signals, specifically Residuals $_{ZCI2M2}$, have to be compared with those corresponding to the synthesised signals. Since the number of data sets considered in this case are different from those in Section 4.5, hence the Residuals of the actual recorded LH and RH signals in this selected ZCI2M2 class have been denoted as LHRes and RHRes respectively and their statistical characteristics have been determined afresh. Their cdf plots have been shown in Figures 5.3(e) and (f), while their statistics are tabulated in Table 5.2.

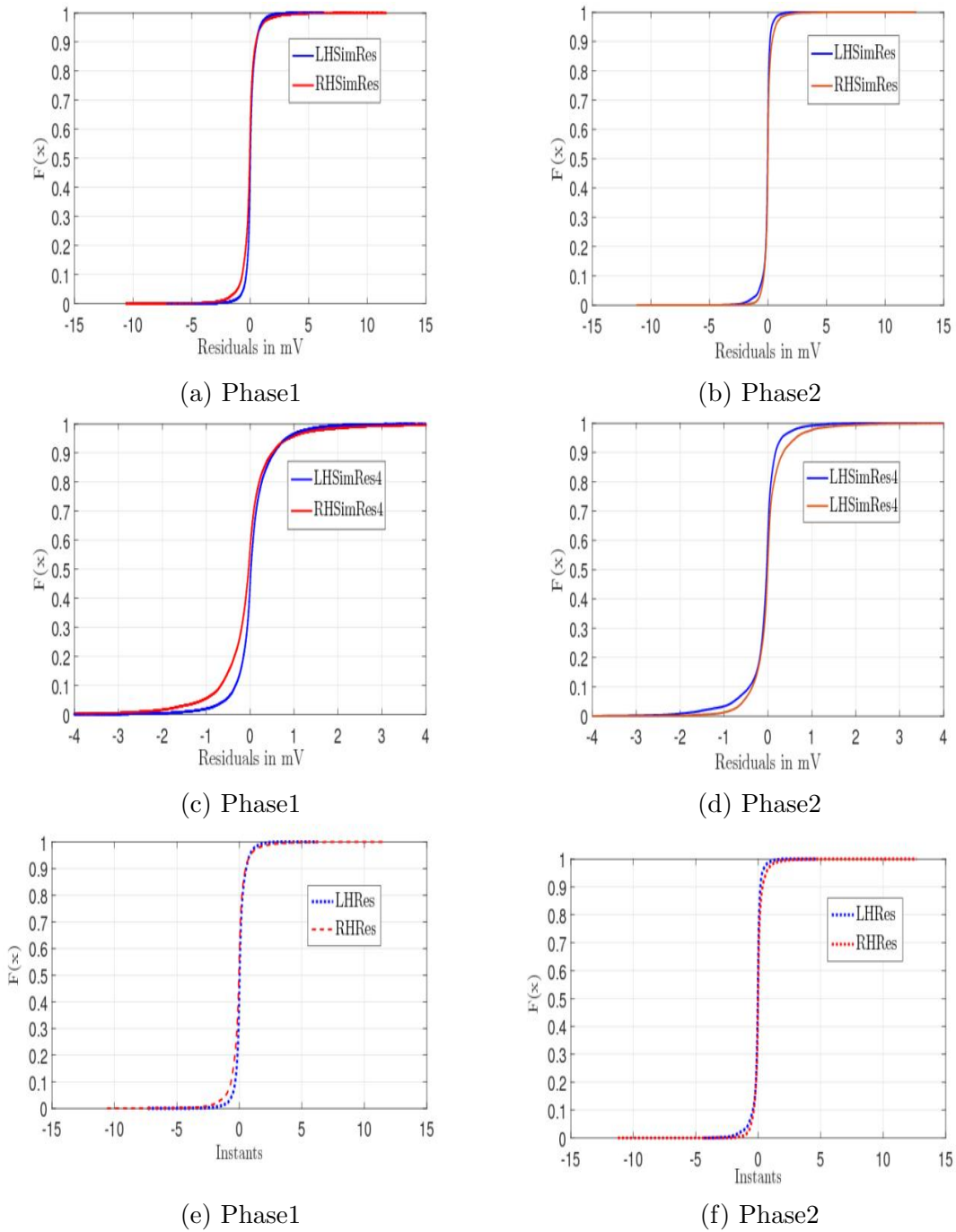


Figure 5.3: Cdf plots of LHSimRes, RHSimRes, LHSimRes4, RHSimRes4, LHRes and RHRes

Table 5.2: Statistical characteristics of Residuals of synthesised and actual signals

Parameters	Range		Span	Median	Mean	SD	Skewness	Kurtosis
	Min	Max						
Residuals of synthesised pair of signals in mV								
Phase1								
LHSimRes	- 7.32	6.92	14.24	0.02	0.06	0.50	-0.30	22.06
RHSimRes	-10.59	11.62	22.21	-0.04	-0.06	0.78	0.16	29.01
Phase2								
LHSimRes	-4.33	4.72	9.05	0.02	-0.07	0.39	-2.14	20.12
RHSimRes	-11.22	12.68	23.90	-0.01	-0.01	0.44	2.20	45.32
Residuals of synthesised pair of signals within $\pm 4\text{mV}$								
Phase1								
LHSimRes4	-4.00	3.99	7.99	0.02	0.06	0.47	0.21	12.23
RHSimRes4	-4.00	3.99	7.99	-0.03	-0.07	0.65	0.00	11.07
Phase2								
LHSimRes4	-3.99	3.97	7.96	-0.03	-0.09	0.42	-2.32	17.70
RHSimRes4	-3.88	3.99	7.81	-0.01	0.00	0.41	1.23	16.6
Residuals of selected actual signals in mV								
Phase1								
LHRes	-7.32	6.92	14.24	0.02	0.06	0.50	-0.30	22.06
RHRes	-10.95	11.59	22.53	-0.03	-0.06	0.78	0.06	29.65
Phase2								
LHRes	-4.33	4.72	9.05	0.02	-0.07	0.39	-2.14	20.12
RHRes	-11.26	12.64	23.90	-0.01	-0.00	0.44	1.52	45.08

The observations from Figure 5.3 and Table 5.2 are stated herewith.

1. It is observed in Table 5.2 that LHSimRes and LHRes are identical in both phases. This is to be expected by virtue of the synthesis procedure for LHSim. However, this is not so for RHSim and the trendline for RH. Hence, as expected, the characteristics for RHSimRes and RHRes vary, but only slightly. The mean, median, SD as well as the kurtosis values are very close to each other, while the skewness values vary slightly in both the phases.

So, it is inferred that the characteristics of the Residuals for both the synthesised signals and the actual signals are almost identical.

2. As in case of LHRes and RHRes, the total corpus of LHSimRes and RHSimRes in both phases are also centered around zero with their mean and median values very close to each other and almost zero.
3. The span of RHSimRes, as well as RHRes, are almost identical in both phases while the corresponding span of the LH Residuals are smaller in Phase2 depicting the effect of prolonged rest. This observation is similar to that of the overall corpus of Residuals analyzed in Section 4.4.3.
4. For this selected class of signals also, the distributions of both LHSimRes and RHSimRes, as well as LHRes and RHRes, in Phase1 can be considered as symmetric since the values are within ± 0.5 . The corresponding distributions for the Residuals for Phase2 are not symmetric in any of the 4 cases. The corresponding kurtosis values for all these cases are slightly larger than those for a normal distribution, as observed earlier also in Section 4.4.3.
5. The zoomed cdf plots in Figures 5.3(c) and (d) show that more than 99% of LHSimRes and RHSimRes values lie within $\pm 4\text{mV}$ for both the phases. The analysis of LHSimRes4 and RHSimRes4 show that these data are even more symmetric in Phase1 and less skewed in Phase2 as compared to LHSimRes and RHSimRes. The kurtosis values are also smaller in all cases than those of LHSimRes and RHSimRes.
6. The results of Pearson distribution tests for LHRes, RHRes, LHSimRes, RHSimRes, LHSimRes4 and RHSimRes4 are tabulated in Table 5.3. As in case of the overall statistical characteristics, the results are identical for LHRes and LHSimRes while those of RHRes and RHSimRes are very close. The results for the Residuals restricted within $\pm 4\text{mV}$, LHSimRes4 and RHSimRes4, are also very close to those of LHSimRes and RHSimRes respectively.

As expected, it is found that more than 80% of the Residuals of all these 6 classes in both phases belong to the class of 4 parameter Beta distributions.

Table 5.3: Comparative Pearson distribution test results for Residuals of actual and synthesised signals

Parameters	Type with % count			Type with % count		
	Class1	Class4	Class6	Class1	Class4	Class6
	Phase1			Phase2		
LHSimRes	87.6	6.8	5.6	80.0	15.7	4.3
RHSimRes	94.0	4.4	1.6	87.9	8.6	3.6
LHSimRes4	88.0	6.8	5.2	79.3	16.4	4.3
RHSimRes4	94.0	4.4	1.6	88.6	7.9	3.6
LHRes	87.6	6.8	5.6	80.0	15.7	4.3
RHRes	91.2	6.4	2.4	91.4	7.9	1.4
Class1:Four parameter Beta distribution						
Class4:Not related to any standard distribution						
Class6:F location-scale distribution						

Thus, it is established that the characteristics of the stochastic components of the actual and the synthesised signals are the same. Furthermore, more than 99% of the Residuals of the synthesised signals lie within $\pm 4\text{mV}$ and more than 80% of these instantaneous values can be generated from the class of 4 parameter beta distribution.

It is known that amongst the 4 parameters of this distribution, two parameters are the minimum and maximum values [117], which are in this case -4mV and 4mV respectively. The other two are shape parameters, typically denoted as α and β . It is also known that for unskewed data, as in the case of Phase1 Residuals, both the shape parameters are equal. In such cases, only one of these shape parameter is required to describe these Residuals and this can be derived as follows: [118], [117]

$$\text{Excess Kurtosis} = \frac{-6}{(3 + 2\alpha)} \quad (5.1)$$

$$\text{and Kurtosis} = \text{Excess Kurtosis} + 3. \quad (5.2)$$

$$\text{So, Kurtosis} = 1 + (4\alpha)/(3 + 2\alpha) \quad (5.3)$$

Thus, considering the minimum and maximum values to be $\pm 4\text{mV}$, the values

of α for LHSimRes4 and RHSimRes4 in Phase1 can be determined using the corresponding stated values of kurtosis in Table 5.2 as -1.83 and -1.87 respectively. For Phase2, the minimum and maximum values can still be considered to be $\pm 4\text{mV}$ and the instantaneous values for LHSimRes and RHSimRes can be generated using both the shape parameters α and β in a standard beta distribution [118].

It is therefore established that there exists a structural hierarchy of two layers in the synthesis of these pairs of passive EDA biopotentials. The inner layer comprises of the LH and PS deviation signals, LHSimdev and PSSimdev, which can be represented as trendlines using suitable choices of their respective ZCI and slope m . The LHSimdev and PSSimdev combine to generate the deterministic trendline for the RH Deviation, RHSimdev.

The upper layer consists of a deterministic and a stochastic component. The deterministic component comprises of two suitable parameters LHmean and RHmean, which add on to the deviation trendlines LHSimdev and RHSimdev to generate the signal trendlines LHSim and RHSim. The stochastic component comprises of two sets of instantaneous values LHSimRes4 and RHSimRes4, which are generated from suitable 4 parameter beta distributions with limits within $\pm 4\text{mV}$. These add to the respective deterministic components to generate the realistic signals.

5.4.2 Qualitative Analysis:

In Chapter 3, it has been observed that the acquired signals as well as the derived signals show day to day as well as person to person variations for both the hands. These signals show Positive, Negative and Transitive values and also depict three different trends in different sets of 2 minute duration. Furthermore, it has been observed that a pair of such LH and RH signals show 4 possible patterns of variation.

Hence, the next task is to verify whether the synthesised signals are capable of representing all these various polarities, trends and pair patterns observed in the original signals. For this, sample pairs of synthesised signals are taken from both Phase1 and Phase2. The synthesised trendlines (LHSim and RHSim) are shown

along with the corresponding LH and RH signals. The residuals LHSimRes and RHSimRes of both LH and RH signals are also shown simultaneously.

Converging Pair: A synthesised Converging signal pair with corresponding Residuals are shown in Figures 5.4(a) and (b). It is observed that LHSim and RHSim are both Positive but the values of RHSim are less than that of LHSim. Also, while LHSim has a Decreasing trend, RH is Constant with initial and final values within 4mV. This combination of trends leads to a Converging pair of signals. The corresponding Residuals, LHSimRes and RHSimRes, are both observed to vary randomly within $\pm 0.5\text{mV}$ with no particular pattern but with a general tendency of having higher initial values and a minimum value near zero at the middle epoch. This is to be expected since the signal trendlines are designed to pass through the ZCI in this region.

Diverging Pair: A synthesised Diverging signal pair with its corresponding Residuals are shown in Figures 5.4(c) and (d). As can be seen, the LHSim and RHSim signals are both Negative in this case with the LHSim values being smaller than those of RHSim. In this case also, both trendlines exhibit different trends with RHSim being Constant while LHSim is Decreasing in nature. In this case also, both the Residuals, LHSimRes and RHSimRes, vary randomly with no particular pattern and with minimum value of zero at the middle epoch. The range of variation of the Residuals in this case is within $\pm 0.8\text{mV}$.

Parallel Pair: A synthesised Parallel signal pair with corresponding Residuals are shown in Figures 5.4(e) and (f). In this case, the LHSim trendline is Positive with slightly Decreasing trend, while the RHSim trendline is Negative with Constant trend. However, the pair of trendlines are together seen as a Parallel pair of signals since their relative initial and final differences are within 4mV. In this case also, both the Residuals, LHSimRes and RHSimRes, vary randomly with no particular pattern except initial large Residuals upto 2mV in case of RHSimRes.

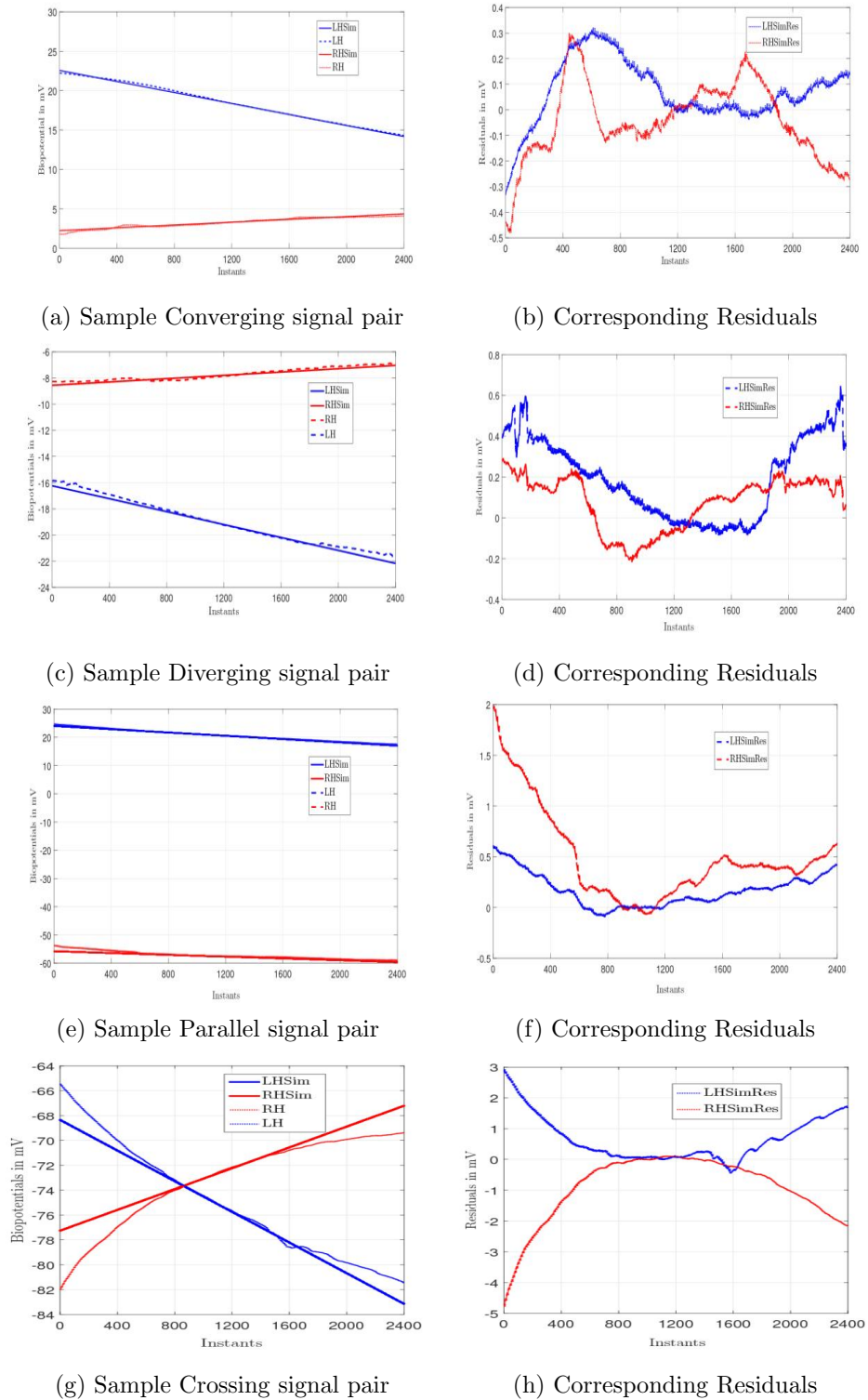


Figure 5.4: Sample synthesised pairs of signals

The bulk of the Residuals are, however, observed to lie within $\pm 0.5\text{mV}$ in both cases.

Crossing Pair: A synthesised Crossing signal pair with corresponding Residuals are shown in Figures 5.4(g) and (h). The LHSim and RHSim trendlines are both Negative but with opposite trends. The LHSim has a Decreasing trend, while the RHSim has an Increasing trend and together, they are seen as a Crossing pair of signals. The Residuals for LHSim and RHSim are seen to vary randomly, but in opposing manners. The LHSimRes values start from a maximum positive value, gradually decrease till a minimum value of zero at the middle epoch and then increase again to end at a positive value slightly lower than the initial value. The corresponding RHSimRes values follow just the reverse pattern.

Thus, it is observed that the signal trendlines give rise to the whole set of functional variations in terms of polarities, trends and pairwise patterns in the biopotentials and the associated Residuals guarantee that no two sets of signals are identical to each other.

5.5 Discussions

The objective of this Chapter is to synthesise realistic pairs of biopotentials on the basis of the observations for the acquired and derived signals, as well as their Deviations stated in earlier Chapters. For this, a minimal set of their essential characteristic features have been identified. There are two distinct components required for the synthesis of realistic signals: the deterministic component and the stochastic component. The deterministic component can be further divided into two layers: the Deviation layer and the signal layer. The essential components for generating the left and right hand Deviation trendlines, denoted as LHSimdev and RHSimdev are the Zero Crossing Instants, ZCI, and slopes m of the LH signal and its corresponding Pair Sum, PS, signal. The RHSimdev is generated from this combination of an

acquired Deviation signal and an interdependence Deviation signal. Thereafter, the addition of the respective setwise means yield the synthesised LH and RH trendlines, LHSim and RHSim respectively. The addition of the stochastic components to these trendlines generates the realistic signals.

In order to validate this synthesis procedure, a total of 250 pairs of signals in Phase1 and 141 pairs of signals in Phase2 were selected such that their respective LHdev and PSdev signals belonged to the ZCI2M2 class, with ZCI within 801 to 1600 instants and slopes within ± 0.01 mV/instant. It was ascertained that the Residuals of the actual pairs of LH and RH signals as well as the synthesised LHSimRes and RHSimRes have similar ranges, spans and statistical characteristics. It was also ascertained that in case of both the actual as well as the synthesised Residuals, more than 99% of the Residuals lie within ± 4 mV and more than 80% of the data belong to the class of 4 parameter beta distributions.

Thereafter, it has been verified for sample generated signal pairs that all possible polarities, signal trends as well as possible patterns seen in a pair of actual recorded signals can be generated using this procedure. This is so since the proper choice of the ZCI and slopes in the LH and PS Deviation signals yields the trends and pairwise patterns for the LH and RH signals and the choice of their respective setwise means provide the signal polarities.

Thus, there exists a clear hierarchy in two levels in the biopotentials. The surface level is defined by the deterministic setwise mean values and the stochastic Residuals, while the inner level is marked by the values of the ZCI and slopes of the acquired LH and the interdependent PS Deviations. This structural complexity leads to the functional complexity in signals, characterised by their different polarity, trends and patterns of variations. It can thus be inferred that a simple 2 layer structural hierarchy leads to the plethora of functional complexity observed in the biopotentials recorded simultaneously from the left and right hand of human subjects.

Chapter 6

Conclusions and Scope for Future Work

6.1 Conclusions:

The aim of this study is to determine the qualitative and quantitative features and parameters of biopotentials that are measured simultaneously from both hands of healthy human subjects using endosomatic EDA technique. These are to be used to characterize healthy human subjects at rest and to devise a procedure using a minimal set of the identified parameters to synthesise realistic pairs of biopotentials.

In order to acquire real-time data for the study, the experiment has been meticulously designed while taking into consideration various aspects. The inclusion and exclusion criteria for selecting subjects have been decided carefully so as to consider healthy subjects only. The experiments are conducted on subjects while they are supine on a fixed bed placed in a well ventilated, low lit, silent cubicle with the temperature and humidity maintained at comfortable levels using air-conditioners at particular settings. This is done to ensure that the diversity in the sensed characteristics are studied with respect to internal causes only, without any external forced disturbances to the system. Accordingly, the locations on the human body for mea-

asuring the signals are also chosen to be non-organ specific, that is, away from major organs in the body. Records of the conditions of the subjects as well as their essential health parameters, specifically blood pressure, pulse rate and oxygen saturation level, have been maintained for every session.

In order to record the desired biopotential signals for subsequent analysis of the inherent characteristics of the human system, a simple, yet safe, instrumentation system was devised without any additional filter or filtering technique. This system was analysed with respect to its static characteristics to ensure the compatibility of the system with the sensors for this application.

This is an observational analytical type of study in which the data from a fixed number of human subjects are acquired using suitable non-invasive, contact type, passive sensors and these are subsequently analysed to identify the features and parameters. The research study has been conducted in two phases, denoted by Phase1 and Phase2, with data recorded from 16 subjects in Phase1 and 14 subjects in Phase2 during different times of the year. Both male and female subjects, who belong to the eastern region of India and are within the age group of 20 to 58 years, were considered for the study. A structured proforma has been designed in the first stage on the basis of similar study materials and preliminary trials. This pretested proforma has been followed for the Phase1 set of studies, where only one set of data was measured in a day. Thereafter, it has been suitably modified in order to study the effect of prolonged duration of rest on the subjects. This second proforma has then been followed in Phase2, where multiple sets of data were measured sequentially, while the subjects lay supine over this extended period. In both phases, each data set lasted for a duration of 2 minutes. The study type was longitudinal in both the phases, in which the data have been acquired repeatedly from each of the subjects, as per their availability and convenience and with mutual consent regarding the time, duration and tenure of the experimental work.

Since the study involves human subjects, so some protocols have been maintained to ensure the objectivity of the study as well as the subject privacy. No compensation

or remuneration in any form were given to any of the subjects for their participation in the research study. The confidentiality of the research data is ensured even during data analysis and publication of results.

Biopotentials, in mV, were recorded from the two fingers of left hand (LH) and right hand (RH) simultaneously for 2 minutes for all the subjects. The total number of samples recorded for a duration of 2 minutes is 2400, with a time interval of 0.05s. A total of 715 such pairs of data have been considered in the two phases, 384 pairs in Phase1 and 331 pairs in Phase2. The general characteristics of the measured signals have been studied and it was found that variability in all senses is the essential feature of these measured LH and RH biopotentials measured from the human subjects. Both the signals vary continuously with time, with different values and trends for each hand. This is so for the same person on same or different dates, and also for different persons on same date. A major observation is that the LH and RH biopotentials remain bounded in a limited range of $\pm 300\text{mV}$ in both phases, yet, in a span of 2 minutes, the data sets vary within few tens of mV only. Hence, these signals may be treated as slowly changing baseline biopotentials of human subjects,

The individual LH and RH signals were checked for their variations in terms of polarity and trends. The signals were classified into three categories of wholly Negative polarity, Positive polarity and Transitive data, where the data set changes its polarity from Negative to Positive or vice versa. The data sets were also segregated with respect to their trends as Increasing, Decreasing or Constant signals, with the limit for constancy being considered as $\pm 4\text{mV}$. Further, the data sets were also classified in terms of their pairwise patterns of variation. Accordingly, all the simultaneously acquired pairs of LH and RH data sets were categorized as Converging, Diverging, Parallel or Crossing pairs of signals.

Another key observation is that while the LH and RH biopotentials remain bounded, yet they are never identical over any set of 2min recording and may exhibit any of the polarities or trends or pairwise patterns in the various sets. Thus, despite their inherent variability, there seems to be an interdependence between the signals.

In order to explore this interdependence, two new signals were proposed: the Gap signal, which records the instantaneous difference between the simultaneously recorded LH and RH signals, and the Pair Sum (PS) signal to record the corresponding instantaneous sum. The general characteristics, polarity and trends of these proposed signals have also been studied.

It is observed that in all the four types of signals, namely LH, RH, Gap and PS signals, the longer duration of rest in Phase2 data sets corroborates with a significant increase in the counts of Negative polarity and Constant trend. The number of Parallel pairs of signals are also significantly more in Phase2. Another interesting observation is that if all the combinations of a Constant trend in any one hand, LH and/or RH, with any of the other trends in the other hand are considered, then almost 72% of the data sets in Phase1 and 97% of the data sets in Phase2 fall in this category. Hence, the other combinations are quite less likely, typically only about 28% data sets in Phase1 and about 3% data sets in Phase2. Yet, all four pairwise patterns are observed in both phases. Of these, the Crossing pattern is the least likely and is observed to occur mostly during the midday.

The characteristics of the Gap and PS signals are observed to be different in the two phases. In Phase1, where the data were collected only once a day from a subject, the occurrences of all the trends are almost equal for PS signals, while they differ in case of Gap signals. Associated with this, in Phase2, the Positive Gap signals are almost as likely as the Negative Gap signals, but most PS signals are Negative in Phase2, as is to be expected for subjects in relaxed condition. Thus, it may be inferred that the PS signals are more representative of the baseline nature of the interdependence of the measured LH and RH signals.

The quantitative analysis of the overall data recorded in the two phases for all these four signal types is done by determining their statistical parameters. It is observed that the LH signals show a consistent unimodal nature in both the phases and the data are clustered tighter in Phase2 than in Phase1, indicating the effect of prolonged rest. However, while the RH data in Phase1 shows a similar unimodal

characteristic, an anomaly was observed in the RH data in Phase2, where it showed a multimodal nature with significantly high variability. An analysis ascertained that this was not due to any particular subject(s), but was due to data recorded from all subjects on a few specific dates. It was also observed that the individual sets of the LH as well as RH signals, as recorded in a set of 2min, showed limited variation in all cases. Thus, among the LH and RH signals, it is observed that the LH signals are more consistent over both the phases.

In a subsequent analysis, it has been established that the overall characteristics of the data in the two phases for all four types of signals are almost identical to those of their overall corpus of setwise means, $Mean_{set}$, in the two phases and this includes the anomaly observed in the RH signals in Phase2. This is to be expected since a set of data varies only within few mVs. The low values of the corresponding setwise standard deviations (SD), denoted as SD_{set} , for both the phases substantiate this fact. It is also observed that, as expected, the values of SD_{set} are smaller in Phase2 than in Phase1. Thus, the $Mean_{set}$ has been considered to be a representative parameter of the corresponding signal.

In order to provide a common basis for studying the time-series characteristics of these signals, the $Mean_{set}$ has been deducted from each signal and the resulting set has been termed as the Deviation signal. The four types of Deviation signals are termed as LHdev, RHdev, Gapdev and PSdev signals.

The statistical parameters of all four types of Deviation signals in both the phases have been studied. For all these signals, the total range is limited within $\pm 30\text{mV}$, which is almost 1/10th of that of the corresponding original signal. Since these are Deviation signals, the mean of all these signals are 0mV and it is observed that their median values are also very close to 0mV. However, the variation in LHdev, as well as the SD, is significantly smaller, within $\pm 20\text{ mV}$ in both Phase1 and Phase2, as compared to that in RHdev. It is also observed that while prolonged rest stabilizes the overall as well as the Deviation signals, yet induced sleep and other motor disturbances affect the RHdev signals more than the LHdev signals. The larger vari-

ability of RHdev leads to corresponding variations in Gapdev and PSdev signals. This indicates the stability of the LHdev signals as compared to the RHdev signals.

The cdf plots of all four Deviation signals in both phases show a common unimodal nature. Thus, the larger variability in the RHdev signals is not associated with any anomalous multimodal nature, unlike the RH signals. In general, the four types of Deviation signals are neither left nor right skewed in Phase1, while Phase2 signals show slight left or right skewed characteristics. However, all these unimodal signals show a high kurtosis, particularly in Phase2, which seems to indicate a reduction in signal variability due to elongated periods of rest. This is corroborated by the earlier observation that the SD values in Phase2 are smaller as compared to those in Phase1. It is further seen that that 80% of the Deviation signals lie within $\pm 3\text{mV}$ for Phase1 and within $\pm 2\text{mV}$ for Phase2.

All these signals in both phases have also been studied in terms of their general characteristics, polarity and trend, as well as the pairwise patterns of the LHdev and RHdev signals. It is observed that the corpus of all these signals exhibit a butterfly like pattern in time with the signals crossing zero typically in the middle epoch, within 801 to 1600 instant. This indicates that the $Mean_{set}$ typically occurs at this point of time in an acquired or derived signal. These signals are all Transitive in nature, but they show all 3 different trends. In view of the observation that 70% of the individual SD values for all subjects lie within $\pm 2\text{mV}$ for both the phases, the constancy of these signals are considered within these limits. It is observed that in case of Deviations also, Constant trend dominates in Phase2 and its prevalence in Phase2 increases from that in Phase1 for all 4 types of signals.

In case of the pairwise patterns, it is observed that in both phases, irrespective of whether the original LH and RH signal pairs are Converging, Diverging or Crossing in nature, the Deviation signal pairs, LHdev and RHdev, are typically Crossing in nature. On the other hand, when the signal pairs are Parallel, then the Deviation signal pairs are almost overlapping in nature and typically exhibit multiple Crossings.

Thereafter, these Deviation signals have been fitted with regression models. It is

observed that most of the Deviation signals follow an almost linear variation around zero value, which occurs typically in the middle epoch. Thus, a linear regression model has been determined for these signals using the zero crossing instant, ZCI, and the corresponding slope of the trendline, m . The values of ZCI and m for all the Deviation signals in both phases have been determined and the validity of the regression model has been ascertained in terms of goodness of fit factor R^2 and the characteristics of the corresponding Residuals for each case.

It is observed that most of the values of ZCI as well as m are limited within narrow ranges, while the Residuals are also tightly bound with almost 99% of them lying within $\pm 4\text{mV}$. The efficacy of the trendline fit is also established since the R^2 values are typically better than 0.5 for all types of Deviation signals in both phases. These characteristics indicate that the model fits well with the Deviation signals. However, the span of Residuals for RHdev signals is almost 1.5times more than that for LHdev in both phases. This indicates that the non-determinism or stochasticity of RHdev, and hence RH signals, are more than that of LHdev and LH signals.

In view of the tight clustering of the ZCI and m values, their interrelationship has been studied by grouping the values in 3 classes and the corresponding counts in each combination class has been noted. For all four types of Deviation signals, it is observed that most of the slope m values lie within ± 0.01 mV/instant (Class M2) with the corresponding ZCI values in the middle epoch, within 801 to 1600 instant (Class ZCI2). The R^2 values for this ZCI2M2 class of signals, R^2_{ZCI2M2} , were checked and it was found that the mean R^2_{ZCI2M2} values are about 0.9 for all four types of Deviation signals of Phase1 and are about 0.8 for Phase2. The instantaneous Residuals of this class, denoted as Residuals $_{ZCI2M2}$, were also studied. It is observed that the Residuals $_{ZCI2M2}$ also remain limited within $\pm 4\text{mV}$ for more than 99.2% of all the four types of Deviation signals in both phases. Hence, it can be inferred that most of the Deviation signals can be well represented by trendlines with ZCI within 800 to 1600 and slopes within ± 0.01 mV/instant. It has also been established that more than 80% of the sets of Residuals of LHdev and RHdev signals in this

combination class belong to a 4 parameter beta distribution.

However, it has also been observed that both in Phase1 and Phase2, there are a significant number of sets for which the ZCI lies in ZCI1, for which the corresponding slopes are very close to 0. It has also been noted that in case of Phase2, where the subjects are in prolonged periods of rest, the ZCI are almost equally likely to lie in the classes ZCI1 and ZCI2, within 1 to 1600.

Using the identified features and parameters, a procedure has been proposed in this study to synthesise a realistic pair of LH and RH signals using a deterministic component and a stochastic component. The deterministic component consists of a Deviation layer and a signal layer. The essential components for generating the LH and RH Deviation trendlines, denoted as LHSimdev and RHSimdev, are the ZCI and m of the LH signal and its corresponding PS signal. The RHSimdev is generated from this combination of an acquired Deviation signal and a derived Deviation signal. Thereafter, the respective setwise means are added to form the synthesised LH and RH trendlines, LHSim and RHSim respectively. The addition of the stochastic components to these trendlines finally generates the realistic signals.

This synthesis procedure has been validated using 250 pairs of signals in Phase1 and 141 pairs of signals in Phase2, which were selected such that their respective LHdev and PSdev signals belonged to the ZCI2M2 class. It was ascertained that the Residuals of the actual pairs of LH and RH signals as well as the Residuals of the synthesised trendlines, denoted as LHSimRes and RHSimRes, have similar ranges, spans and statistical characteristics with more than 99% of the Residuals within $\pm 4\text{mV}$ and more than 80% of the data belonging to the class of 4 parameter beta distributions.

Thus, there exists a clear hierarchy in two levels in the biopotentials. The surface level is defined by the deterministic setwise mean values and the stochastic Residuals, while the inner level is marked by the values of the ZCI and slopes of the acquired LH and the interdependent PS Deviations. This structural complexity leads to the functional complexity in signals, since the proper choice of the ZCI and slopes in the

LH and PS Deviation signals yields the trends and pairwise patterns for the LH and RH signals, the choice of their respective setwise means provides the signal polarities and the selection of suitable sets of stochastic Residuals guarantees the uniqueness of each signal.

It can thus be concluded that a simple 2 layer structural hierarchy leads to the plethora of functional complexity observed in the endosomatic EDA biopotentials recorded simultaneously from the left and right hand of human subjects.

6.2 Scope for future work

The investigation of these biopotentials performed in this study has indicated the existence of interrelations between LH and RH signals. These are also indicative of the essential bilaterality of the human system. Further detailed studies are required to explore the various aspects associated with this bilaterality. In order to do so, the study must be extended to include endosomatic signals from other bilateral non-organ specific locations in the body.

Using this study as a basis, features related to endosomatic as well as exosomatic studies of subjects subjected to known tasks or disturbances can be identified and characterized. In particular, orthostatic tests using these biopotentials can be used to identify the effect of posture change on biopotential levels.

In the present study, a linear regression model has been derived for the Deviation signals using the ZCI and m values in the ZCI2M2 class. This procedure can be adapted to model the signals in the ZCI1M2 class also since these constitute a significant proportion of the total number of signals, particularly in Phase2. The modelling of these signals can further be extended to generic higher order regression fits using ACF and Kalman filter based approaches, which might be more useful to model certain human conditions and/or particular external stimulations. Further, modelling of this response using time series analysis techniques; deterministic models and/or other methods like Fuzzy and Neural Network techniques can also be done

to model dynamic scenarios like those during orthostatic tests.

This study can also be used as a baseline for determining characteristic features of established medical conditions like stress or hypertension in the EDA potentials. Such studies can be expected to provide features in the biopotentials that can be correlated with some standard health parameters like blood pressure (BP), pulse rate (PR), ECG or EEG and might be useful in providing a simple, safe, low cost, non-invasive health monitoring device.

Annexure

Consent Form

Note to the subjects:

You are being asked to take part in the research study described below. There are no known risks associated with this research. If you do not take part in the study, there will be no penalty. If you choose to take part, you have the right to stop at any time. However, we encourage you to talk to the research group so that we know why you are leaving the project. If there are any new findings during the study that may affect you, you will be told about them. Your part in this study is confidential. None of the information will identify you by name. All records will be maintained in codes so that identity is not disclosed. If you decide to participate in this study, your involvement will be required in 2 or 3 phases for the experimental portion only and this may last for about 10-12 weeks per phase. The results of this research study may be presented at meetings or in publications; however, your identity will not be disclosed at any point of time.

About the Research Topic:

Topic: “Study and Characterization of Non-organ specific Biopotential Signals acquired from the Human System”

It is known that EEG and ECG measures the electrical activity of the brain and heart respectively. On the other hand, the endosomatic method of measurement of electrodermal activity (EDA) consists of passive reception of electrical activity of the dermal substrate. Thus, a huge variety exists in the type of biopotentials that can be recorded from a human subject from relatively convenient locations on the surface, eliminating the need to invade the system. The present research aims to determine the qualitative and quantitative features and parameters of biopotentials that are measured simultaneously from both hands of healthy human subjects using endosomatic EDA technique. These are to be used to characterise healthy human subjects at rest and to devise a procedure using a minimal set of the identified parameters to synthesise realistic pairs of biopotentials. The biopotentials are acquired without any external stimulus and non-invasively from the human subjects using a simple instrumentation system comprising of 2 sets of multimeters with compatible adapter for online recording of the data to the PC without any additional filter or filtering technique, using two pairs of EDA sensors (Ag-AgCl electrodes), one pair of sensors for each hand. These measured signals will be analysed statistically to characterize and identify representative features of the human system.

I, Mr./Mrs./Dr./Ms. ----- resident of -----
----- do hereby give consent voluntarily to record my biopotentials and other data pertaining to the research work being conducted by Mrs. Aditi Roy(Bhattacharya) under the guidance of Dr. Ratna Ghosh and Dr. Bhaswati Goswami in Instrumentation and Electronics Engineering Department, Jadavpur University. I have no objection to publication of my case study details without my name in any journal or any other reviews. I am signing this consent form voluntarily, out of free will, without any pressure and in my full senses.

Date: _____ Full Signature : _____
Place: _____

Consent form explained/witnessed by: -----

Date: _____ Full Signature : _____
Place: _____

Questionnaire for subjects

SUBJECT CODE : S _ _ _				
Full name	পুরো নাম			
Sex (Male/Female)	লিঙ্গ (ছেলে/মেয়ে)			
Age (years)	বয়স (বছর)			
<i>Please Answer the following - (write Y for yes and N for no):</i>	<i>নিম্নলিখিত প্রশ্নগুলির (হ্যাঁ বা না দিয়ে) উত্তর দিন</i>	<i>Mention Y or N For any disease you may have or had</i>	<i>Do you take any medicine prescribed by doctor?</i>	<i>Do you take any medicine on your own?</i>
1. Do you have any disease from the following list (any history of Chronic illness)? (Y/N)	আপনার নিচের লেখা ব্যাধিগুলি থেকে, এক বা একের বেশী কোনো ব্যাধি (দীর্ঘস্থায়ী অথবা দুরারোগ্য) আছে? (হ্যাঁ বা না)	কোনো রোগ থাকলে, হ্যাঁ বা না দিয়ে উত্তর দিন Y/N	আপনি কি ডাক্তারের বলা কোনো ওষুধ খান? Y/N	আপনি কি নিয়মিত নিজে থেকে কোনো ওষুধ খান? Y/N
High Blood Pressure/ Hyper tension	উচ্চ রক্তচাপ			
Diabetes	মধুমেহ			
Kidney problem	কিডনির সমস্যা			
High Cholesterol	কোলেস্টেরল বেশী			
Chronic Constipation	দীর্ঘস্থায়ী কোষ্ঠ-কাঠিন্য			
Chronic Cardiac problem	দীর্ঘস্থায়ী হার্টের সমস্যা			
Chronic Indigestion	দীর্ঘস্থায়ী বদহজমের সমস্যা			
Any other Chronic illness	আর অন্য কোনো দীর্ঘস্থায়ী ব্যাধি			
Prone to cold infection	সর্দি-কাশীর ধাত			
Asthma	হাঁপানি			
Headache	মাথা ব্যথা			
Migraine	মাইগ্রেন			
Prostrate problem	প্রস্টেট সমস্যা			
Jaundice	ন্যাড়া/পাণ্ডুরোগ			
Dengue	ডেঙ্গু			
Chicken pox	চিকেন-পক্স			
Menstrual problem	মাসিকের সমস্যা			
Others (mention)	অন্য কোনো সমস্যা (থাকলে জানান)			
Mumps	মাম্পস্			
Toncil	টনসিল			
<i>Answer these questions in Yes/No</i>	<i>নিচের প্রশ্নগুলির হ্যাঁ বা না তে উত্তর দাও</i>	<i>Yes (Y)</i>	<i>No (N)</i>	
2 Do you have any dominant or recurrent pain?	আপনার কোনো দীর্ঘস্থায়ী বা রোজকার বেথা আছে?			
If yes (Y), please specify region.	হ্যাঁ হলে কোথায়?			
3 Have you had surgery before?	আপনার কোনো অস্ত্রপচার হয়েছে?			
If yes (Y), please specify	হ্যাঁ হলে কোথায়?			
4 For females only: Any Hormone replacement (HR) therapy done?	মহিলাদের জন্য: আপনার কোনো হরমোনের চিকিত্সা হয়েছে?			
5 Are you a consumer of alcohol?	আপনি কি মদ্যপান করেন?			

Questionnaire for subjects

	if yes (Y) then, daily/weekly/monthly/occasional? is it more than 2 pegs or less?	হ্যা হলে, কি রোজ/সপ্তাহে/মাসে/মাঝে মধ্যে? ২ পেগের বেশি না কম?		
6	Do you smoke?	আপনি কি ধূমপান করেন?		
	if yes (Y), then what (cigarette/ biri/ cigar) ?	হ্যা হলে (সিগারেট/বিড়ি/সিগার)?		
	Is it more than 10 nos. daily or less?	দিনে ১০টার বেশি না কম?		
7	Do you take drugs?	আপনি কি মাদক সেবন করেন?		
	if yes (Y), then daily/weekly/monthly/occasional ?	হ্যা হলে, রোজ/সপ্তাহে/মাসে/মাঝে মধ্যে?		
8	Do you take Jarda paan?	আপনি কি জর্দা পান খান?		
9	Do you take Jarda masala / pan parag/ chutki /gutkha?	আপনি কি জর্দা মশলা/পান পরাগ/চুটকি/ গুটখা খান?		
	If yes (Y), please tell what?, How much?	হ্যা হলে কোনটি? কতটা?		
10	Are you left handed?	আপনি কি বাম হাতে কাজ করেন?		
	Measured Physical parameters -	শারীরিক পরিমাপ		
	Weight in kg.	ওজন কিলোগ্রামে		
	Height in meters	উচ্চতা মিটারে		
	BMI (Body mass Index) in metric	BMI সংখ্যায়		
	Waist measure in cm.	কোমর সেন্টিমিটারে		
	Hip measure in cm.	নিতম্ব সেন্টিমিটারে		
	WHR (Waist to Hip Ratio)	কোমর ও নিতম্বের অনুপাত		

Bibliography

- [1] J. D. Bronzino, *Biomedical Engineering Handbook*. CRC press, 1999, vol. 2.
- [2] W. Boucsein, *Electrodermal Activity*. Springer Science & Business Media, 2012.
- [3] R. L. Veech, Y. Kashiwaya, and M. T. King, “The resting membrane potential of cells are measures of electrical work, not of ionic currents,” *Integrative Physiological and Behavioral Science*, vol. 30, no. 4, pp. 283–307, 1995.
- [4] R. F. Yazıcıoğlu, C. Van Hoof, and R. Puers, “Biopotential readout front-end asics,” in *Biopotential Readout Circuits for Portable Acquisition Systems*. Springer, 2009, pp. 39–78.
- [5] V. H. Rice, *Handbook of Stress, Coping, and Health: Implications for Nursing Research, Theory, and Practice*. Sage, 2012.
- [6] C. L. Edelman, C. L. Mandle, and E. C. Kudzma, *Health Promotion Throughout the Life Span-E-Book*. Elsevier Health Sciences, 2017.
- [7] L. Jensen and M. Allen, “Wellness: The dialectic of illness,” *Image: the Journal of Nursing Scholarship*, vol. 25, no. 3, pp. 220–224, 1993.
- [8] M. S. Eberhardt, D. D. Ingram, D. M. Makuc, E. Pamuk, V. Freid, S. Harper, C. Schoenborn, and H. Xia, “Urban and rural health chartbook,” *Health, United States*, 2001.

- [9] D. Callahan, "The WHO definition of 'health'," *Hastings Center Studies*, pp. 77–87, 1973.
- [10] (2003) WHO definition of 'Health'. [Online]. Available: <http://www.who.int/about/definition/en/print.html>
- [11] S. Bok, "Rethinking the who definition of health," *Harvard Center for Population and Development Studies Working Paper Series*, vol. 14, no. 7, 2004.
- [12] S. Mackey, "Towards an ontological theory of wellness: A discussion of conceptual foundations and implications for nursing," *Nursing Philosophy*, vol. 10, no. 2, pp. 103–112, 2009.
- [13] D. B. Ardell, "High Level Wellness Strategies," *Health Education*, vol. 8, no. 4, pp. 2–2, 1977, pMID: 406244. [Online]. Available: <https://doi.org/10.1080/00970050.1977.10618258>
- [14] M. Neuman, "Biopotential electrodes - The Biomedical Engg Handbook," *CRC Press LLC, Boca Raton*, 2000.
- [15] L. Geddes and L. Baker, "Principles of Applied Biomedical Instrumentation," *Journal of Clinical Engineering*, vol. 2, no. 1, p. 86, 1977.
- [16] R. Plonsey, "Bioelectric phenomena," *Wiley Encyclopedia of Electrical and Electronics Engineering*, 2001.
- [17] R. Plonsey and R. C. Barr, *Bioelectricity: a quantitative approach*. Springer Science & Business Media, 2007.
- [18] R. C. Barr and J. D. Bronzino, "Basic electrophysiology," *The Biomedical Engineering Handbook*, vol. 2, 2000.
- [19] L. Cromwell, F. J. Weibell, and E. A. Pfeiffer, *Biomedical Instrumentation and Measurements*. Prentice Hall, 1980.

- [20] C. D. McCaig, B. Song, and A. M. Rajnicek, “Electrical dimensions in cell science,” *Journal of cell science*, vol. 122, no. 23, pp. 4267–4276, 2009.
- [21] S. Ghatak, B. Roy, R. Choudhuri, and S. Bandopadhaya, “Modulation of autonomous nervous system activity by gyrosonic stimulation,” 03 2010.
- [22] B. Roy, R. Choudhuri, A. Pandey, S. Bandopadhyay, S. Sarangi, and S. K. Ghatak, “Effect of rotating acoustic stimulus on heart rate variability in healthy adults,” *The open neurology journal*, vol. 6, p. 71, 2012.
- [23] R. L. Bailey, “Electrodermal activity (EDA),” *The International Encyclopedia of Communication Research Methods*, pp. 1–15, 2017.
- [24] R. Edelberg, “Electrical activity of the skin: Its measurement and uses in psychophysiology,” *Handbook of Psychophysiology*, pp. 367–418, 1972.
- [25] S. Yagi, “Computational discourse analysis for interpretation,” *Meta: Journal des traducteurs/Meta: Translators’ Journal*, vol. 44, no. 2, pp. 268–279, 1999.
- [26] H. S. Burr and F. S. C. Northrop, “The electro-dynamic theory of life,” *The Quarterly Review of Biology*, vol. 10, no. 3, pp. 322–333, 1935.
- [27] P. Venables and M. Christie, “Mechanisms, instrumentation, recording techniques, and quantification of responses,” *Electrodermal activity in psychological research*, 2012.
- [28] W. Prokasy, *Electrodermal activity in Psychological research*. Elsevier, 2012.
- [29] J. G. Webster and H. Eren, *Measurement, instrumentation, and sensors handbook: spatial, mechanical, thermal, and radiation measurement*. CRC press, 2014, vol. 1.
- [30] N. V. Thakor, “Biopotentials and electrophysiology measurement,” *The Measurement, Instrumentation, and Sensors Handbook*, vol. 74, 1999.

- [31] H. Carim *et al.*, “Bioelectrodes,” *Encyclopedia of Medical Devices and Instrumentation*, vol. 1, pp. 195–226, 1988.
- [32] Y. M. Chi, T.-P. Jung, and G. Cauwenberghs, “Dry-contact and noncontact biopotential electrodes: Methodological review,” *IEEE reviews in biomedical engineering*, vol. 3, pp. 106–119, 2010.
- [33] D. C. Fowles, M. J. Christie, R. Edelberg, W. W. Grings, D. T. Lykken, and P. H. Venables, “Publication recommendations for electrodermal measurements,” *Psychophysiology*, vol. 18, no. 3, pp. 232–239, 1981.
- [34] E. McAdams, “Bioelectrodes,” *Encyclopedia of medical devices and instrumentation*, 2006.
- [35] R. Edelberg, “Electrical properties of the skin,” *Methods in psychophysiology*, 1967.
- [36] J. G. Webster, *Medical Instrumentation Application and Design*. John Wiley & Sons, 2009.
- [37] H. J. Baek, G. S. Chung, K. K. Kim, and K. S. Park, “A smart health monitoring chair for nonintrusive measurement of biological signals,” *IEEE transactions on Information Technology in Biomedicine*, vol. 16, no. 1, pp. 150–158, 2012.
- [38] I. Hjermann, I. Holme, K. V. Byre, and P. Leren, “Effect of diet and smoking intervention on the incidence of coronary heart disease: Report from the Oslo Study Group of a randomised trial in healthy men,” *The Lancet*, vol. 318, no. 8259, pp. 1303–1310, 1981.
- [39] B. Rifkind, “The lipid research clinics coronary primary prevention trial results. I. Reduction in Incidence of Coronary Heart Disease,” *J Am Med Assoc*, vol. 251, pp. 351–364, 1984.

- [40] S. Bandopadhyay, M. K. Mandal, P. P. Chakrabarti, S. K. Ghatak, R. Chowdhury, and S. Ray, “Moving sound reduces arousal in psychosomatic patients,” *International Journal of Neuroscience*, vol. 116, no. 8, pp. 915–920, 2006.
- [41] A. Kumar, “Effect of gyrosound on brain: A magnetoencephalographic study,” Ph.D. dissertation, School of Medical Science and Technology, Indian Institute of Technology, Kharagpur, 2007.
- [42] P. Puska, J. Tuomilehto, A. Nissinen, J. T. Salonen, E. Vartiainen, P. Pietinen, K. Koskela, and H. J. Korhonen, “The north karelia project: 15 years of community-based prevention of coronary heart disease,” *Annals of Medicine*, vol. 21, no. 3, pp. 169–173, 1989.
- [43] D. Bari, H. Aldosky, C. Tronstad, H. Kalvøy, and Ø. Martinsen, “Electrodermal responses to discrete stimuli measured by skin conductance, skin potential, and skin susceptance,” *Skin Research and Technology*, vol. 24, no. 1, pp. 108–116, 2018.
- [44] D. Callahan, “The WHO definition of ‘Health’,” vol. 1, pp. 77–88, 02 1973.
- [45] J. S. Larson, “The World Health Organization’s definition of health: Social versus spiritual health,” *Social Indicators Research*, vol. 38, no. 2, pp. 181–192, 1996.
- [46] Huber *et al.*, “How should we define health?” *BMJ, formerly the British Medical Journal*, vol. 343, pp. d–4163, 2011.
- [47] J. Guckenheimer, “Organisms as complex systems.” [Online]. Available: <http://www.mathaware.org/mam/2011/essays/complexsystemsGuckenheimer.pdf>
- [48] J. Guckenheimer and J. M. Ottino, “Foundations for complex systems research in the physical sciences and engineering,” in *Report from an NSF Workshop in September*, 2008.

- [49] G. R. Cooper and C. D. McGillem, *Probabilistic methods of signal and system analysis*. Oxford University Press, 1986, no. BOOK.
- [50] R. Shiavi, *Introduction to applied statistical signal analysis: Guide to biomedical and electrical engineering applications*. Elsevier, 2010.
- [51] J. Muthuswamy, “Biomedical signal analysis,” *Standard Handbook of Biomedical Engineering and Design*, pp. 18–1, 2004.
- [52] M. Shinji, “A study of the association with blood pressure difference causing body temperature 37.5 c and hypertension in department of primary care,” *Clinical physiology and functional imaging*, vol. 33, no. 6, pp. 441–449, 2013.
- [53] M. J. Joyner, N. Charkoudian, and B. G. Wallin, “Sympathetic nervous system and blood pressure in humans: individualized patterns of regulation and their implications,” *Hypertension*, vol. 56, no. 1, pp. 10–16, 2010.
- [54] C. E. Clark, R. S. Taylor, A. C. Shore, O. C. Ukoumunne, and J. L. Campbell, “Association of a difference in systolic blood pressure between arms with vascular disease and mortality: a systematic review and meta-analysis,” *The Lancet*, vol. 379, no. 9819, pp. 905–914, 2012.
- [55] C. Roffe, S. Sills, K. Wilde, and P. Crome, “Effect of hemiparetic stroke on pulse oximetry readings on the affected side,” *Stroke*, vol. 32, no. 8, pp. 1808–1810, 2001.
- [56] K. Shelley and S. Shelley, “Pulse oximeter waveform: photoelectric plethysmography,” *Clinical Monitoring, Carol Lake, R. Hines, and C. Blitt, Eds.: WB Saunders Company*, pp. 420–428, 2001.
- [57] J. Allen, “Photoplethysmography and its application in clinical physiological measurement,” *Physiological measurement*, vol. 28, no. 3, p. R1, 2007.

- [58] K. H. Shelley, "Photoplethysmography: beyond the calculation of arterial oxygen saturation and heart rate," *Anesthesia & Analgesia*, vol. 105, no. 6, pp. S31–S36, 2007.
- [59] A. Challoner and C. Ramsay, "A photoelectric plethysmograph for the measurement of cutaneous blood flow," *Physics in Medicine & Biology*, vol. 19, no. 3, p. 317, 1974.
- [60] A. Reisner, P. A. Shaltis, D. McCombie, and H. H. Asada, "Utility of the photoplethysmogram in circulatory monitoring," *Anesthesiology: The Journal of the American Society of Anesthesiologists*, vol. 108, no. 5, pp. 950–958, 2008.
- [61] C. L. Lim, C. Byrne, and J. K. Lee, "Human thermoregulation and measurement of body temperature in exercise and clinical settings," *Annals Academy of Medicine Singapore*, vol. 37, no. 4, p. 347, 2008.
- [62] J. Y. Kim, P. Farmer, D. B. Mark, G. J. Martin, D. M. Roden, A. E. Dunaif, R. L. Barbieri, J. T. Repke, and W. C. Lau, "Harrisons principles of internal medicine," *Women's Health*, vol. 39, no. 5, pp. 24–39, 2008.
- [63] A. E. M. Ash and J. W. T. Roope, "Detecting small potential differences in a mammalian body," Nov. 18 1975, US Patent 3,920,003.
- [64] C. Demoulin, J.-M. Crielaard, and M. Vanderthommen, "Spinal muscle evaluation in healthy individuals and low-back-pain patients: a literature review," *Joint Bone Spine*, vol. 74, no. 1, pp. 9–13, 2007.
- [65] T. J. Roberts and A. M. Gabaldón, "Interpreting muscle function from emg: lessons learned from direct measurements of muscle force," *Integrative and comparative biology*, vol. 48, no. 2, pp. 312–320, 2008.
- [66] V. Alvarez, C. Reinsberger, B. Scirica, M. H. OBrien, K. R. Avery, G. Henderson, and J. W. Lee, "Continuous electrodermal activity as a potential novel

- neurophysiological biomarker of prognosis after cardiac arrest—a pilot study,” *Resuscitation*, vol. 93, pp. 128–135, 2015.
- [67] E. B. Prince, E. S. Kim, C. A. Wall, E. Gisin, M. S. Goodwin, E. S. Simmons, K. Chawarska, and F. Shic, “The relationship between autism symptoms and arousal level in toddlers with autism spectrum disorder, as measured by electrodermal activity,” *Autism*, vol. 21, no. 4, pp. 504–508, 2017.
- [68] K. Shankar, M. Manivannan, and P. Fernandez, “Gsr analysis of hypnotic analgesia,” *International Journal of Systemics, Cybernetics and Informatics (ISSN 0973-4864)*, Jan, pp. 08–06, 2008.
- [69] R. S. Behnke, *Kinetic Anatomy With Web Resource*. Human Kinetics, 2012.
- [70] G. Schulter and I. Papousek, “Bilateral electrodermal activity: reliability, laterality and individual differences,” *International Journal of Psychophysiology*, vol. 13, no. 3, pp. 199–213, 1992.
- [71] J. S. Gross and J. A. Stern, “An investigation of bilateral asymmetries in electrodermal activity,” *The Pavlovian journal of biological science: official journal of the Pavlovian*, vol. 15, no. 2, pp. 74–81, 1980.
- [72] G. R. Tomkinson and T. Olds, “Physiological correlates of bilateral symmetry in humans,” vol. 21, no. 08. Georg Thieme Verlag Stuttgart· New York, 2000, pp. 545–550.
- [73] R. Zangróniz, A. Martínez-Rodrigo, J. M. Pastor, M. T. López, and A. Fernández-Caballero, “Electrodermal activity sensor for classification of calm/distress condition,” *Sensors*, vol. 17, no. 10, p. 2324, 2017.
- [74] R. Trivers, B. Fink, M. Russell, K. McCarty, B. James, and B. G. Palestis, “Lower body symmetry and running performance in elite jamaican track and field athletes,” vol. 9, no. 11. Public Library of Science, 2014, p. e113106.

- [75] R. Wyatt and B. Tursky, "Skin potential levels in right- and left-handed males," *Psychophysiology*, vol. 6, no. 2, pp. 133–137, 1969.
- [76] M. Bracco, P. Turriziani, D. Smirni, R. G. Mangano, and M. Oliveri, "Relationship between physiological excitatory and inhibitory measures of excitability in the left vs. right human motor cortex and peripheral electrodermal activity," *Neuroscience Letters*, vol. 641, pp. 45–50, 2017.
- [77] V. Serdyuk, *Scoliosis and Spinal Pain Syndrome: New understanding of their origin and ways of successful treatment*, 1st ed. Byword Books, 12 2013.
- [78] M. J. van Putten, J. M. Peters, S. M. Mulder, J. A. de Haas, C. M. Bruijninx, and D. L. Tavy, "A brain symmetry index (bsi) for online eeg monitoring in carotid endarterectomy," vol. 115, no. 5. Elsevier, 2004, pp. 1189–1194.
- [79] M. Yan *et al.*, "A bilateral brain symmetry index for analysis of eeg signal in stroke patients," in *4th International Conference on Biomedical Engineering and Informatics (BMEI)*, Shanghai, Oct. 2011, pp. 8–11.
- [80] M. Bryden, *Laterality functional asymmetry in the intact brain*. Elsevier, 2012.
- [81] D. R. Mahapatra, N. Chakraborty, S. Bandopadhyay, and B. Balachandran, "Gyrosonics: Signature analysis and reduced-order models," in *ASME 2010 International Mechanical Engineering Congress and Exposition*. American Society of Mechanical Engineers, 2010, pp. 419–424.
- [82] O. Pabst, C. Tronstad, S. Grimnes, D. Fowles, and Ø. G. Martinsen, "Comparison between the ac and dc measurement of electrodermal activity," *Psychophysiology*, vol. 54, no. 3, pp. 374–385, 2017.
- [83] A. Greco, A. Lanata, L. Citi, N. Vanello, G. Valenza, and E. P. Scilingo, "Skin admittance measurement for emotion recognition: A study over frequency sweep," *Electronics*, vol. 5, no. 3, p. 46, 2016.

- [84] F. Shaffer, D. Combatalade, E. Peper, and Z. M. Meehan, “A guide to cleaner electrodermal activity measurements,” *Biofeedback*, vol. 44, no. 2, pp. 90–100, 2016.
- [85] D. S. Bari, H. Y. Y. Aldosky, C. Tronstad, H. Kalvøy, and Ø. G. Martinsen, “Influence of relative humidity on electrodermal levels and responses,” *Skin Pharmacology and Physiology*, vol. 31, no. 6, pp. 298–307, 2018.
- [86] R. G. Hicks, “Experimenter effects on the physiological experiment,” *Psychophysiology*, vol. 7, no. 1, pp. 10–17, 1970.
- [87] K. W. Back, S. R. Wilson, M. D. Bogdonoff, and W. G. Troyer, “Racial environment, cohesion, conformity and stress,” *Journal of psychosomatic research*, vol. 13, no. 1, pp. 27–36, 1969.
- [88] R. G. Hicks, “Converging operations in the psychological experiment,” *Psychophysiology*, vol. 8, no. 1, pp. 93–101, 1971.
- [89] J. W. Mason and J. V. Brady, “The sensitivity of psychoendocrine systems to social and physical environment,” *Psychobiological Approaches to Social Behavior*, pp. 4–23, 1965.
- [90] R. Rosenthal, “Experimenter effects in behavioral research (new york: Appleton-century-crofts, 1966),” *See also*, no. 55, 1969.
- [91] M. J. Christie and P. H. Venables, “Site, state, and subject characteristics of palmar skin potential levels,” *Psychophysiology*, vol. 9, no. 6, pp. 645–649, 1972.
- [92] P. A. James *et al.*, “2014 evidence-based guideline for the management of high blood pressure in adults: report from the panel members appointed to the eighth joint national committee (jnc 8),” *JAMA (The Journal of American Medical Association)*, vol. 311, no. 5, pp. 507–520, 2014.

- [93] Puavilai *et al.*, “Diagnostic criteria for diabetes mellitus and other categories of glucose intolerance: 1997 criteria by the expert committee on the diagnosis and classification of diabetes mellitus (ada), 1998 WHO consultation criteria, and 1985 WHO criteria,” *Diabetes Research and Clinical Practice*, vol. 44, no. 1, pp. 21–26, 1999.
- [94] Devara *et al.*, “Laboratory investigation of dyslipidemia,” *Laboratory Medicine*, vol. 29, no. 7, pp. 432–436, 1998.
- [95] R. K. Shiva, “Thyroid function test and its interpretation,” vol. 4, pp. 584–590, March, 2014.
- [96] K. Park, “Park’s textbook of PREVENTIVE AND SOCIAL MEDICINE,” *Preventive Medicine in Obstet, Paediatrics and Geriatrics*, 2005.
- [97] “Rishmulti18s datasheet, [online]. available: [http://www.rishabh.co.in/index.php/products/product/118.](http://www.rishabh.co.in/index.php/products/product/118)”
- [98] *RISH Multi 18S*, Rishabh Instruments Pvt. Ltd. [Online]. Available: http://rishabh.co.in/uploads/product/15030919_RISH_multi_18S_manual_with_back_new.pdf
- [99] “Rishmulti si 232 datasheet, [online]. available: [http://www.rishabh.co.in/index.php/products/product/121.](http://www.rishabh.co.in/index.php/products/product/121)”
- [100] E. A. Lipman. (2007) Electrical safety information. [Online]. Available: http://web.physics.ucsb.edu/~phys13CH/electrical_safety.pdf
- [101] *RISH Multi SI 232*, Rishabh Instruments Pvt. Ltd. [Online]. Available: http://rishabh.co.in/uploads/product/SI_232_MANUAL_10-2011_NEW-1.pdf
- [102] A. C. Guyton and J. E. Hall, *Guyton and Hall Textbook of Medical Physiology, 12e*, 12th ed. Elsevier Saunders, 6 2010.

- [103] E. O. Doebelin and D. N. Manik, “Measurement systems: application and design,” 2007.
- [104] A. K. Ghosh, *Introduction to Measurements and Instrumentation*. PHI Learning Pvt. Ltd., 2012.
- [105] D. V. S. Murty, *Transducers and Instrumentation*. PHI Learning Pvt. Ltd., 2010.
- [106] E. W. Weisstein, “Accuracy,” *from MathWorld—a Wolfram Web Resource*. <http://mathworld.com/Accuracy/html>, 2008.
- [107] R. Myatt, “Pulse oximetry: what the nurse needs to know,” *Nursing Standard (2014)*, vol. 31, no. 31, p. 42, 2017.
- [108] M. J. Christie and P. H. Venables, “Sodium and potassium electrolytes and basal skin potential levels in male and female subjects,” *The Japanese journal of physiology*, vol. 21, no. 6, pp. 659–668, 1971.
- [109] D. C. Fowles and P. H. Venables, “Endocrine factors in palmar skin potential,” *Psychonomic Science*, vol. 10, no. 11, pp. 387–388, 1968.
- [110] C. Therrien and M. Tummala, *Probability and random processes for electrical and computer engineers*. CRC press, 2011.
- [111] D. C. Fowles and P. H. Venables, “The effects of epidermal hydration and sodium reabsorption on palmar skin potential.” *Psychological Bulletin*, vol. 73, no. 5, p. 363, 1970.
- [112] M. A. Idowu, “Lognormal distribution and its applications in biological and medical sciences,” in *Biometrics and Biostatistics*, 2015.
- [113] D. Lykken, R. Rose, B. Luther, and M. Maley, “Correcting psychophysiological measures for individual differences in range.” *Psychological Bulletin*, vol. 66, no. 6, p. 481, 1966.

- [114] B. Lahcene, “On pearson families of distributions and its applications,” *African Journal of Mathematics and Computer Science Research*, vol. 6, no. 5, pp. 108–117, 2013.
- [115] N. L. Johnson, S. Kotz, and N. Balakrishnan, “Continuous univariate distributions, vol. 2 of wiley series in probability and mathematical statistics: applied probability and statistics,” 1995.
- [116] N. Balakrishnan, “Continuous multivariate distributions,” *Wiley StatsRef: Statistics Reference Online*, 2014.
- [117] M. J. Panik, *Advanced statistics from an elementary point of view*. Academic Press, 2005, vol. 9.
- [118] A. K. Gupta and S. Nadarajah, *Handbook of beta distribution and its applications*. CRC press, 2004.